Stability of Rock Mass*

by

T. Ramamurthy**

Introduction

My involvement in soil mechanics has been for quite some years, right from the beginning of my career. I was fascinated by soil mechanics activity when I made a casual visit to the Andhra Pradesh Engineering Research Laboratories. I joined their Soil Mechanics Laboratory to make a career for myself.

I was contemplating to deliver this lecture on one of the following aspects...

(*i*) Strength and deformation response of choesionless soils in general stress system including plane strain,

(*ii*) crushing phenomena and response of cohesionless soils under high stresses including modelling of rockfills, or

(*iii*) stability of soil slopes and some important considerations in the design of high earth and rockfill dams.

During the last few years, at IIT Delhi, a base has been laid in the area of rock mechanics. In view of this I have accepted the advice of my colleagues to deliver this IGS Lecture on rock mechanics. Some results are beginning to come out of our research; I therefore chose "stability of rock mass" as the topic of this Lecture. I will confine myself to the strength aspect of intact—isotropic and anisotropic rocks, rock masses, to the stability of rock slopes and underground openings in squeezing grounds. Characterization of rocks and rock masses is essential for any realistic analysis of rock slopes, foundations of dams, or rock mass around tunnels. Numerous problems are being faced during open excavations in rock mass. On many occasions work in underground excavations had to be stopped for months in highly squeezing grounds in the Himalayas and therefore the relevance of the topic is being emphasized in this lecture.

Probably this is the first in the series of lectures on rock mechanics to be delivered in the country and I do hope many more will soon follow and generate considerable research activity. For the numerous problems we are facing both in hard and soft rock formations in this country, we alone have to find solutions to them by our active involvement.

Rock mechanics activity in terms of teaching, research and practice has been a recent phenomenon in India. Teaching at the post-graduate

---

*Eight IGS Annual Lecture delivered on the occasion of its 27th Annual General Session held at Roorkee, India.

**Professor and Head, Civil Engineering Department, Indian Institute of Technology, New Delhi-110016, INDIA.

level was first started through an elective course at the Indian Institute of Science in 1964. During 1972, the subject was being taught as an elective only at four Institutes. To the undergraduates it was first introduced at the Indian Institute of Technology, Delhi, during 1971 and to the post-graduates, a set of courses in Rock Mechanics was offered for minor specialization during 1976. In 1977 at this Institute, a fullfledged master's programme in rock mechanics was started for civil engineers for the first time in this country. This programme has been opened to mining engineers in July, 1985 and is the only programme currently being offered.

Research in rock mechanics has been considerably slow. Reasonably good facilities now exist at some of the educational institutions like Banaras Hindu University, Indian School of Mines, Regional Engineering College, Kurukshetra, and to some extent at the University of Roorkee and the Indian Institutes of Technology located at Bombay and Kanpur. Some of the national research institutes like, Central Soil and Material Research Station, Central Mining Research Institute, National Geophsical Research Institute and Central Water and Power Research Station have acquired good facilities for testing and research over the years. State research laboratories have also built up some testing facilities and started some research activities through the funds provided by the Central Board of Irrigation and Power. Of late, research publications have been increasing in number both at the national and international levels.

At IIT Delhi we have been steadily building research facilities in rock mechanics in terms of laboratory testing and computer programmes. Apart from various laboratory testing equipment some of the important facilities that are availabe are:

(*i*) High pressure triaxial equipment to test rock specimens under confining pressures upto 1400 kg/cm^2— it includes volume measuring system as well,

(*ii*) A biaxial loading frame for testing rock specimens upto $70 \times 70 \times 70$ cm size with maximum loading upto 500 t vertical and 100 t horizontal with electrical and manual loading and unloading and rate control facility,

(*iii*) Geomechanics modelling facility to test scaled models (3 m long and 1 m high) for the study of deformation pattern and failure modes for underground and open excavations and also stability of fundations of dams,

(*iv*) Data logging system connected to LVDTs and load cells and pressure transducers, and

(*v*) Field testing facilities to load upto 500 t.

Rock and Rock Mass

An intact rock is considered to be an aggregate of minerals without any structural defects. Such rocks are treated as isotropic, homogeneous and continous. A rock mass includes structural features induced in it by the force field of its physical environment. These features *viz.*, bedding planes, shear planes, fault planes, joint planes and fracture planes, render rock mass anisotropic, nonhomogeneous and discontinuous. Heavily fractured

rock and intact rock are often treated as continum. Because of the size and persistence or otherwise of the structural defects, testing of specimens of rock mass in the laboratory has become restrictive in practice. To a large extent, more than in the case of soils, greater relevance is placed on insitu evaluation of the response of rock mass in the anticipated stress range and stress field. Estimation of relevant parameters for the design of civil and mining engineering works is of paramount importance. Sometimes comprehensive data collection both from field and laboratory is carried out primarily to perform a realistic analysis of the rock mass, that is, to predict its deformational response and stability.

Strength of intact rock is influenced mainly by (*i*) geological, (*ii*) lithological, (*iii*) physical, (*iv*) mechanical, and (*v*) environmental factors, as presented in Table 1.

TABLE 1

Factors Effecting the Intact Rock Strength

INTACT ROCK STRENGTH

Geological	*Lithological*	*Physical*	*Mechanical*	*Environmental*
Geological Age	Mineral Composition	Density/ Specific gravity	Specimen preparation	Moisture content
Weathering and other alterations	Cementing Material	Void Index	Specimen geometry	Nature of pore fluids
	Texture and Fabric	Porosity	End contact/ end restraint	Temperature
	Anisotropy		Type of testing machine	Confining Pressure
			Rate of loading	

Strength Criteria for Intact Rocks

Under a given situation, geological, lithological, physical, environmental and most of the mechanical aspects remain constant and the influence of confining pressure is predominant. The effect of confining pressure on the strength of intact rock has been investigated extensively starting with von Karman (1911) who conducted pioneering experiments on Carrara marble in copper jackets and observed a nonlinear variation of strength with confining pressure. All the subsequent investigations conducted to study the influence of confining pressure confirm this nonlinear response. An important aspect of rock behaviour under triaxial condition is the change in behaviour from brittle to ductile nature at high confining pressures (Grigg 1936, Donath 1970, Mogi 1972, Hoshino et al. 1972, Ramamurthy and Goel 1973).

For argillaceous sandstone and siltstone, brittle to ductile transition occurs under confining pressure range of 1000—3000 kg/cm^2 (Handin and Hager 1957, Hoshino et al 1972). For rock salt and gypsum this pressure

is as low as 200–400 kg/cm². This transition was usually observed when σ_1/σ_3 is in the range of 3 to 5 (Schwarz 1954, Mogi 1965). A rare exception to this nonlinearity is in the case of highly crystalline rocks like quartzite and granite which tend to exhibit linear response. The well known Navier-Coulomb theory based on maximum shear stress criterion predicts a linear behaviour. The classical Griffith's criterion based on failure of rocks in tension predicts to some extent a nonlinear response. However, these classical theories, though simple in concept and also in use, fail to predict rock behaviour universally. Hence a need has been felt to develop a failure criterion applicable to most rock types.

To overcome this inadequacy, an empirical power law was suggested by Murrell (1968) as

$$\sigma_1 = \sigma_c + B(\sigma_3)^A \qquad ...(1)$$

or

$$\tau = \tau_0 + b\,\sigma_n^a \qquad ...(2)$$

In the non-dimensional form these equations may be written as

$$\left(\frac{\sigma_1}{\sigma_c}\right) = 1 + B\left(\frac{\sigma_3}{\sigma_c}\right)^A \qquad ...(3)$$

and

$$\frac{\tau - \tau_0}{\sigma_c} = K\left(\frac{\sigma_n}{\sigma_c}\right)^a \qquad ...(4)$$

where A, B, K, a and b material constants,

τ = shear strength at failure,

τ_0 = shear strength at zero normal stress σ_n,

σ_c = uniaxial compressive strength, and

σ_1 & σ_3 = major and minor principal stresses.

An alternate form of this power law was suggested by Hoek (1968) in terms of maximum shear stress and associated normal stress as

$$\frac{\sigma_m - \tau_0}{\sigma_c} = D\left(\frac{\sigma_m}{\sigma_c}\right)^C \qquad ...(5)$$

where

$$\tau_m = \frac{\sigma_1 - \sigma_3}{2}, \quad \sigma_m = \frac{\sigma_1 + \sigma_3}{2},$$

and C and D are material constants.

For sandstones $D = 0.76$ and $C = 0.85$; similar values for other rock types are not available.

Jaeger (1971) and Franklin (1971) elegantly summarized the failure criteria applicable to intact rocks. Figure 1 presents various forms of

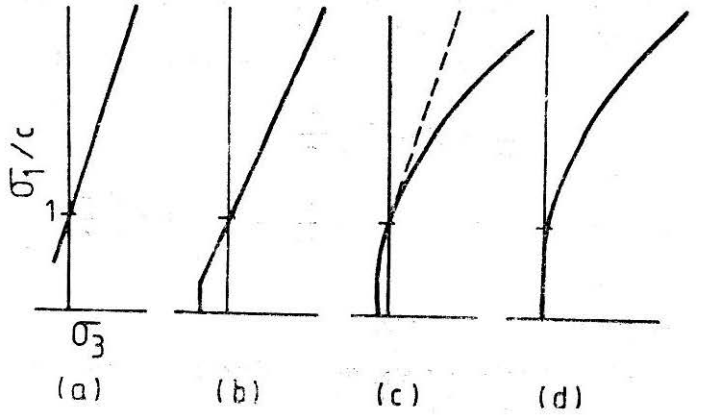

FIGURE 1 Failure Criteria : (a) Coulomb, (b) Poncelet, (c) Griffith, (d) Power law (Jaeger 1971)

criteria in vogue upto early 1970. Before 1974, no systematic attempt was made to relate the constants of failure criteria with the lithologic classification of rocks. Using the normalized forms, many empirical criteria were evolved but the one suggested by Bieniawski (1974) has gained popularity and is expressed as

$$\frac{\sigma_1}{\sigma_c} = 1 + B\left(\frac{\sigma_3}{\sigma_c}\right)^{\alpha} \qquad ...(6)$$

where α = slope of the plot between $\left(\frac{\sigma_1}{\sigma_c} - 1\right)$ versus $\left(\frac{\sigma_3}{\sigma_c}\right)$ on log-log plot, and

B = a material constant.

From a study of a range of South African rocks, Bieniawski had the distinction of linking up the constants of the failure criterion with the lithology of some rocks. He suggested that

$\alpha = 0.75$ for all rock types

and $B = 3.0$ for siltstone and sandstone,

4.0 for sandstone,

4.5 for quartzite, and

5.0 for norite.

Based on test results of four rock types, Brook (1979) modified Hoek's expression (1968) to take the form of

$$\frac{\tau_m}{\sigma_c} = A\left(\frac{\sigma_m}{\sigma_c}\right)^{n} \qquad ...(7)$$

Conforming to non-linear response of strength with confining pressure through trial and error process, Hoek and Brown (1980) suggested the following equation,

$$\sigma_1 = \sigma_3 + [m\ \sigma_c\ \sigma_3 + s\ \sigma_c^2\ ]^{\frac{1}{2}} \qquad ...(8)$$

where m and s are material parameters; $s = 1$ for intact rocks and m depends on rock type and has a wide range.

Yudbir et al. (1983) gave a general form to Bieniawski's expression as

$$\frac{\sigma_1}{\sigma_c} = A + B\left(\frac{\sigma_3}{\sigma_c}\right)^{\alpha} \qquad \ldots(9)$$

where α = slope of plot between $\left(\frac{\sigma_1}{\sigma_c} - A\right)$ and $\left(\frac{\sigma_3}{\sigma_c}\right)$ on log-log scale,

B = material constant, and

A = dimensional parameter which depends on rock quality; for intact rocks its value is unity.

Based on very limited data they proposed on the lines of Bieniawski a value of

B = 2 for tuff, shale and limestone,

3 for siltstone and mudstone,

4 for sandstone, quartzite, and

5 for norite and granite.

When the analysis of test data was carried out by adopting the criteria referred to in the foregoing, sometimes significant deviations were observed suggesting the need for developing a more realistic criterion to be applicable at least in the first instance to intact rock, with a possibility of extending it to estimate rock mass strength.

Proposed Strength Criterion

In order to develop a simple mathematical expression which would enable prediction of strength sufficiently accurate not only for intact but also of anisotropic rocks and fractured rock masses covering the entire brittle and ductile regions, an attempt has been made through Mohr-Coulomb failure criterion (Rao 1984, Ramamurthy, Rao and Rao 1985 and Rao, Rao and Ramamurthy 1985) as detailed hereunder :

As per Mohr-Coulomb criterion,

$$(\sigma_1 - \sigma_3) = 2c \cos\phi + (\sigma_1 + \sigma_3)\sin\phi \qquad \ldots(10)$$

where c = cohesion intercept, and

ϕ = friction angle.

By normalising and rearranging, Eq. 10 be written as

$$\left(\frac{\sigma_1 - \sigma_3}{\sigma_3}\right) = \frac{2c\cos\phi}{\sigma_3(1-\sin\phi)} + \frac{2\sin\phi}{1-\sin\phi} \qquad \ldots(11)$$

The term $\frac{2\,c\,\cos\phi}{1-\sin\phi}$ is equal to σ_c (unconfined compresssive strength) when $\sigma_3 = 0$.

$$\text{Therefore, } \frac{\sigma_1-\sigma_3}{\sigma_3} = \frac{\sigma_c}{\sigma_3} + \frac{2\sin\phi}{1-\sin\phi}$$

$$= \frac{\sigma_c}{\sigma_3}\left[1 + \frac{\sigma_3}{\sigma_c}\cdot\frac{2\sin\phi}{1-\sin\phi}\right] \qquad ...(12)$$

To take care of the variations in c and ϕ with increase of confining pressure σ_3 and also to account for the non-linear behaviour, Eq. 12, is modified as

$$\left(\frac{\sigma_1-\sigma_3}{\sigma_3}\right) = B\left(\frac{\sigma_c}{\sigma_3}\right)^{\alpha} \qquad ...(13)$$

where B = rock material constant; function of rock type and quality, and

α = slope of plot between $\frac{\sigma_1-\sigma_3}{\sigma_3}$ and $\frac{\sigma_c}{\sigma_3}$ on log-log plot.

The above expression is applicable for all values of $\sigma_3 > 0$.

To establish the applicability of this expression, initially four sandstones selected from different geological formations ranging from the Vindhyans to recent Siwalik, were tested (Rao 1984) using simple triaxial cell (Ramamurthy 1975). These sandstones were

(*i*) Kota sandstone, belonging to Bhander series of Upper Vindhyans (600 m.y.),

(*ii*) Singrauli sandstone, belonging to Purewa bottom series of Raniganj group of the Gondwana system (150 m.y.).

(*iii*) Jhingurda sandstone, Singrauli coal fields, belonging to Purewa top series of Raniganj group of the Gondwana system (150 m.y.), and

(*iv*) Jamrani sandstone from a hydel project, U.P. belonging to the lower Siwalik of eastern Himalayas (25 m.y.).

In addition to the data of these four sandstones, similar data of 80 different rock types published in the literature were analysed. These include sedimentary (argillaceous, arenaceous, and chemical), metamorphic and igneous rocks. Plots of the data in terms of $(\sigma_1-\sigma_3)/\sigma_3$ versus σ_c/σ_3 for argillaceous rocks (shales and slates), arenaceous (sandstone and quartzite), chemical (limestone, dolomite, anhydrite, rock salt and marble) and igneous rocks (granite, andesite, norite, basalt, gabbro and syenite) are presented in Figs. 2 to 5. The results of the four Indian sandstones are presented in Fig. 6.

All these plots are straight lines and are nearly parallel on log-log graph with the value of α falling in a very narrow range of 0.75 to 0.85.

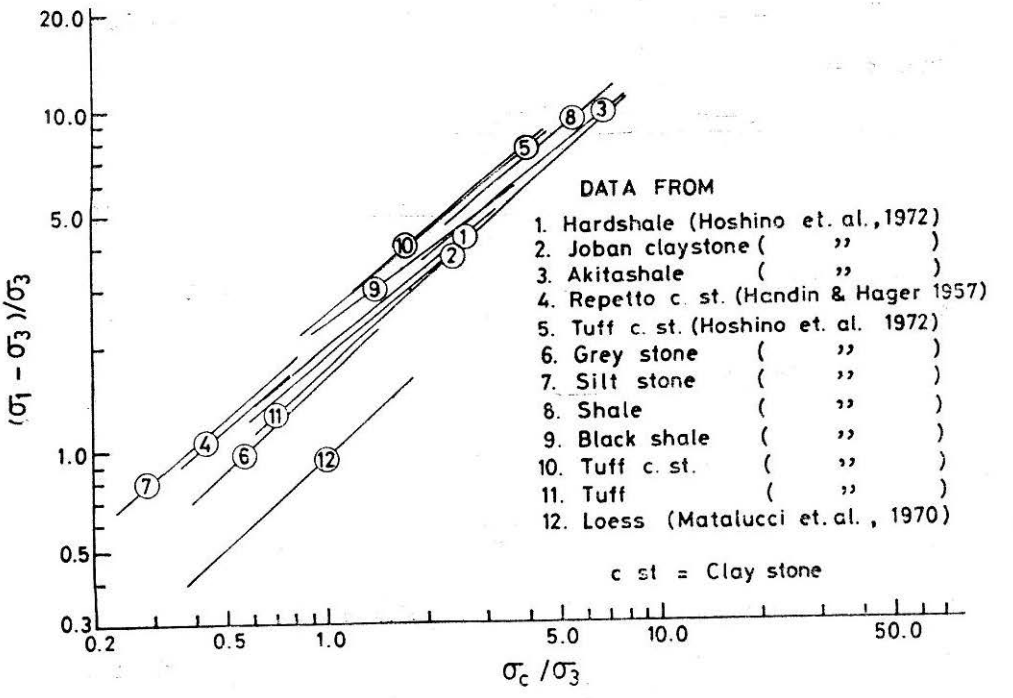

FIGURE 2 Plot of Proposed Criterion for Argillaceous Rocks

An average value of 0.8 is suggested for all rock types without significantly sacrificing accuracy in the prediction of strength. The data on igneous rocks presented in Fig. 5 has been shown in Fig. 7, as per Bieniawski's criterion to emphasise that definite values cannot be assigned to constants in Eq. 6. The values of α obtained from Bieniawski's expression vary over a wide range, i.e. from 0.4 to 1.2. These values vary from one rock group to another and also even within the same rock group. Therefore, the assumption of a constant value of α from such wide variation is difficult to justify.

Using a constant value of $\alpha = 0.8$, and the values of strength (σ_c) and σ_1 for various values of σ_3, the values of B were calculated from Eq. 13. These values of B for the four sandstones fall in a close range from 2.13 to 2.69. Adopting $s=1$ in Hoek-Brown criterion (Eq. 8), the values of m were estimated. The values of m vary widely from 1.42 to 13.26 (Table 2), whereas the suggested values of m for such rocks by Hoek and Brown (1980) is 15. Table 2 also presents the values of coefficient of determination (r^2). These values of the coefficient are better for the proposed criterion than that for Hoek-Brown criterion suggesting definite advantage of the proposed criterion. A good agreement between the experimental results and proposed criterion is also reflected in Fig. 8.

A wide scatter in the values of m for different groups of rocks was observed and is indicated in Table 3, along with the values suggested by Hoek and Brown (1980).

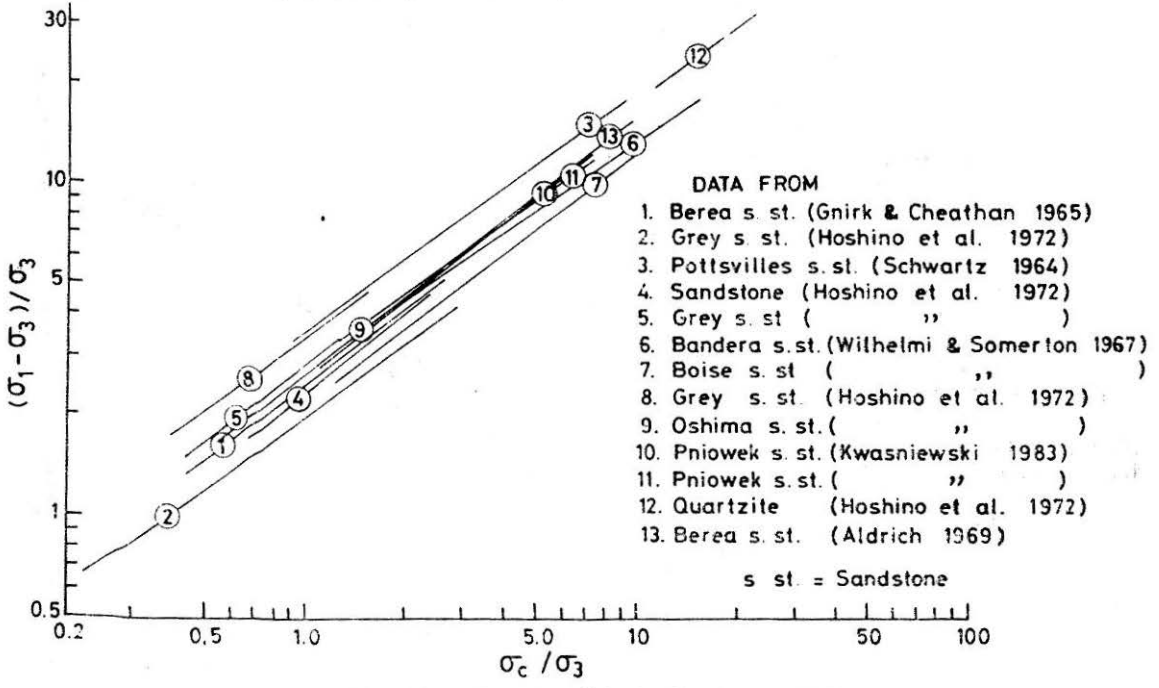

FIGURE 3 Plot of Proposed Criterion for Arenaceous Rocks

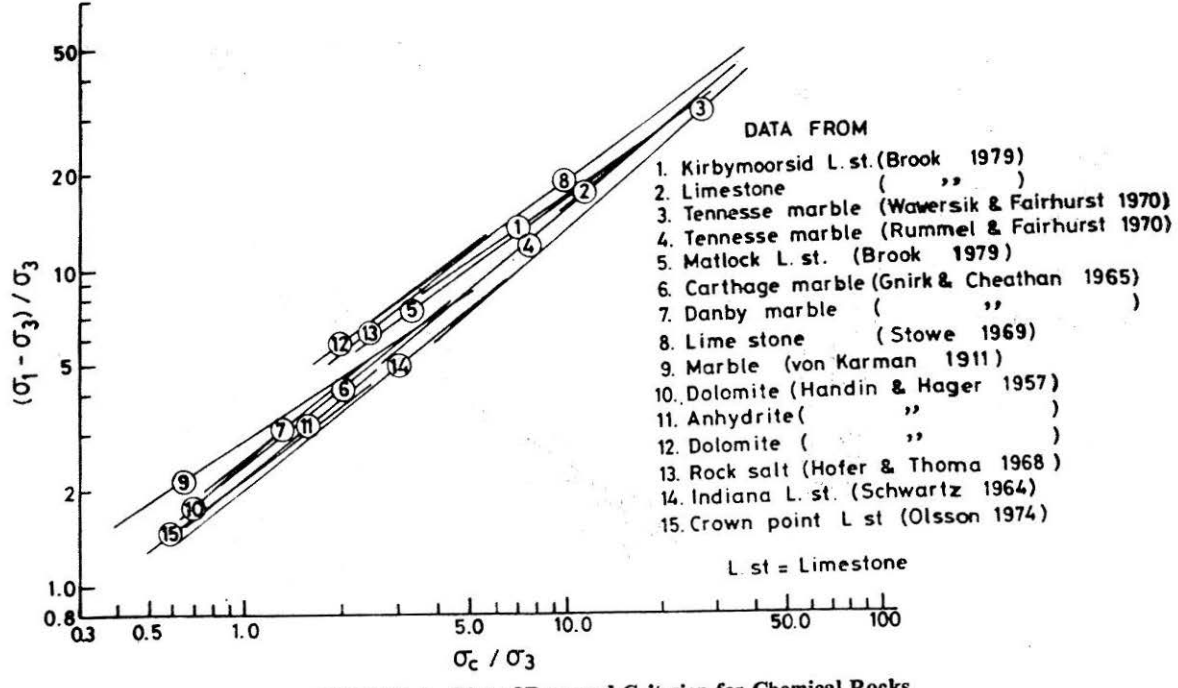

FIGURE 4 Plot of Proposed Criterion for Chemical Rocks

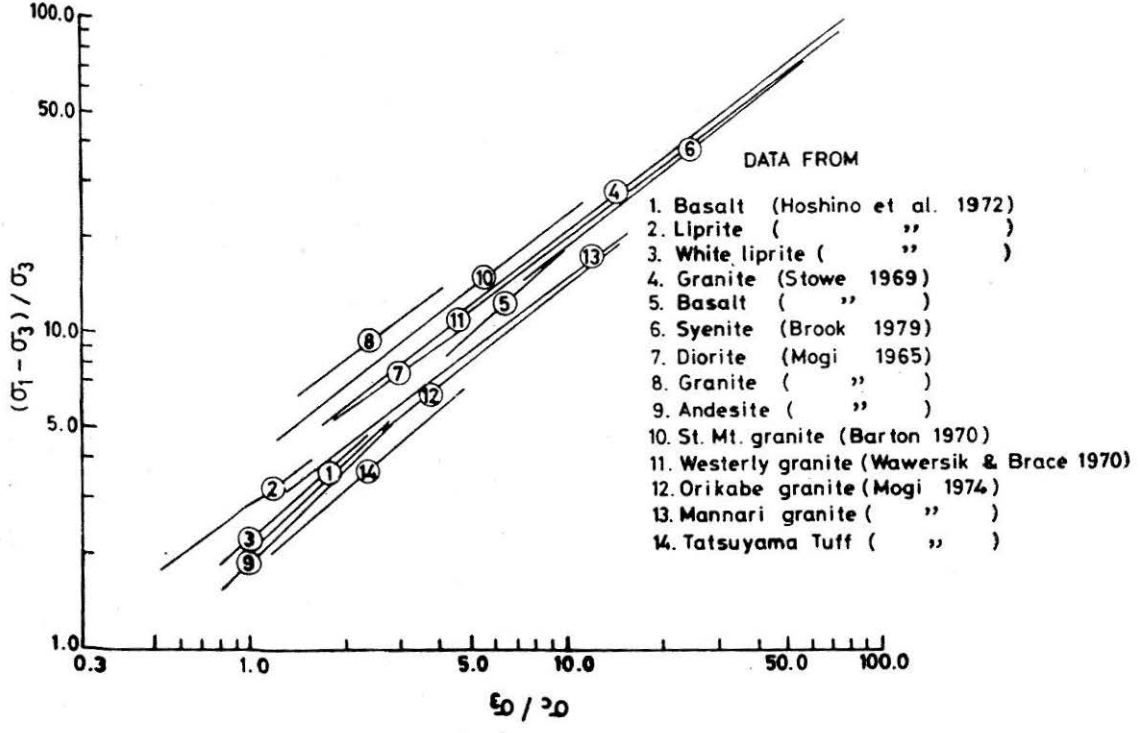

FIGURE 5 Plot of Proposed Criterion for Igneous Rocks

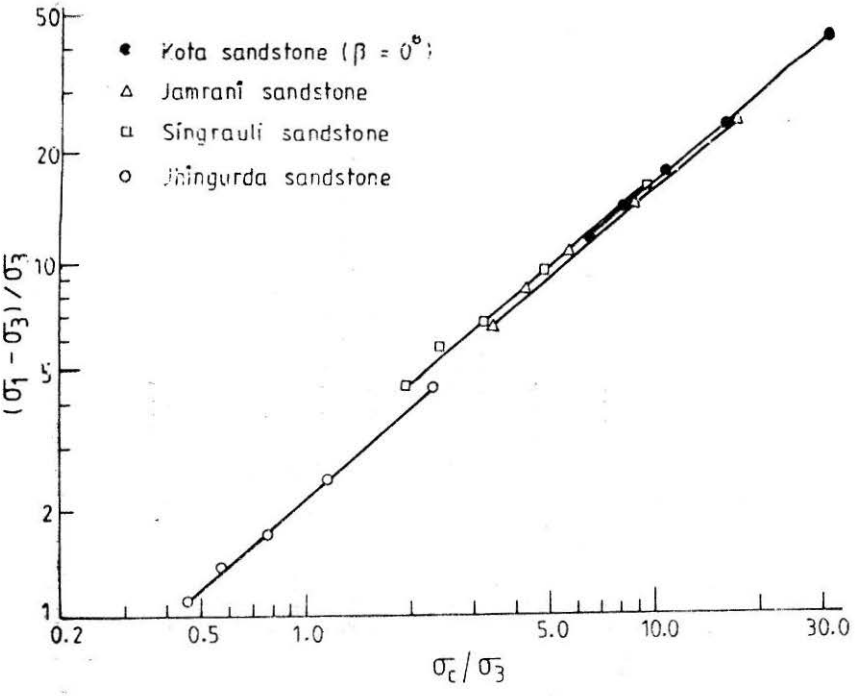

FIGURE 6 Plot of Proposed Criterion for Four Indian Sandstones

Table 4 has been prepared from test results (as an illustration) on Indiana limestone (Schwartz 1964). The values of B and m are listed for different confining pressures. The values of B are nearly same but the values of m vary considerably over the range of confining pressures of 7.03 to 562.40 kg/cm.^{2} The values of m decrease with increasing confining pressure suggesting that it will be difficult to assume a constant value of m for any rock type. On the contrary, the value of B for a particular rock type could be very reliably obtained from tests carried out at least at any one convenient confining pressure.

Further, to verify the applicability of the proposed criterion in the range of brittle to ductile region, Mogi's transition line has been plotted in Fig. 9, for Indiana limestone and Talsuyma tuff. For both the rocks, coefficient of determination for the proposed criterion was higher than that for the Hoek—Brown criterion. The proposed criterion has the potential of predicting the strength in the compression range spreading over brittle and ductile regions more accurately. On the other hand the predicted strength from Hoek-Brown criterion is higher at lower σ_3 and lower at higher σ_3. At still higher σ_3, this criterion overpredicts the strength.

Based on the detailed study of over 80 rocks and the four sandstones, Table 5 has been developed to enable a choice of the value of B based on lithologic classification. This table covers different rock types, namely, igneous, sedimentary and metamorphic. The mean and standard deviation in the values of B and m for rock types classified in Table 5 are given in Table 6.

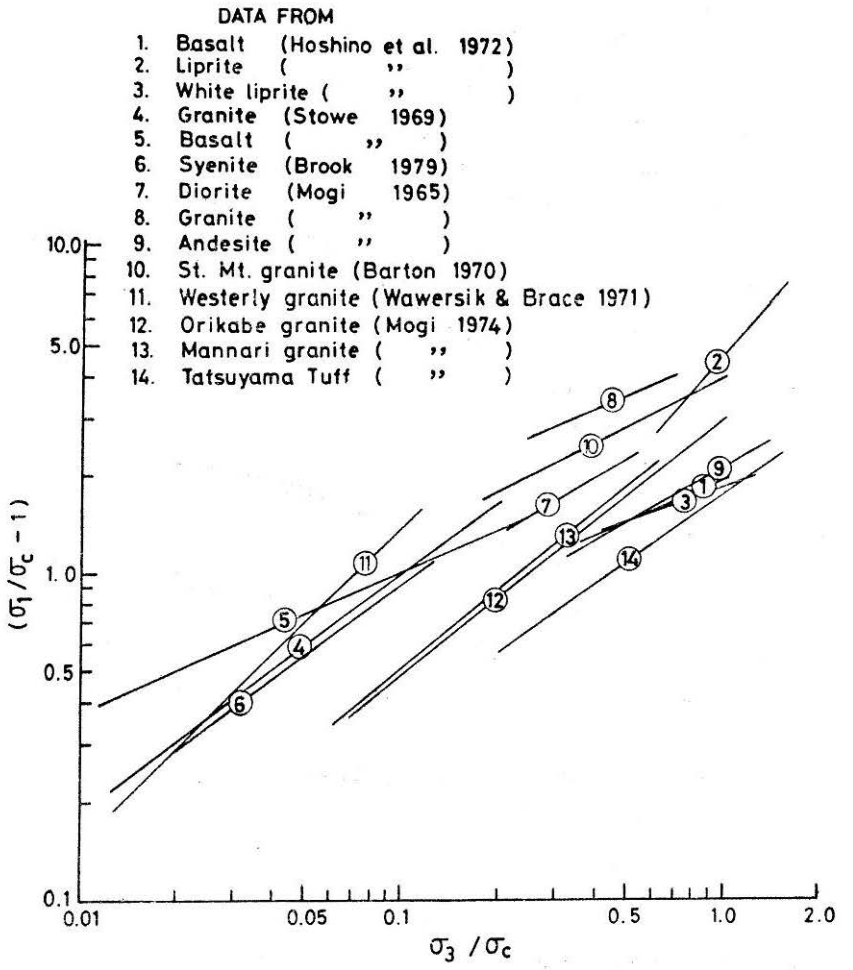

FIGURE 7 Plot of Bieniawski's Criterion for Igneous Rocks

TABLE 2

Parameters Evaluated for Sandstones

Rock Type	Proposed Criterion			Hoek-Brown Criterin	
	B ($\alpha=0.8$)	r^2	σ_c^* (kg/cm²)	m ($s=1$)	r^2
Kota sandstone $\beta = 0°$	2.6900	0.999	903.31	13.2500	0.953
Jamrani sandstone	2.5299	0.972	516.36	7.3379	0.896
Singrauli sandstone	2.6286	0.998	305.01	6.4555	0.935
Jhingurda sandstone	2.1373	0.955	82.65	1.4163	0.841

* Calculated from the triaxial test data

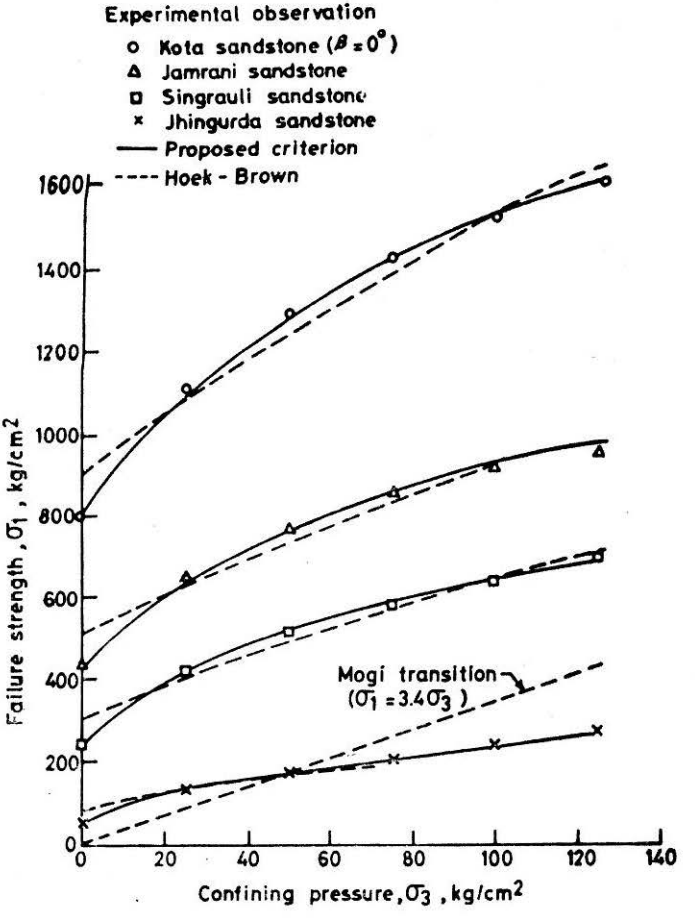

FIGURE 8 Comparison Between Predicted and Measured Strength of Sandstones

TABLE 3

Estimated Range and Suggested values of m for Different Rocks

Rock Types	Values of *m*	
	Estimated range	Values Suggested by Hoek & Brown (1980)
1. Argillaceous	—0.091 to 10.20 (average 3.84)	10.0
2. Arenaceous	—3.17 to 21.0 (average 4.85)	15.0
3. Chemical	1.32 to 14.42 (average 5.75)	7.0
4. Igneous	0.95 to 32.84 (average 11.41)	25.0

TABLE 4

Values of B and m for Indiana Limestone (Schwartz 1964) at Different Confining Pressures, $\sigma_c = 445.20$ kg/cm²

σ_3 kg/cm²	σ_1 kg/cm²	B ($\alpha = 0.8$)	m ($s = 1$)	$\sqrt{m}$
70.3	679.6	1.94	5.54	2.35
140.6	855.3	1.99	4.89	2.21
210.9	1007.6	2.06	4.65	2.16
281.2	1089.7	1.98	3.64	1.90
351.5	1230.3	2.06	3.59	1.89
421.8	1288.8	1.97	2.88	1.69
492.1	1347.4	1.88	2.38	1.54
562.4	1429.4	2.02	2.16	1.46
Average		1.98	3.72	1.89

It is observed that the value of B is low for soft rocks and high for hard ones within the group. Rocks of similar composition which become stronger due to further changes (say siltstone to shale) or due to metamorphosis (from limestone to marble), clearly indicate an increase in the values of B. Such a sensitivity to lithology of rocks is somewhat similar to what one finds in Deere and Miller's classification as well.

In the absence of any facilities of triaxial testing of rock specimens, this table serves as a good guide in the preliminary evaluation of strength envelope. One needs to know from laboratory tests only the uniaxial compressive strength of rock. When facilities exist it would be sufficient to conduct careful tests at least at any one convenient confining pressure to evaluate a realistic value of B for generating the strength envelope. The proposed theory is thus simple and realistic to represent the strength criterion of intact rocks.

Strength Criterion for Anisotropic Rocks

An idealized cylindrical specimen of anisotropic rock with an oblique plane of weakness making an angle of β with the axis of major principal stress (σ_1) is shown in Fig. 10. A large amount of experimental data (to quote a few, Donath 1964 on slate, Chenvert and Gatlin 1965 on sandstone. Attewell and Sandford 1974 on slate Hoek and Brown 1980 on slate) clearly shows that the strength for all rocks is maximum for $\beta = 0$ and/or 90 degrees and minimum for β in the range of 20 to 30°. It is also known that the degree of anisotropy considerably diminishes with increasing confining pressure.

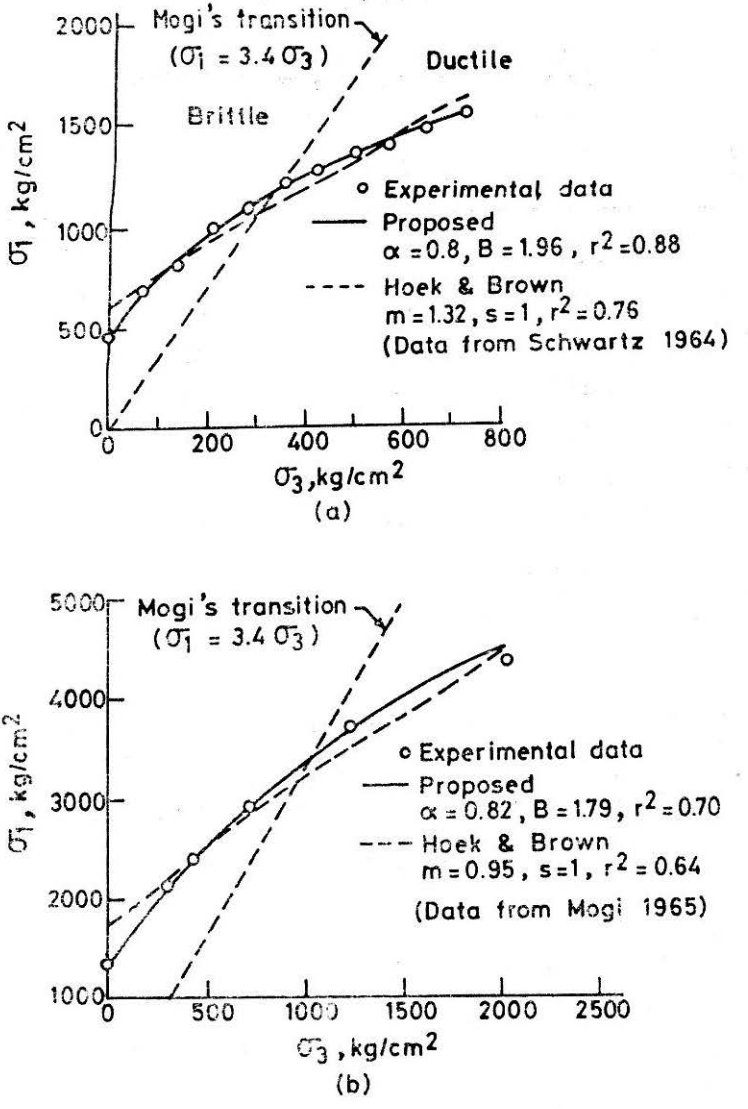

FIGURE 9 Validity of the Proposed Criterion in the Brittle ductile Region for, (a) Indiana Limestione and (b) Talsuyama Tuff.

A number of empirical strength criteria have been proposed based on the classical Navier-Coulomb and Griffith's failure criteria. Some of the widely used theories for anisotropic rocks are those of Jaeger (1969), Walsh and Brace (1964) and of McLamore and Gray (1967). To evaluate these failure criteria, it is necessary to conduct triaxial tests at a minimum of three different confining pressures on specimens of at least three different orientations of β. These theories due to their obvious limitations cannot be used for evaluating the strength of rocks and to quantify the parameters with lithologic classification of rocks.

TABLE 5

Mean Values of parameter *B* for different rocks

Rock Type	Sedimentary and Metamorphic Rocks						Igneous Rocks	
	Argillaceous		Arenaceous		Chemical Rocks			
	Silt stone	Shales	Sand-stone	Quar-tzite	Limestone	Marble	Ande-site	Granite
	Clays	Slates			Anhydrite	Dolo-mite	Diorite	Charno-ckite
	Tuffs	Mud-stone			Rocksalt		Norite	
	Loess	Clay-stone					Liprite Basalt	
Parameters *B*	1.8	2.2	2.2	2.6	2.4	2.8	2.6	3.0

TABLE 6

Mean and Standard Deviation of *B* and *m* parameters for Different Intact Rocks

	Argillaceous		Arenaceous		Chemical		Igneous	
	B	*m*	*B*	*m*	*B*	*m*	*B*	*m*
Mean	2.10	4.04	2.15	5.18	2.51	5.74	2.73	11.12
Standard Deviation	0.29	3.27	0.34	4.99	0.34	4.27	0.43	9.58

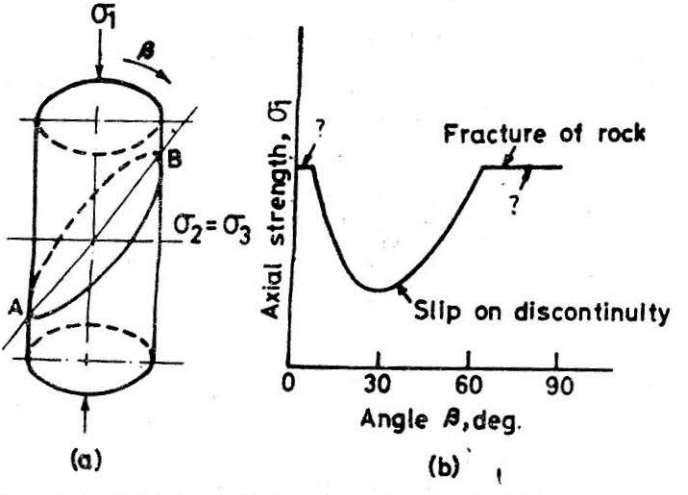

FIGURE 10 (*a*) Typical Anisotropic Specimen Showing Variable Parameters during Testing and

(*b*) σ_1—β Failure Pattern for Anisotropic Rock

Using the non-linear failure envelope predicted by Griffith's theory for plane compression and through a process of trial and error, Hoek and Brown (1980) presented an empirical failure criterion applicable for both isotropic and anisotropic rocks,

$$\sigma_1 = \sigma_3 + \left(m\,\sigma_c\,\sigma_3 + s\sigma_c^2\right)^{\frac{1}{2}} \qquad \ldots (8)$$

wherein

$s = 1$ for intact rock, and

$= 0$ for crushed rock,

$m =$ varies widely—a function of type and quality of rock.

In order to predict the strength of anisotropic or jointed rock from the proposed criterion, Eq. 13 can be written as :

$$\frac{(\sigma_1 - \sigma_3)_j}{\sigma_3} = B_j \left(\frac{\sigma_{cj}}{\sigma_3}\right)^{\alpha} \qquad \ldots (14)$$

where σ_{cj} = uniaxial compressive strength of rock with a weak plane or a a joint oriented at β greater than zero degrees, and

B_j = material constant for the joint orientation.

The strength predicted from Walsh and Brace, Jaeger, Hoek and Brown and also from the proposed theory at $\sigma_3 = 25$ and 125 kg cm^2 for Kota sandstone are presented in Fig. 11 along with the experimental results. Both Walsh and Brace and Jaeger criteria yield poor prediction. Using the proposed criterion, the value of B_j at $\beta = 0°$ is 2.69 whereas at $\beta = 30°$, this value is 2.51. The values of B_j for other orientations ($\beta = 65°$ and $\beta = 90°$) fall in between these two values indicating that the variation of B_j with β is small. Thus one can consider B_j to be a constant for a particular rock, and the prediction of strength will be sufficiently accurate for general use. On the other hand, for Kota sandstone using Hoek-Brown criterion, the variation in m is from 13 25 to 7.77 and that in s is from 1 to 0.63 for different values of β. Also for the proposed criterion, the coefficient of determination (r^2) at different orientation is above 0.999 whereas in the case of Hoek-Brown criterion, it is around 0.94, indicating an excellent matching of experimental results with the proposed criterion.

The applicability of this proposed criterion was verified (Rao 1984) for the results of other anisotropic rocks like Green river shale, Arkansas sandstone and permean shale (Chenevert and Gatlin 1965), Martinsburg shale (Donath 1964), Texas Slate, Green river shale-1 and 2 (McLamore and Gray 1967), Barnsly hard coal (Pomeray et al 1971), fractured sandstone (Horino and Ellickson 1970) and Penrhyn slate (Attewell and Sandford 1974). The analysis of the data of these rocks indicates that except for Texas slate and Penrhyn slate, the values of α for all other rocks is around 0.80. The variation between B and B_j for these rocks is small, while the variation in m and m_j, and s and s_j is large. The variation of B_j with β is also very small when compared with the variation in m_j and s_j for these rocks. The predictions using these values are presented only for two rocks in Figs. 12 and 13. Experimental results superimposed for comparison in these figures suggest better prediction of strength from the proposed criterion. Higher values of coefficient of determination also

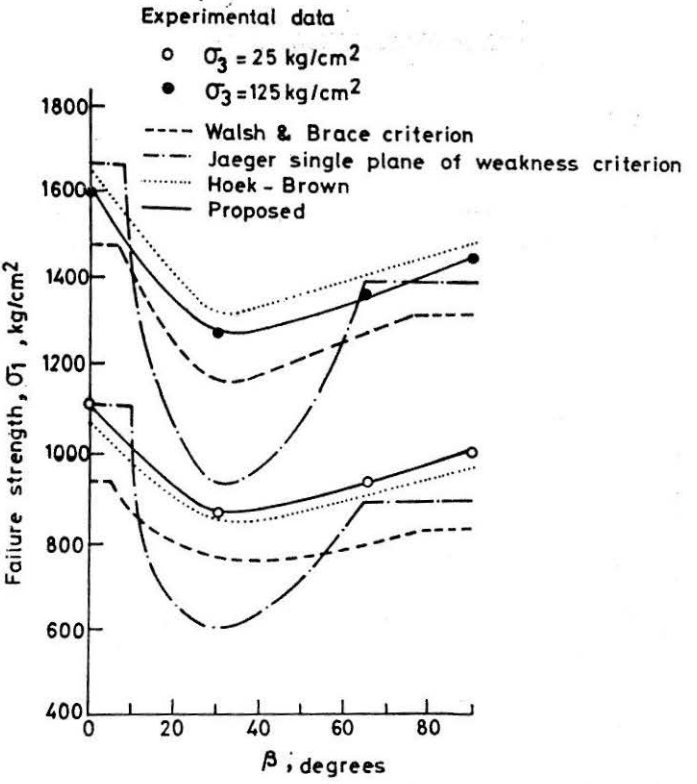

FIGURE 11 Comparison between Predicted and Measured Strengths for Kota Sandstone

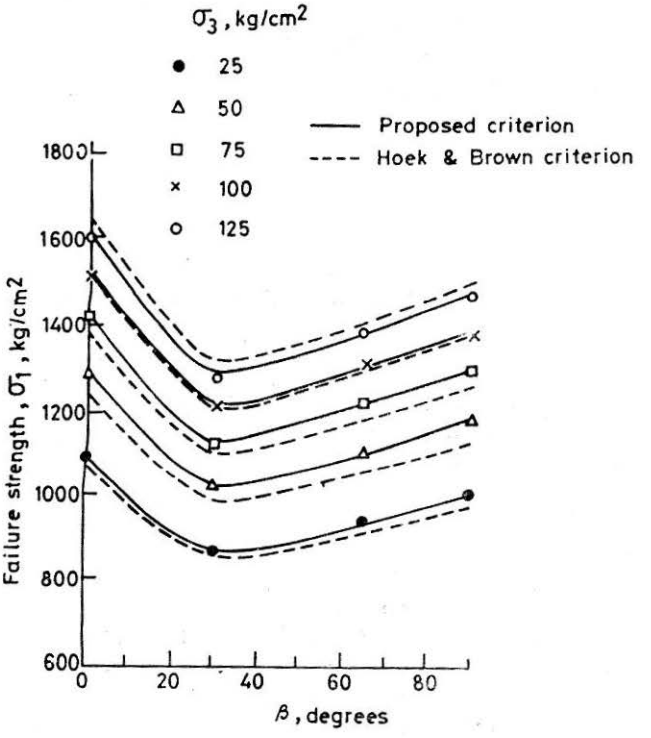

FIGURE 12 Comparison between Predicted and Measured Strengths for Kota Sandstone

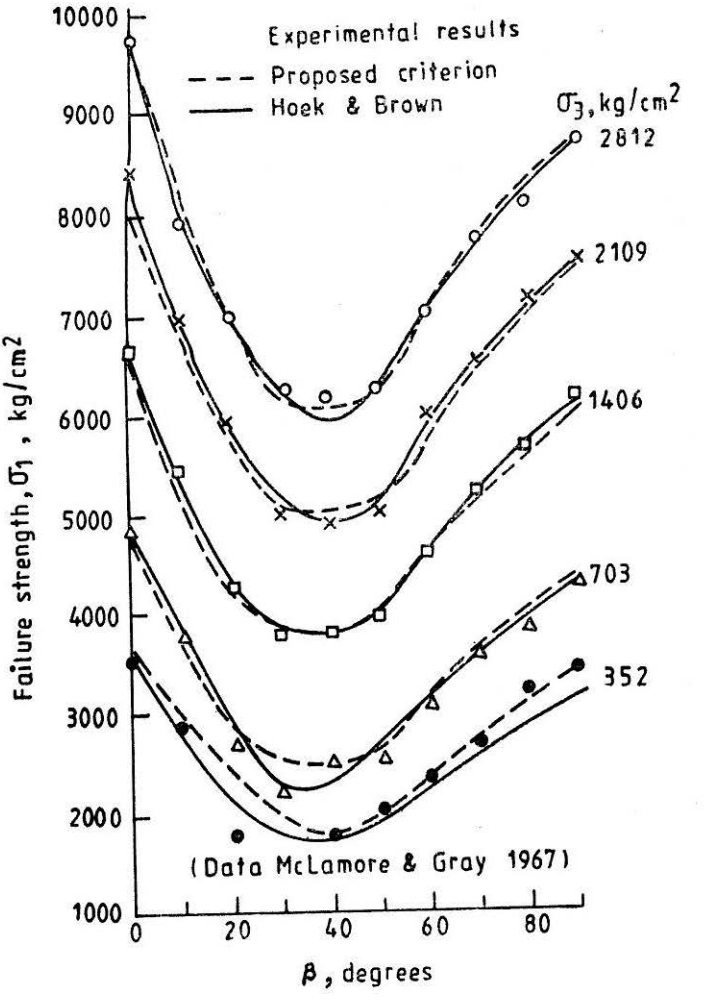

FIGURE 13 Comparison between Predicted and Measured Strengths for Texas Slate

confirmed the versatility of the approach. Further the validity of B values suggested for isotropic rocks has been confirmed for adoption even for anisotropic rocks, and thus the values of B suggested for various rock types in Table 5, for intact isotropic rocks are applicable for anisotropic rocks as well.

Rock Mass Strength

Using the limited data available from tests on Panguna Andesite (Hoek and Brown 1983) the input parameters for the proposed criterion have been estimated. The ratios of σ_{cm}/σ_c and B_m/B (subscript m for rock mass) alongwith the rating obtained from rockmass rating (RMR) classification of Bieniawski (1974) and rock mass quality index (Q—system) of Barton *et al* (1974) have been presented in Fig. 14. With the relationship proposed (Bieniawski 1974) between RMR and Q

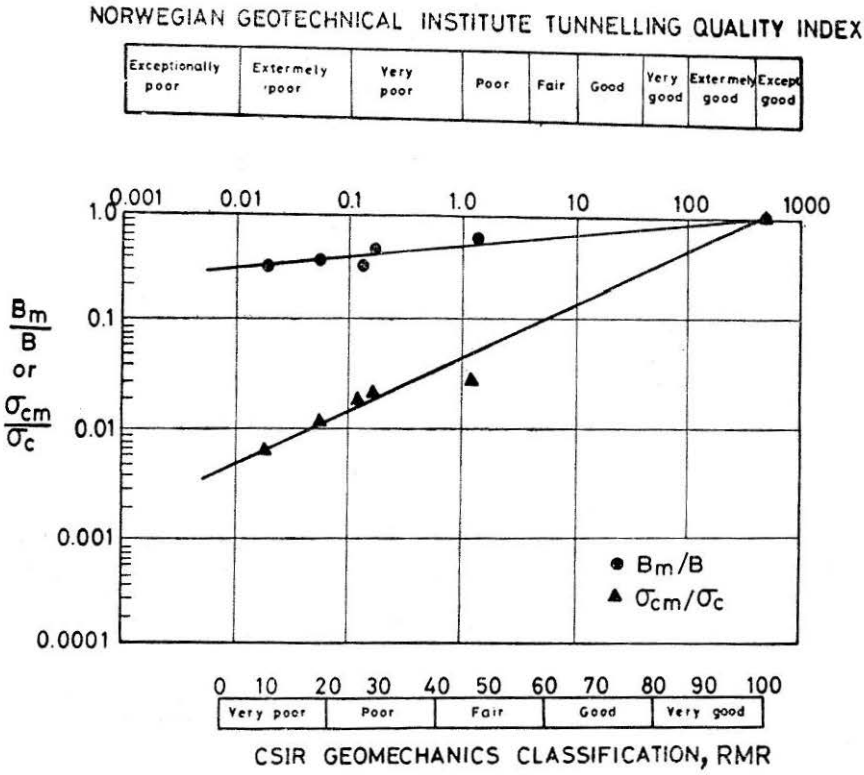

FIGURE 14 Plot of σ_m/σ_c and B_m/B for Panguna Andesite against Rock Mass Classifications

system, namely, RMR = 9 $\log_e Q$+44, the positions of the scales have been fixed in this figure. With this limited data, the following empirical relationships are suggested for predicting the values of σ_{cm} and B_m when RMR or Q ratings of rock mass are known :

$$\sigma_{cm} = \sigma_c \exp\left[\frac{RMR-100}{18.75}\right] \quad \ldots (15)$$

where σ_c = intact rock strength in unconfined compression, and

σ_{cm} = rock mass strength in unconfined compression,

and

$$B_m = B \exp\left[\frac{RMR-100}{75.5}\right] \quad \ldots (16)$$

where B = material constant for intact rock, and

B_m = material constant for rock mass.

By assessing the rating values of rock mass from the field, estimation of B_m and σ_{cm} could be conveniently made either from Eqs. 15. and 16 or from the values given in Table 7.

TABLE 7

Values of B_m/B for Panguna Andesite (σ_c = 2655 kg/cm²)

Ratio	RMR									
	100	90	80	70	60	50	40	30	20	10
σ_{cm}/σ_c	1.0	0.58	0.34	0.20	0.12	0.07	0.04	0.02	0.01	0.008
B_m/B	1.0	0.87	0.77	0.67	0.59	0.52	0·45	0.39	0.35	0.304

With these values of B_m and σ_{cm}, the strength of rock mass can be estimated by modifying Eq. 13 to the form

$$\frac{(\sigma_1 - \sigma_3)_m}{\sigma_3} = B_m \left(\frac{\sigma_{cm}}{\sigma_3} \right)^{\alpha} \qquad ...(17)$$

It should be noted that the relationships proposed above (Eqns. 15 and 16) for the evaluation of σ_{cm} and B_m are based on very limited but reliable field experimental data. More field data is essential to refine these relationships. However, these relations could be very well adopted for the analysis of most preliminary designs.

The great advantage and most significant aspect of the proposed criterion is that, based on lithologic classification, only one parameter B has to be appropriatly chosen from the Table 5. When no laboratory facilities exist to test intact rock specimens under a range of high confining pressures, this Table 5 and Eq. 17 provide a means to arrive at the most appropriate parameters for design. When once the failure envelope is arrived at, the shear strength parameters c and ϕ could be easily estimated for the appropriate stress range anticipated.

If some minimum laboratory facilities exist, at least one intact rock specimen could be tested at a convenient confining pressure. Using the values of σ_1 and σ_3 from the test, choosing $\alpha = 0.8$ and knowing σ_c of the intact rock, B could be estimated and checked with the values given in Table 5, and adopted to generate the entire failure envelope. With this value of B, using Eqs. 15 and 16, σ_{cm} and B_m for the rock mass could be estimated and the strength envelope for the rock mass could be predicted. The proposed failure criterion has therefore wide application.

Influence of a Single Plane of Weakness

In a laboratory test, orientation of the plane of weakness with respect to principal stress directions remains unaltered. Variation of the orientation of this plane can only be achieved by obtaining cores in different directions. In a field situation either in the foundations of dams, around underground or open excavations, the orientation of joint system remains stationary but the directions of principal stresses rotate resulting in a change in the strength of rock mass.

Jaeger and Cook (1979) developed a theory to predict the strength of rock containing a single plane of weakness. It assumes that the failure

will take place as a consequence of sliding along the plane of weakness or a joint plane and is expressed as

$$(\sigma_1 - \sigma_3) = \frac{2c + 2\sigma_3 \tan \phi}{(1 - \tan \phi \cot \beta) \sin 2\beta} \quad \ldots(18)$$

where ϕ = friction angle.

Failure by sliding will occur for all values of β falling between $\phi°$ and 90°. The minimum strength is obtained when $\tan 2\beta = -\cot \phi$, i.e.

$$(\sigma_1 - \sigma_3)_{min} = 2 (c + \sigma_3 \tan \phi) [(\tan \phi^2 + 1)^{\frac{1}{2}} + \tan \phi] \quad \ldots(19)$$

This suggests that one has to first estimate the values of c and ϕ along the joint plane. It is not clear whether the values of c and ϕ are constant or vary with the orientation of joint plane. The test results reported by various investigators on anisotropic strength of rocks indicate only the variation of $(\sigma_1 - \sigma_3)$ and not the variation of c or ϕ with β.

An experimental programme was executed (Yaji 1984) on cylindrical specimens of plaster of Paris, red sandstone from Kota region of Rajasthan and on pink granite of Guledgudda quarries in Karnataka with different orientations of cut planes. These three materials cover a wide range of compressive strength commonly observed for weak to extremely hard intact rocks. Table 8 provides their physical and engineering properties. This study was conducted with an objective to obtain answers to the

TABLE 8

Physical and Engineering Properties of Rocks used for Joint Studies

Property/Parameter	Material		
	Plaster of Paris	Sandstone	Granite
1. Mass density (kN/m³)	12.25	22.5	26.5
2. Specific Gravity	2.61	2.63	2.69
3. Porosity (per cent)	60	12	<1
4. Uniaxial Compressive Strength σ_c (MN/m²)	9.5	70	123
5. Tensile Strength (MN/m²)	2.6	7.8	14.7
6. Tangent Modulus E_t (GPa)	1.0	5.1	10.8
7. Cohesion Intercept (MN/m²)	2.17	14.0	25.5
8. Angle of Friction (ϕ)°	40.5	44.0	46.5
9. Deere and Miller (1966) Classification	EL	CL	BL

following aspects:

1. Does failure always take place by sliding along the plane of weakness? Could it be that fracture takes place across the weak plane for some orientations?

2. How should one account for the variation of σ_c, c and ϕ with the orientation of weak plane?

3. How does the roughness along the joints alter the values of σ_c, c and ϕ?

Studies on the three materials mentioned above revealed some interesting findings which are covered under various subheads in the following.

Study on Planar Joints

This study is significantly different from the previous studies conducted on joints by Patton (1966), Ladanyi and Archambault (1971), Barton (1973), Barton and Choubey (1976) and Schneider (1976) wherein direct shear tests were carried out on joint planes and failure was by sliding over the joint plane or by shearing of the asperities. Also, the mode of failure was influenced by the material strength and stress level.

In the present investigation plaster of Paris specimens were cast to have the joint plane at desired orientation using matching metal castings to obtain joint planes within the permissible limits of tolerance. For sandstone and granite, the specimens were cut along the desired inclinations and lapped to the specifications of ISRM to match the joint. Unconfined compression and triaxial tests conducted on these three materials revealed the following:

1. The modes of failure of specimens with planar joint under different confining pressures are summarised in Table 9. It is very clearly brought out that failure occurs predominetly by sliding for values of β ranging from about 30°– 60°. For other rangers of β, the failure pattern changes from vertical splitting to shearing across the joint plane, ignoring the presence of joint to propagate sliding. Splitting and slabbing are observed at lower confining pressure ranges which changed to shear failure across the joint plane at higher σ_3. Therefore, it is concluded that the mode of failure is a function of both β and σ_3.

2. σ_{cj} of specimens with horizontal or vertical joints was about 80 per cent of the σ_c of the intact rock.

3. The unconfined compressive strength was minimum when β was between 30° — 45°.

4. The variation of σ_{cj} from $\beta = 0°$ to $\beta = 90°$ can be represented by a polynomial (Fig. 15) of the second order, namely

$$\sigma_{cj} = A\beta^2 + B\beta + C \qquad \ldots (20)$$

The constants A, B and C are given in Table 10.

TABLE 9

Modes of Failure in Planar Joint Specimens

Confining Pressure	Mode of failure				
	Intact	Joint inclination range			
		0—15°	30—60°	75—90°	90°
Low ($\sigma_3 \simeq 0$)	Vertical splitting and local shearing, violent failure	Vertical splitting and local shearing	Sliding on preformed joint plane	Tensile splitting	Longitudinal slabbing
Medium ($\sigma_3 <$ 5 percent of intact σ_c)	Tensile splitting combined with shearing	Spalling tensile and/shear combinations	Mostly sliding	Tensile splitting accompanying fracture	Mostly tensile splitting
High $\sigma_3 \simeq$ 10 per cent of intact σ_c	Fracturing along a shear plane inclined at about $(45+\phi/2)$ to the horizontal	Shearing across the joint plane ; Joint is ignored.	Sliding with local shear	Shearing across the joint and no influence of joint plane	Tensile fracturing and shearing across the joint plane

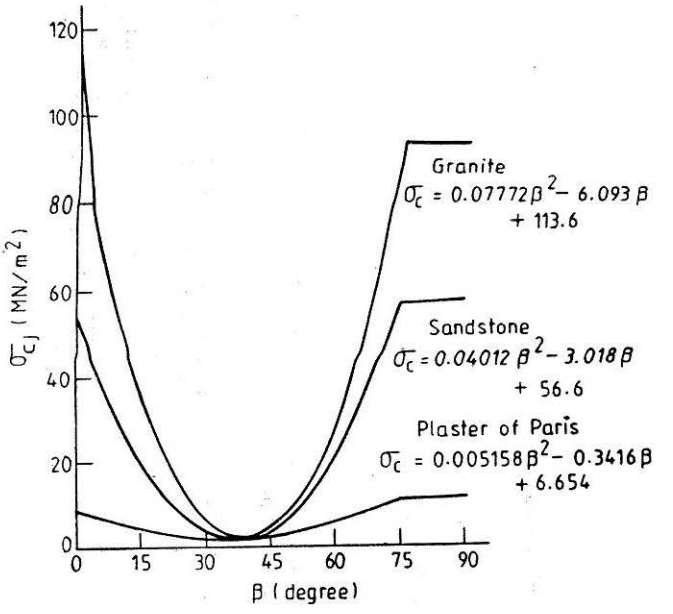

FIGURE 15 Variation of σ_{cj} with Orientation of Planar Joint

TABLE 10

Values of Constants *A*, *B* and *C* for Estimating σ_{cj}

Materials	Values of Constants		
	A	*B*	*C*
Plaster of Paris	0.005158	−0.3416	6.654
Sandstone	0.04012	−3.018	56.60
Granite	0.07772	−6.093	113.60

Figure 16 shows the variation of the ratio of σ_{cj} to σ_c with β. The trends of variation are similar except that a weaker material like plaster of Paris shows greater minimum value in the region of β from 30°—45°.

5. Results of triaxial shear tests revealed that cohesion also varies with β as was observed in the case of σ_{cj}. This variation could be conveniently represented by a polynomial of the second degree (Eq. 20). Figure 17 shows the variation of *c* and its representation by an expression. The values of constants *A*, *B* and *C* are not the same as in the case of σ_{cj}. These constants vary linearly on a semi-log plot and the lines representing these variations are nearly parallel to each other, and therefore, can be represented by the

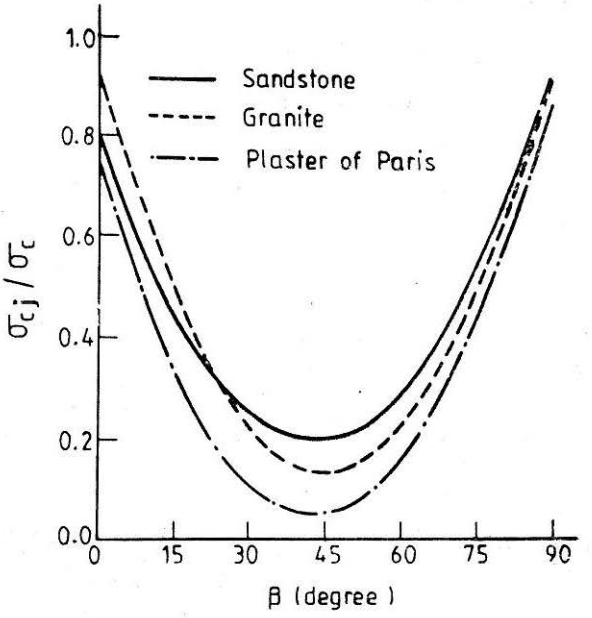

FIGURE 16 Variation of σ_{cj}/σ_c with Orientation of Planar Joint

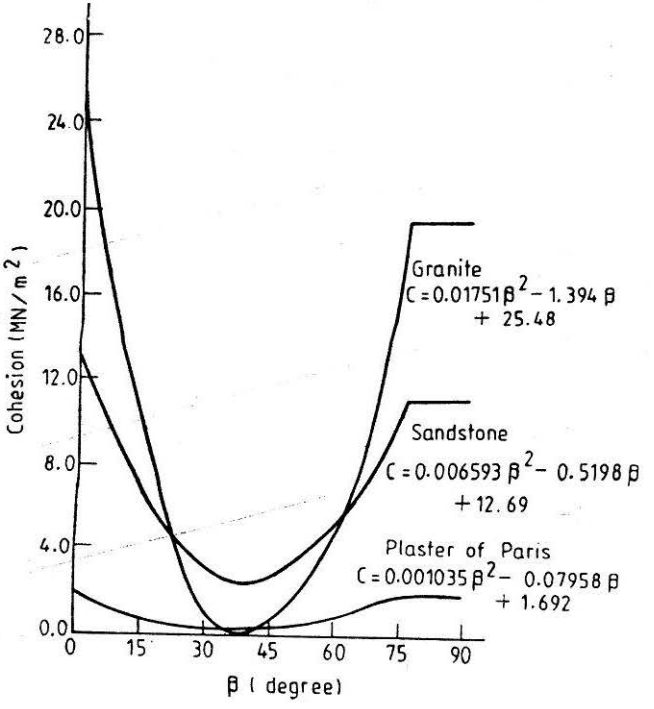

FIGURE 17 Variation of Cohesion with Orientation of Planar Joint

following expressions :

$$A = \exp\,[(\sigma_c - A')/\lambda]$$

$$B = -\exp\,[(\sigma_c - B')/\lambda]$$

$$C = \exp\,[(\sigma_c - C')/\lambda] \qquad \ldots (21)$$

The values of A', B', C' and λ are included in Fig. 18. For known values of σ_c of intact rock, as it appears, one could estimate the constants and evaluate the values of c along planar joint. This study has clearly brought out that the variation of cohesion, c along planar joints cannot be ignored. Therefore, the cohesion in Jaeger—Cook equation (Eq. 18) cannot be assumed to be constant. It also implies that with the rotation of principal stress directions, the cohesion along the joint plane must also be considered accordingly. The variation of the ratio of cohesion of planar joint to that of the inact specimen with β is shown in Fig. 19. Here again the weak rock-like material suggests greater reduction in cohesion compared to stronger rocks.

6. The varation of friction angle, ϕ with β for all the three materials is small. For plaster of Paris, the variation is between 39.6° to 42.4° for values of $\beta = 0°$ to 90° and also for the range of confining pressures adopted. In the case of sandstone, these values of ϕ fall between 42.4° and 45.5°, and for granite between 40.5° and 46.5°. As such, the variation in the values of ϕ for the three materials having distinct unconfined compressive strengths is

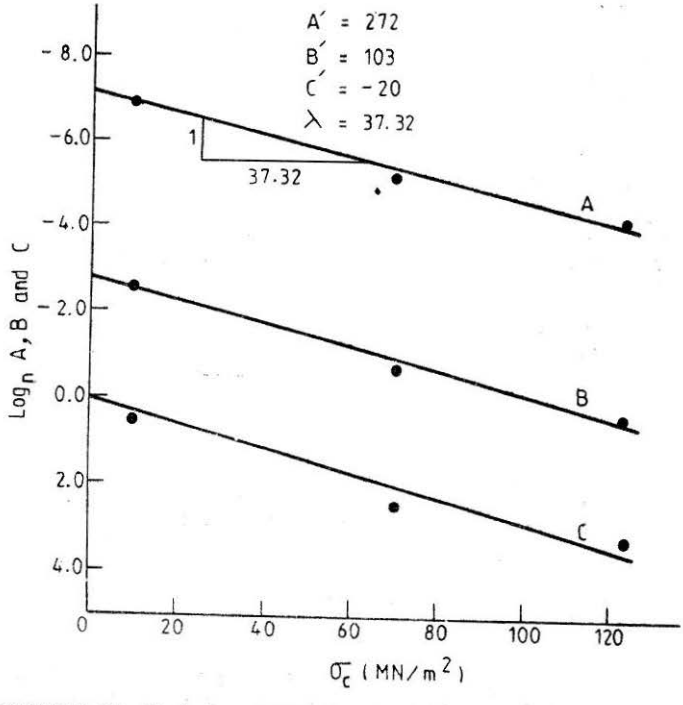

FIGURE 18 Variation of Cohesion Coefficients A, B and C with σ_c

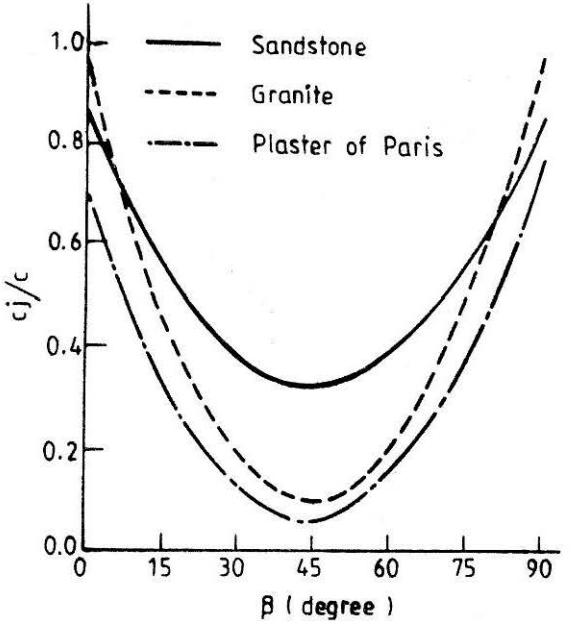

FIGURE 19 Variation of c_j/c with Orientation of Planar Joints

indeed small. Therefore, the values of ϕ to be adopted with rotation of principal stress directions could be considered to be constant over the range of β.

Study on Rough Joints

More than 30 different types of step-shaped and berm-shaped joints were produced in cylindrical specimens of plaster of Paris, with varying number of steps or berms along the length of different inclinations of β. These specimens were tested in unconfined compression and triaxial states. Some of the interesting findings are summarized below :

1. Roughness produces interlocking effect along the joint planes. Greater the roughness greater is the interlocking effect. Consequenly, longitudinal spilitting at lower confining pressures and clear well defined shear failure across the joint plane were observed.

2. Increase of roughness results in higher σ_{cj} approaching the strength of intact specimen.

3. Figure 20 for different roughnesses produced along the joint planes inclined at $\beta = 45°$ or $60°$ suggests that the ratio of cohesion of joint specimen (c_j) to that of intact specimen (c) increases with roughness. The roughness is defined as the ratio of amplitude of the protrusion on the joint surface to the joint length. When the roughness is almost equal to zero, this ratio of cohesion values also becomes nearly zero as suggested by tests on planar joints in plaster of Paris for similar values of β.

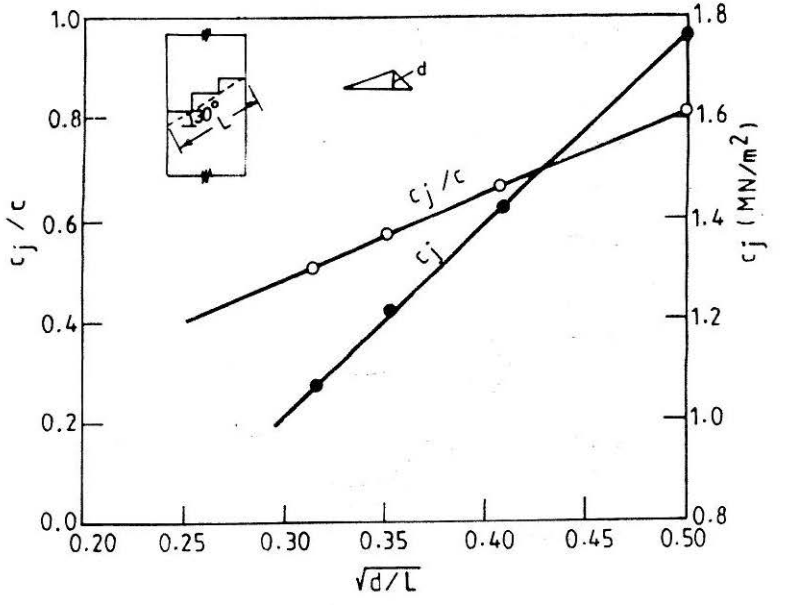

FIGURE 20 Variation of Cohesion with Amplitude of Protrusion for Stepped Shaped Joint ($\beta = 60°$)

4. The value of friction angle did not change irrespective of the type of rough joints and its inclination and was close to that of an intact and a planar joint specimen.

5. Contrary to what has been observed in the case of planar joints rough joints indicate increase of c_j/c up to a maximum value of 0.72 when $\beta = 45°$, due to the high degree of interlocking. A similar trend of higher values of σ_{cj} at $\beta = 45°$ was also observed. From Mohr-Coulomb criterion, the uniaxial compressive strength σ_c of intact rock can be expressed as

$$\sigma_c = \frac{2\,c\cos\phi}{1-\sin\phi}$$

$$i.e.\ \frac{\sigma_c}{c} = \frac{2\cos\phi}{1-\sin\phi} \qquad \ldots(22)$$

Most rocks which are coarse grained, massive, crystalline or arenaceous and having similar values of friction angle will have similar σ_c/c ratios. For all the three materials, ϕ varies from 40.5° to 46.5°, the ratio σ_c/c varies from 4.4 to 5.0. For most rocks when ϕ varies from 25 to 45°, this ratio may range from 3 to 5. One very interesting observation from the study of various joints of these three materials is that the values of ratio σ_c/c or σ_{cj}/c_j essentially lie between 4 and 5. Planar joints exhibited lower ratios.

From the above findings it is obvious that whenever rotation of

principal stress directions takes place, the following may be expected :

(*i*) The corresponding changes in σ_c and c may have to be appropriately considered ;

(*ii*) Further, whenever first order protrusions on the joint planes do not interfere *i.e.* the gouge material is thick enough, one would expect considerable reduction in c with the rotation of principal stresses as was observed in the case of planar joints ;

(*iii*) If the protrusions on the joint plane interfere and produce interlocking as is the case often with closed joints, the variation in c with the rotation of principal stresses may not be significant for consideration ;

(*iv*) Even the values of Modulus number, K, and modulus exponent n, of Janbu's (1965) expression relating initial tangent modulus (E_i) with confining pressure σ_3 also undergo considerable change with the rotation of principal stresses ;

(*v*) The value of K attains a minimum and the value of n attains a maximum in planar joints for $\beta = 45°$. The variation in K is similar to that of c in planar joints.

(*vi*) The variation of friction angle with the rotation of principal stresses may not be significant, more so, with rough joints.

Influence of Number and Location of Joints

For plaster of Paris representing weak rock, the variation of number of horizontal joints per meter length (J_n joint frequency) with the ratio of unaixial strenghts of joint and intact specimens under unconfined compression has been presented in Fig. 21. The ratio of moduli of jointed specimen to that of the intact specimen is also included in this figure. The reduction of strength is observed to be lower than the modulus values with joint frequency. When there are 10 joints/m, the reduction in strength is only 10 per cent, whereas for 100 joints/m the corresponding reduction is 50 per cent. On the other hand, the reduction in modulus is about 70 per cent for 100 joints/m.

The location of a single joint with respect to the loading surface defined by $d_j = D_j/B$ (ratio of depth of joint D_j, to the width or diameter, B, of the loaded area) greatly influences the strength of rock, Fig. 22. When the joint is located very close to the loading face, the strength of jointed rock is about 50 per cent of the intact value. Its effect is as important as the presence of 100 joints/m uniformly spaced. With the location of the joint away from the loading face, the strength of joint rock increases and attains a value, the same as that of the intact rock when the joint is located at about 1.2 B or beyond below the loading face. The ratio of moduli of joint to intact specimens with the variation of the location of joint is also shown in the Fig. 22. The modulus of the joint rock is higher than that of the intact rock so long as the joint is within the depth equal to the width the loaded areas. In fact, the stiffness of the rock is highest when the joint is close to the loading face contrary to what has been observed for strength. Influence of the location of a joint on the

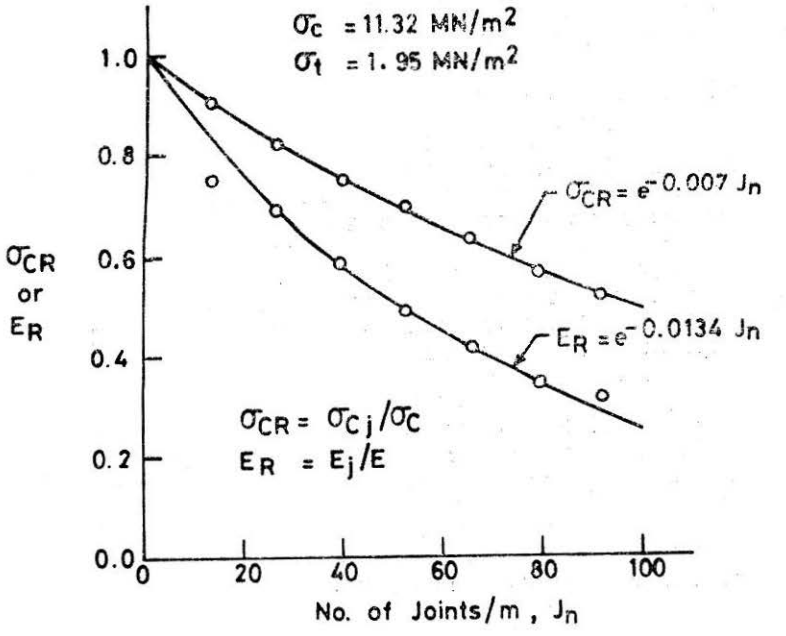

FIGURE 21 Variation of Strength and Modulus with Joint Frequency for Plaster of Paris

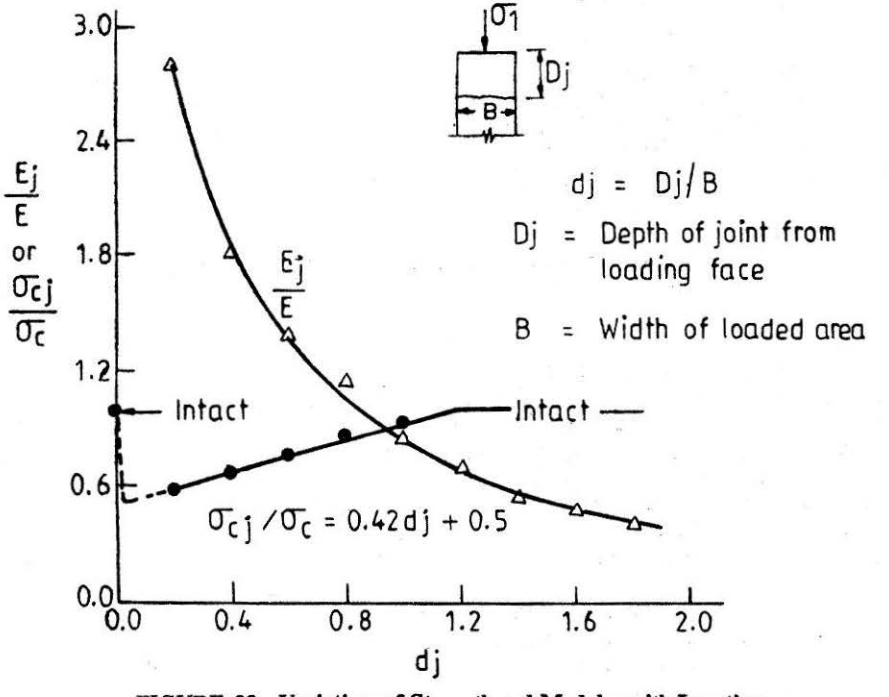

FIGURE 22 Variation of Strength and Modulus with Location of Single Joint ($\beta = 0$) for Plaster of Paris

stiffness continues to decrease even upto a depth twice the width of the loaded area.

Investigations are in progress to know how far this behaviour is also observed in different rocks. The influence of orientation, number of joints and the effect of confinement on the response of different rocks are being studied.

From Fig. 23, one also notes that the influence of anisotropy fast deteriorates for values of σ_c/σ_3 less than 5. When $\sigma_c/\sigma_3 = 1$, in most weak rocks, it appears that only about 10 per cent of strength anisotropy may be observed. For practical purposes one may assume that the effect of anisotropy may not be significant when the insitu hydrostatic stress is the same as the unconfined compressive strength of intact rock in the case of well defined jointed rock mass.

Modulus of Rock Mass

Bieniawski (1978), based on the data collected from field tests, suggested an empirical relation for the estimation of modulus of elasticity (E_m) of the rock mass (in GPa) as

$$E_m = 2\,\text{RMR} - 100 \qquad \ldots(23)$$

This equation suggests that when RMR value is 50, the modulus of rock mass is almost negligible. Even loose soils exhibit values of modulus greater than zero. Test results of Yaji (1984) on smooth and rough joint planes and the data provided in Fig. 21 on the reduction of modulus with number of joints one would expect E_m/E to be greater than zero, (where E_m = modulus of rock mass and E = modulus of intact rock, both the values are in unconfined state). If the joint inclinations are essentially falling between 30° to 45° (with the vertical or major principal stress) E_m/E may be close to zero. But when the joint inclinations are nearly horizontal, E_m/E could as well be equal to about 0.2. This is suggested by some field results reported by Bieniawski. Therefore, one may suggest the following relationships for practical use :

(*i*) For predominantly horizontal joints

$$E_m/E = \exp\,(0.0217\,\text{RMR} - 2.17) \qquad \ldots(24)$$

(*ii*) For predominantly inclined joints, inclined at 30° to 45° to vertical

$$E_m/E = \exp\,(0.0564\,\text{RMR} - 5.64) \qquad \ldots(25)$$

STABILITY OF ROCK SLOPES

Stability of sloping ground has attracted considerable attention of geotechnical engineers during the past few decades due to the importance of controlling and preventing landslides, design and construction of road and railway embankments and cuttings, earth and rockfill dams, open excavations for foundations of dams and open pit mines. Cuts made for roads and railways are sometimes difficult and perpetually problematic. The cost of solving the slope problem connected with mining can be of great economic consideration. A few million tons of extra waste would have to be mined as a result of an average slope being reduced by 3 to 5

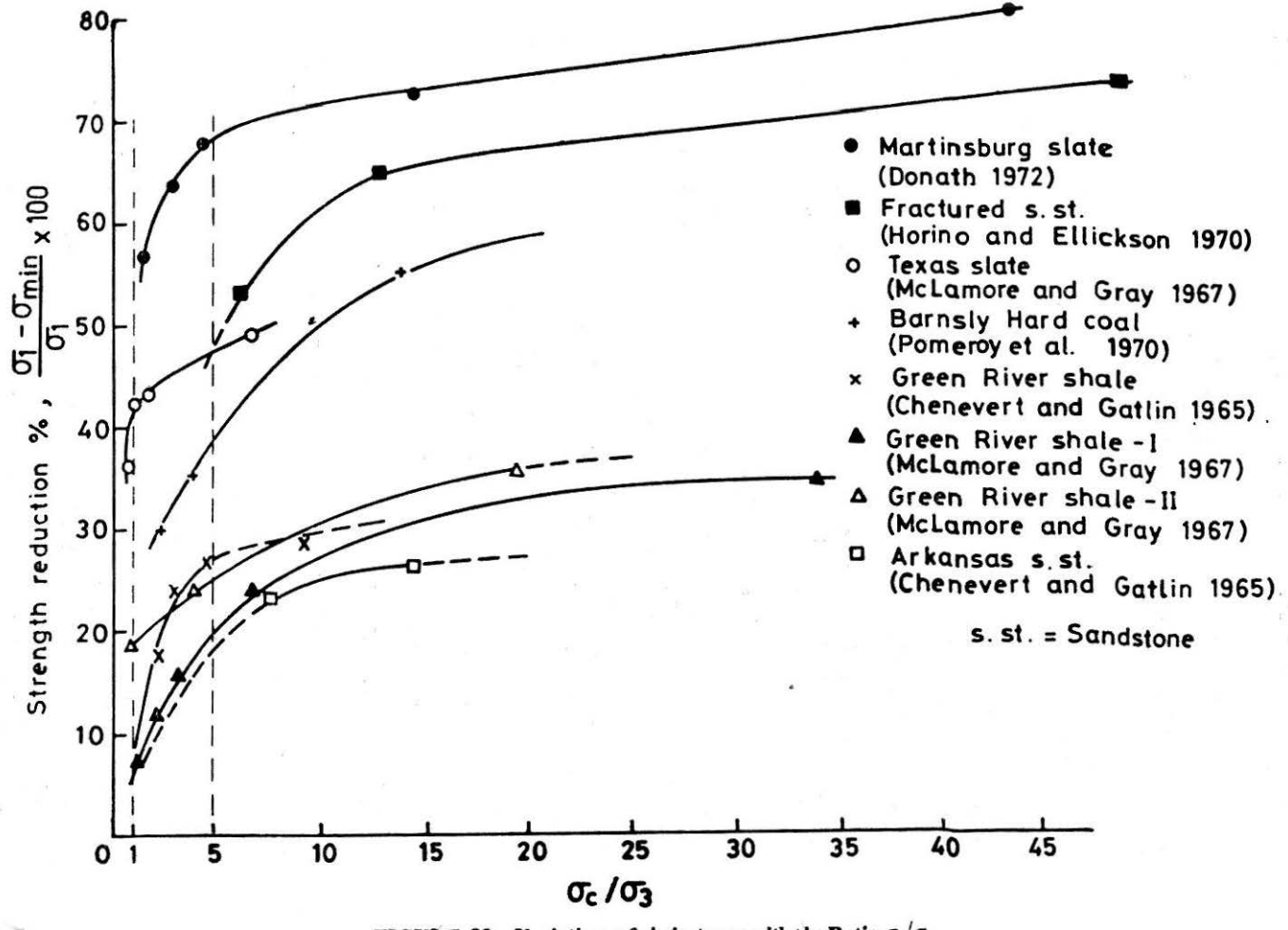

FIGURE 23 Variation of Anisotropy with the Ratio σ_c/σ_3

degrees in an open pit of about 400×400×150 m deep. Unlike soil slopes, rock slope stability is essentially governed by the joint sets, their relative orientation, the gouge material present in the joints and on the extent of excavation with respect to joint spacing. The mode of failure is primarily controlled by them.

Modes of Failure

The modes of failure of rock mass are either circular, planar, wedge or toppling types, (Hoek and Bray 1977).

(*i*) *Circular mode* :— When the sterographic representation of the joints by *pi* diagram does not indicate any well defined planes of orientation one would expect rotational failure of rock mass along a curved surface; more often along a circular surface and mass movement takes place into the excavation. Such failures are expected in heavily fractured rock mass, more so when the joint material is clayey or when the joint faces are decomposed and also in coal tips and rockfills.

(*ii*) *Planar mode* :— When a joint set is highly ordered, represented by a single pole concentration, the mode of failure is planar with the mass moving into the excavation, when the face of excavation is same or inclined to the strike direction of the joint plane. If the face of excavation is in the dip direction, failure by sliding along the joint plane will not result.

(*iii*) *Wedge mode* :— When two or more pole concentrations are exhibited representing intersecting planes, wedge failure is likely to take place with the translatory movement of the rock mass in the form of a tetrahedron when the line of intersection of the planes of sliding daylights into the excavation.

(*iv*) *Toppling mode* :—When the pole concentration lies on the opposite side of the face of excavation, failure by toppling of blocks of rock may take place particularly in steeply dipping column and sheet like rock mass structures.

Some of the rock slopes could remain almost at 45° for heights upto 200 *m* (Hoek 1970), essentially due to high degree of interlocking and roughness along the joint planes. More often, rock slopes have been found to be flatter than 45° when the degree of interlocking is low and the material along the joints has weathered.

Analysis of rotational type of failure of soil and rock slopes along circular or curved surface has drawn considerable attention over the years.

Rotational Approach

Even though the earliest work on stability analysis was carried out by Coulomb (1773) and Collin (1846), significant contributions were largely due to the classical methods developed by Swedish engineers during the period 1915 to 1925. Swedish slip-circle method of slices for rotational slides developed by Fellenius (1927, 1936) has been the most widely used conventional technique for numerous practical problems. Among other

significant contributions in this area are the works of Taylor (1948), Sokolovsky (1960), Janbu (1954), Bishop (1955), Morgenstern and Price (1965), Chugaev (1966) and Spencer (1967, 1968, 1969).

Bishop's (1955) slip circle analysis formed the basis for further research in the stability analysis of slopes. This method is rigorous in its content satisfying both force and moment equilibrium conditions and also considered the presence of inter-slice forces. To circumvent the rather lengthy and involved tedious numerical computations Bishop simplified the original expression by assuming the direction of the interslice forces to be horizontal. The minimum factor of safety obtained by this method is a close approximation to the final value obtained by using the rigorous method. This implied that the of factor safety is insensitive to the distribution of internal forces. This analysis did not justify why an expression to obtain factor of safety not satisfying one of the basic conditions of equilibrium should yield a solution close to the critical equilibrium state.

Morgenstern and Price (1965) suggested a method of analysing a slope using a general slip surface satisfying both force and moment equilibrium conditions and could consider slope sections with varying shear strength parameters and pore pressures. The analysis is based on the principles of limit equilibrium and need *a priori* assumption of the shape of the potential sliding mass as well as the distribution of internal forces. This method and the slip-circle method of Bishop gave similar values of factor suggesting insensitiveness of the factor to the varying distributions of internal forces within the potential sliding mass.

In Table 11, a comparison of some approaches has been made in terms of total and effective stress (Wolfskill and Lambe 1967) from the analysis of the failed slope of Siburua dam.

An alternative method of analysis for circular and logarithmic spiral slip surfaces based on Bishop's approach was presented by Spencer (1967, 1968, 1969). It was observed that a reasonably reliable value of minimum factor of safety can be obtained by assuming the inter-slice forces to be parallel. For lower angles of inclination of the inter-slice forces the factor

TABLE 11

Factors of Safety from Different Approaches

Method	Factor of safety	
	Total Stress	Effective Stress
Rigid free body	0.77	1.00
Slip circle with slices	0.80	0.83
Bishop's simplified	0.80	0.97
Morgenstern & Price	0.96	1.00

of safety is found to be rather insensitive and supported the implications of Bishop's simplified approach.

A detailed study of the approaches referred in the foregoing paragraphs brings forth some of the following shortcomings:

(*i*) None of the analyses illustrate absolute minimum factor of safety of a slope under a given situation,

(*ii*) Their inability is in locating the real critical slip surface,

(*iii*) Being a statically indeterminate problem the assumption of the potential slip surface and internal stress distribution is a must; often circular slip surface is assumed, to know the directions of normal forces on the slip surface and to eliminate moments about the centre of rotation.

Though the assumption of a circular slip surface makes the analysis simpler it lacks physical validity; more often, non-circular slip surfaces have been observed even in soils (Cooling and Golder 1942, Hutchinson 1961, Legget 1962, and Skempton 1964). Therefore, circular slip surface analyses are generally accepted for practical problems as an approximate solution in the stability analysis. The analyses do not justify that the surface obtained leads to an absolute minimum. An analysis with ill-conditioned assumptions should lead to misleading results.

Variational Approach

In order to eliminate the shortcomings of the slip circle method with interslice forces, a rigorous mathematical technique was adopted in the calculus of variations for the analysis of the stability of slopes in terms of effective stresses (Narayan, Bhatkar, Ramamurthy 1976, 1978, 1982, Ramamurthy, Narayan, Bhatkar 1977, Ramamurthy 1984). The slope stability problem was posed as a minimization problem in the calculus of variation (Goldstein 1969) wherein, the stress distribution function was determined to minimize the factor of safety satisfying all equilibrium and boundary conditions and also the Mohr-Coulmb failure criterion was not violated anywhere along the slip surface.

The stability equations are obtained based on limiting equilibrium conditions considering the influence of effective interslice forces. This approach requires no *a priori* assumption regarding

(*i*) the shape of the slip surface,

(*ii*) the internal stress distribution, and

(*iii*) the point of application of horizontal effective thrust line.

Two methods have been developed for obtaining the solution by this apprach, namely,

(*i*) Indirect method (non-local variation)

(*ii*) Direct method (Raleigh-Ritz technique).

By adopting the limit equilibrium method of analysis, the stability equations of any slope in general are obtained by considering the critical state of equilibrium of the various forces acting over an infinitesimal slice situated within the potential sliding mass. Figure 24 shows a section through a slope with a general slip surface and a and b as the boundaries defined by a (x_a, y_a) and b (x_b, y_b) on the slope section. The given slope is represented by any known function $y = y_o(x)$, i.e. DABC in the figure and the potential sliding surface by $y = y(x)$ with a and b as its boundary points on the slope. Functions $y = y_t(x)$ and $y = y_t'(x)$ define the line of action of total and effective horizontal thrust lines respectively. The elemental sliding surface is represented by 1234. Figure 25 shows the various forces acting on the elemental slice and the force polygon of these forces.

The stability equations framed under the limit equilibrium conditions (Ramamurthy, Narayan and Bhatkar 1977) reduce to minimization problem in the calculus of variations. The problem is to find a critical slip surface $y^o(x)$ and shear mobilizing factor function $f^o(x)$ which minimizes an appropriately defined factor of safety.

The overall factor of safety (F_s) along the slip surface and average factor of safety (F_v) along the interslice boundary were written as:

$$F_s = \frac{\int_{x_a}^{x_b} \Big[a_1 (1+y_1'^2) + a_3 \Big(a_2 (y_0 - y_1)(1-h) - y_1' \Big[y_2 \Big\{ y_0' - y_1' - \tfrac{1}{2} a_2 a_3 \{ h' (y_0-y_1)^2 + 2h (y_0-y_1)^2 + 2h (y_0-y_1)(y_0' - y_1') \} \Big\} + y_2' \{ a_2 (y_0-y_1) - \tfrac{1}{2} a_2 a_3 h (y_0-y_1)^2 \} \Big] \Big) \Big] dx}{\int_{x_a}^{x_b} \Big[a_2 (y_0-y_1) y_1' (1-h) + \frac{1}{F_v} [(1+a_3 y_2) \Big\{ a_1 (y_0' - y_1') - \tfrac{1}{2} a_2 a_3 \Big(h' (y_0-y_1)^2 + 2h (y_0-y_1)(y_0' - y_1') \Big) \Big\} + y_2' \{ a_1 (y_0-y_1) - \tfrac{1}{2} a_2 a_3 h (y_0-y_1)^2 \} a_3] y_1' \Big] dx} \quad \ldots(26)$$

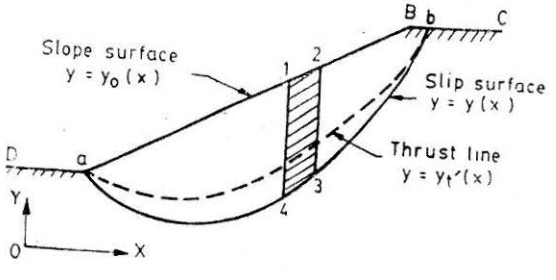

FIGURE 24 Sliding Mass considered in Variational Method

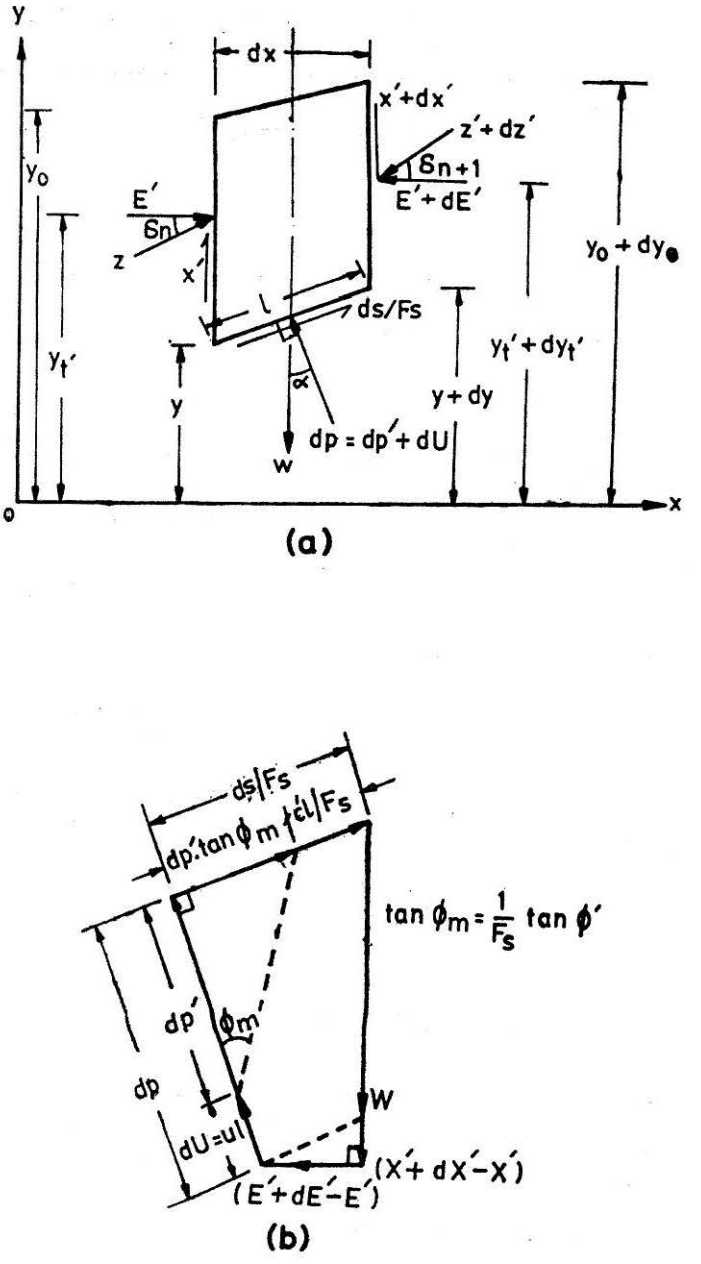

FIGURE 25 (a) Forces on a Slice, (b) Force Polygon

$$F_v = \frac{\int_{x_a}^{x_b} \left[\left(a_1 (y_0 - y_1) - \frac{1}{2} a_2 a_3 h (y_0 - y_1)^2 \right) (1 + a_3 y_2) \right] dx}{\int_{x_a}^{x_b} \left[\left(a_1 (y_0 - y_1) - \frac{1}{2} a_2 a_3 h (y_0 - y_1)^2 \right) (y_1' - y_2) \right] dx} \quad \ldots (27)$$

where

$$a_1 = c',\ a_2 = \gamma,\ a_3 = \tan \phi',\ h(x) = r_u,\ h'(x) = r_u',$$

$$y_1(x) = y(x),\ y_1'(x) = y'(x),\ y_2(x) = f(x) \text{ and}$$

$$y_2'(x) = f'(x).$$

The minimization of the functional of the form $J(y_i)$ given by Eq. 26 can be obtained by using either indirect method or direct method in the calculus of variation. The indirect method was described in detail by Narayan, Bhatkar and Ramamurthy (1976). The direct method (Ramamurthy, Narayan and Bhatakar 1977) is very briefly presented herein for completeness and used to develop slope stability charts.

Direct Method of Minimization

Using the well known Raleigh-Ritz technique (Gelfand and Fomin 1963), the overall factor of safety has been minimized. The method of local variations (Chernovs'ko 1965) could also be adopted. In Ritz method the functional $J[y_1\ y_2]$ defining F_s (Eq. 26) was not considered along arbitrary admissible functions $y_1(x)$ and $y_2(x)$ but along all possible linear combinations.

$$y_1(x) = \sum_{i=1}^{m} a_i \psi_i(x) \quad \ldots (28)$$

$$y_2(x) = \sum_{j=1}^{n} b_j \psi_j(x) \quad \ldots (29)$$

where a_i and b_j are unknown functions and ψ_i and ψ_j are the prescribed functions of the independent variable x. The functions ψ_i and ψ_j are referred to as basis or interpolation functions. The interpolation functions chosen so as to satisfy the given boundary conditions,

$$y_1(x_a) = y_a\ ;\quad y_1(x_b) = y_b \quad \ldots (30)$$

and

$$y_2(x_b) = -\frac{1}{a_3};\ y_2'(x_b) = -\frac{F_v}{a_3} \quad \ldots (31)$$

identically.

Substituting Eqs. 28 and 29 in Eq. 26, the functional $J[y_1, y_2]$ becomes a function $F(a_i, b_j)$ of $(n+m)$ unknown constants. The problem of minimizing $F(a_i, b_j)$ with respect to a_i and b_j is essentially a mathematical programming problem. The coefficients (a_i^0, b_j^0) are determined from the following equation:

$$\frac{\partial F}{\partial a_i^0} = 0 \text{ and } \frac{\partial F}{\partial b_j^0} = 0 \qquad \ldots(32)$$

Equation 32 results in $(n+m)$ simultaneous algebraic equations, solutions of which yield a_i^0 and b_j^0. The minimizing functions y_1^0 and y_2^0 are obtained from the following expressions :

$$y_1^0(x) = \sum_{i=1}^{m} a_i^0 \psi_i(x) \qquad \ldots(33)$$

$$y_2^0(x) = \sum_{j=1}^{n} b_j^0 \psi_j(x) \qquad \ldots(34)$$

Considering a homogeneous slope section and representing the surface of slope and slip surface by fourth degree polynomials and using the above referred equation, numerical results were used to develop stability charts one each for $r_u = 0$, 0.2, 0.3 and 0.4 and presented in Figs. 26 to 29. From the rigorous indirect method it was observed that the slip surface could be represented by a fourth degree polynomial without sacrificing overall absolute minimum factor of safety. These charts are convenient to ascertain the stability of slopes when the material and slope geometry parameters are known.

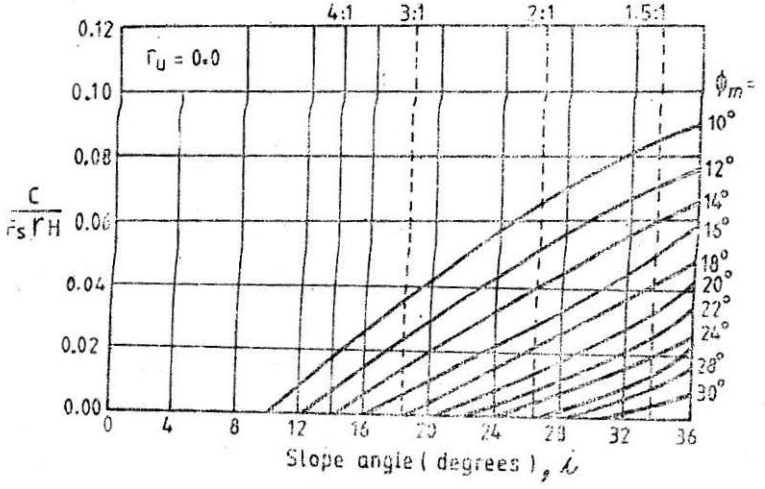

FIGURE 26 Slope Stability Chart for $r_u = 0$

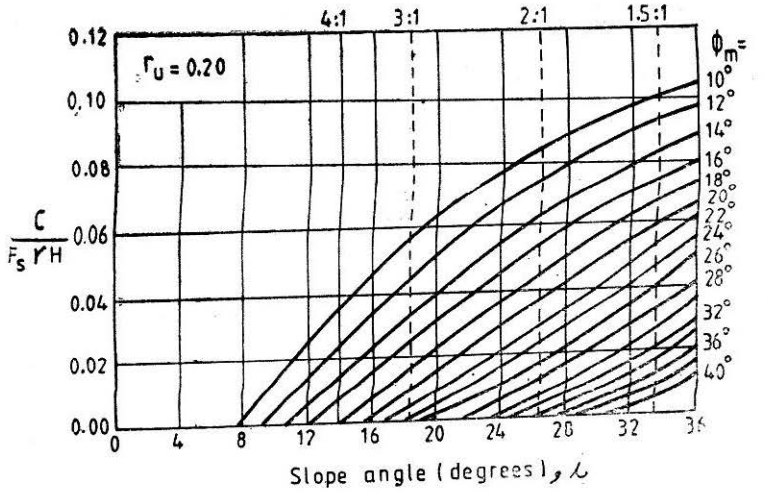

FIGURE 27 Slope Stability Chart for $r_u = 0.2$

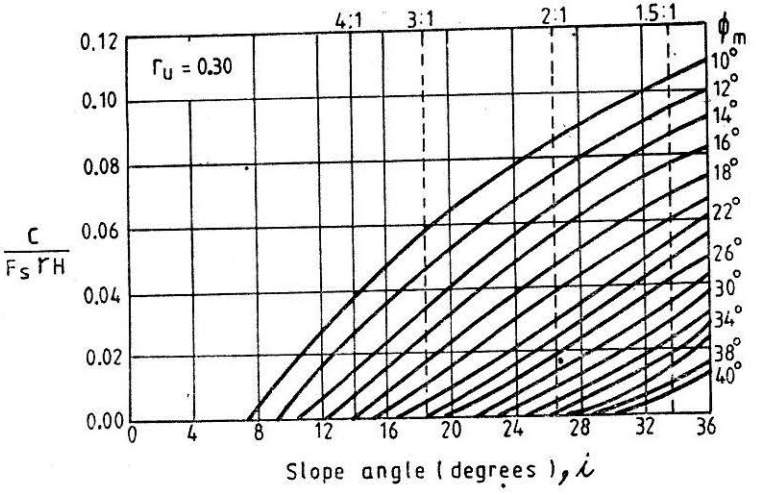

FIGURE 28 Slope Stability Chart for $r_u = 0.3$

The results obtained by the variational method showed variation from those obtained by Spencer (1967). Table 12 shows comparison of factors of safety for a typical case both from direct and indirect methods with that obtained by the procedure suggested by Spencer with the following properties :

Slope angle 26.2°, 30 m height having 30 m crest width, $c'/\gamma H = 0.02$, $\gamma = 1.92 g/cm^3$, $r_u = 0.5$, $\phi' = 40°$.

A definite gain of about 5 per cent in the overall factor of safety along the slip surface is suggested by the variational approach. The critical slip surface associated with the minimum factor of safety obtained by

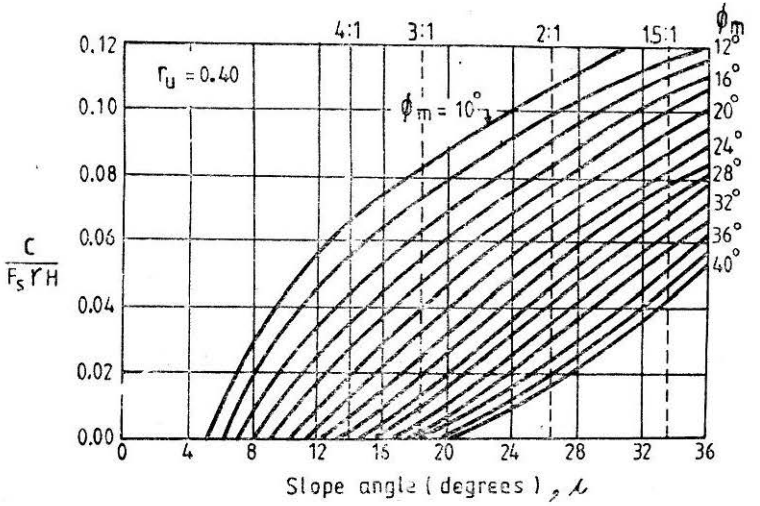

FIGURE 29 Slope Stability Chart for $r_u = 0.4$

variational method considerably deviates from the critical slip circle obtained by conventional approaches. The variational method suggests that any assumption of internal stress distribution within the potential sliding mass may lead to ill-conditioned functions resulting in mis-interpretation of numerical results. The assumed function for internal stress distribution must satisfy all equilibrium and boundary conditions and also the conditions for minimum factor of safety and critical slip surface. The normal stress distribution along the potential sliding surface is related to the critical slip surface. A typical normal stress (σ_n') distribution along a critical slip surface is shown in Fig. 30. The variation of effective inter-slice force, E', along the critical slip surface is shown in Fig. 31. Though the existing methods of analysis yield results which are meaningful by assuming some normal stress distribution, the results themselves do not necessarily refer to the absolute minimum. The factor of safety, slip surface, normal stress distribution, internal stress distribution and the position of horizontal effective thrust line are

TABLE 12

Comparison of Factors of Safety

Method		F_s	F_v	Percentage difference in F_s
Slip-circle analysis Spencer (1967)		1.070	—	—
Variational Method	Direct	1.126	1.454	5.25
	Indirect	1.124	1.451	5.0

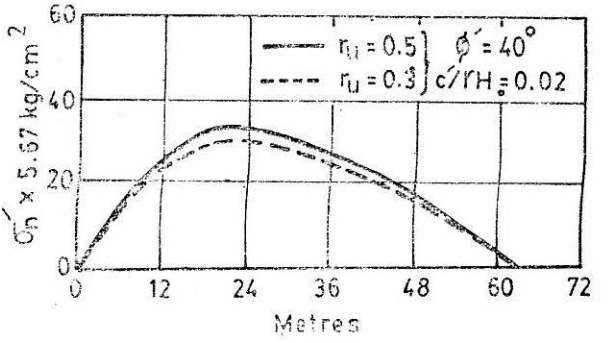

FIGURE 30 ***Variation of Effective Normal Stress along the Slip Surface***

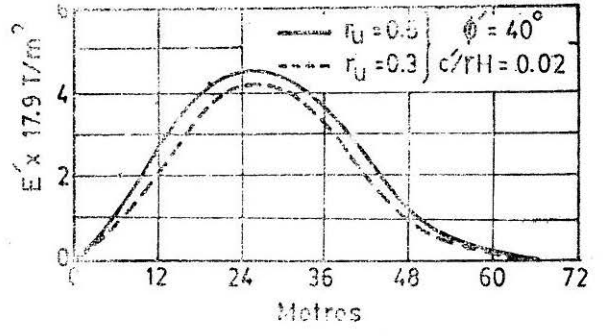

FIGURE 31 Variation of Effective Interslice Force along the Slip Surface

largely influenced by the pore pressure developed along the potential sliding mass.

The slip surfaces obtained by the direct and indirect variational methods lie very close to each other. The slip surface obtained by the variational method has a varying curvature and has its apex towards the lower boundary showing flatter curvature towards the upper portion. It is also interesting to note that the shape of the slip surface closely resembled the shape of slip surface observed for slide in Siburua dam (Wolfskill and Lambe 1967).

By estimating c and ϕ of the rock mass after generating its strength envelope as per Eq. 17 and knowing seepage conditions in the slope in terms of pore pressure (r_u), one could use the stability charts to estimate the factor of safety of a slope.

Stability charts from Finite Element Analysis

Since limit equilibrium methods do not distinguish whether a slope has been formed due to excavation or by construction (Brown and King 1966), the effect of insitu stresses does not figure in this analysis and tension analysis cannot be carried out, a finite element analysis was carried out on cut slopes to develop stability charts for ready use by the designers.

Elasto-plastic analysis of the rock slopes was carried out using elasto-visco-plastic algorithm taking time as a fictitious parameter (Zienkiewicz and Cormeau 1974) in plane strain. The Mohr-Coulomb failure criterion and also Hoek-Brown criterion were used separately to estimate plastic strains.

Seventy six 8-noded parabolic isoparametric elements with 265 nodes have been used for discretization. Due to symmetry, only half of the excavation was considered for the analysis as shown in Fig. 32. The bottom boundary was fixed at a depth of 3 times the depth of the slope from the crest level whereas the side boundary was fixed at 6 times the depth of excavation. The displacements in the horizontal direction at the lateral boundary and also along the central line of excavation were restrained. The bottom boundary was also considered as fully restrained.

The excavation process was simulated in a single step by applying stresses equal and opposite to the insitu stresses on the excavated boundary making the surface stress free. These applied stresses are calculated and converted to equivalent nodal loads. The equivalent nodal loads are given by

$$\{R_e\} = \int_v [B]^T \{\sigma_o\}\, dv \qquad \ldots(35)$$

where

$[B]$ = strain displacement matrix,

$\{\sigma_o\}$ = initial stress vector, and

dv = elementary volume.

The element stiffness was calculated and assembled once for all. Knowing the assembled stiffness matrix, the unknown displacements were calculated. Strains and subsequently, stresses were determined from these displacements using the strain-displacement matrix and elasticity matrix. The yielding Gauss points were identified by comparing the stress level at every Gauss point with reference to the equivalent linear strength envelope given by the equation

$$s = \frac{1}{F}(c_i + \sigma_n \tan \phi_i) \qquad \ldots(36)$$

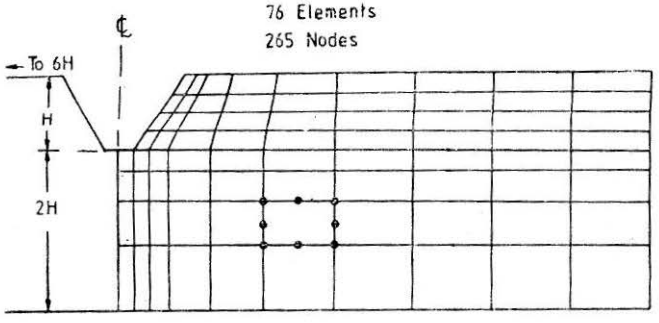

FIGURE 32 Finite Element Discretization

where F is the strength reduction factor or trial value of factor of safety, σ_n is the normal stress and c_i and ϕ_i are the instantaneous cohesion and the angle of friction resistance. The excess shear stress was then converted to equivalent nodal loads and this whole process was repeated until convergence took place Then the excess shear stress is released and redistributed among the neighbouring points in the continuum. The slope was assumed to collapse when the excess shear stress was of such a magnitude that its release and redistribution caused the stress levels of the neighbouring points to exceed their shearing strengths. In this way the failure progressed from one point to another in the continuum which was indicated by lack of convergence with increasing displacement.

The failure was estimated by drawing a curve between the assumed values of factor of safety and the corresponding displacement of a point (preferably the most effected point in the continum). In Fig. 33 the straight line protions of the curve are extended to give point F which decided the factor of safety. A typical development of yielding zones with increase of trial factor of safety is shown in Fig. 34.

For developing stability charts for ready use by the designer, a parametric study was carried out. It was observed that

(*i*) the Young's modulus (E) effects only the magnitude of the displacements and not the factor of safety;

(*ii*) the Poisson's ratio (ν) within the range of 0.15 to 0.35 did not influence the factor of safety; and

(*iii*) the effect of stress ratio (K_o) was insignificant on factor of safety.

The combined effect of c, γ, H and ϕ was considered by introducing a non-dimensional factor $\lambda_{c\phi} = \gamma H \tan \phi/c$ (Janbu 1954). It was observed that nearly same values of $\lambda_{c\phi}$ were obtained for the same factor of safety and same slope angle. Similarly stability number (Taylor 1948) $S_n = (c/F\gamma H)$

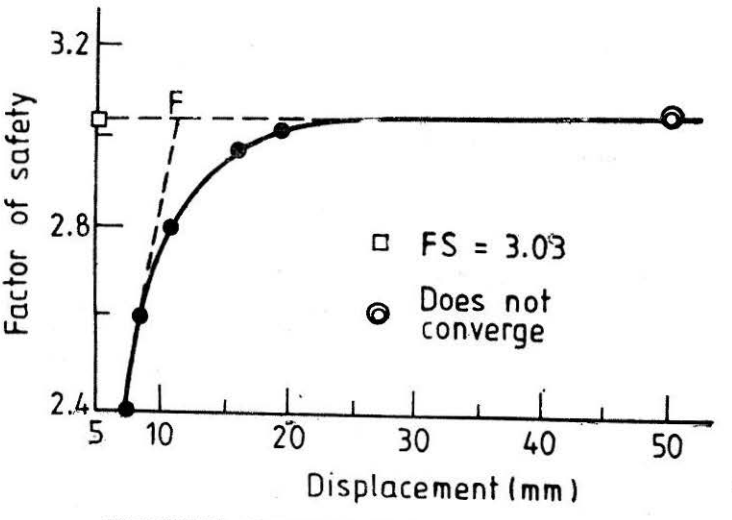

FIGURE 33 Criterion for Defining Factor of Safety

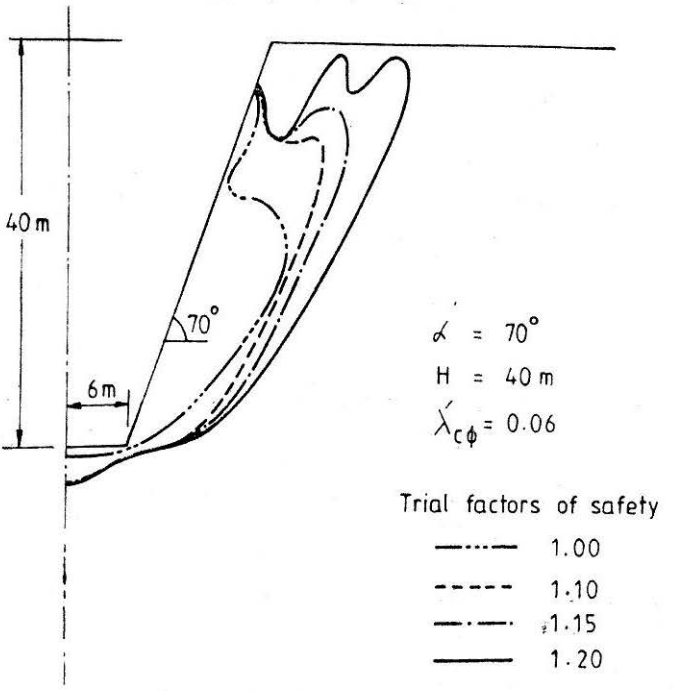

FIGURE 34 Development of Yielding Zone with Factor of Safety

was determined. Figure 35 shows the relationship between S_n and $1/\lambda_{c\phi}$ (using finite element method) for different values of slope angle, i, (Sharma, Ramamurthy and Ailawadi 1984). In this figure the stability number as per Hoek-Bray charts (1977) are also included. The stability numbers as per limit equilibrium method (LEM) obtained by Hoek—Bray charts are higher than from the finite element method (FEM) suggesting underestimation of factor of safety by the former method. For a 90° rock slope, Hoek-Bray charts underestimate factor of safety by about 38 per cent. As the slope angle of cut slopes in rock decreases, the difference in factors of safety from both the approaches decreases. A better appreciation of the comparison of factors of safety obtained by Hoek-Bray charts and finite element approach can be made from Fig. 36.

Using m and s parameters of Hoek-Brown criterion on a similar basis as shown in the foregoing for finite element analysis, stability chart for a dry/drained cut rock slope has been developed (Ramamurthy, Sharma and Ailawadi 1985, Ailawadi 1985). Non-dimensional parameters $\lambda_{ms} = \frac{\sigma_c s}{\gamma H m}$ and stability number, $S'_n = \frac{\sigma_c s^{1/2}}{\gamma H F^{3/2}}$ have been developed to form the stability chart linked through slope angle, i, Fig 37. For limit equilibrium approach adopting Bishop's simplified method (1955) similar stability chart was developed and superimposed on that obtained from the finite element method in Fig. 37. This figure provides a ready comparison of limit equilibrium and finite element methods. The limit equilibrium method may either underestimate or overestimate depending upon the

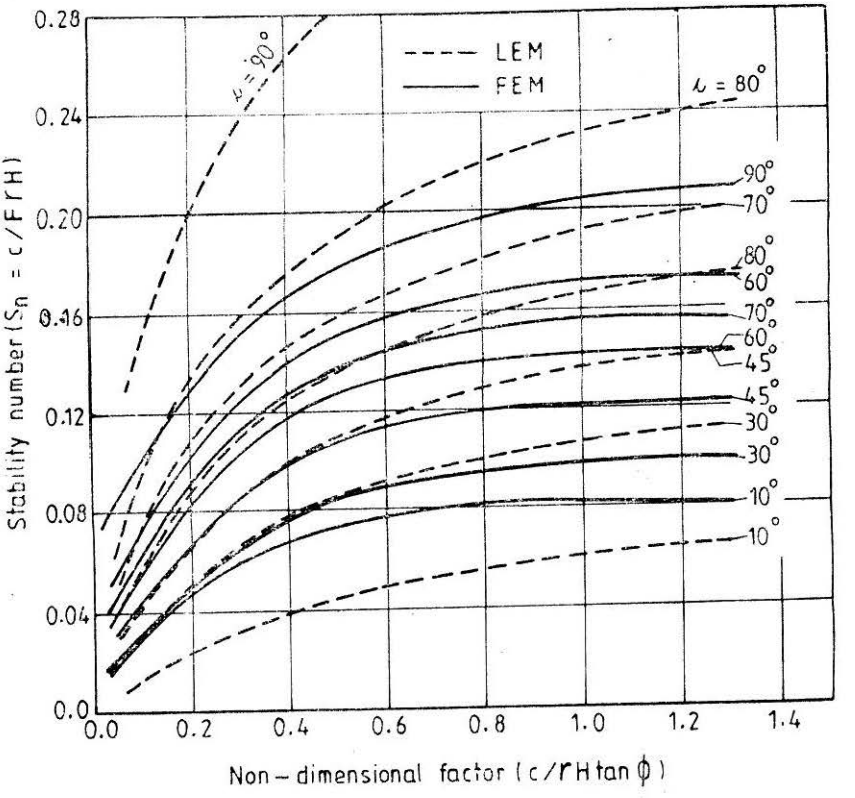

FIGURE 35 Combined Stability Chart by LEM and FEM

slope angle and λ_{ms} value. For a 90° slope with $\lambda_{ms} = 0.001$, the limit equilibrium method underestimates the factor of safety by as much as 50 per cent. For a slope of 45° and $\lambda_{ms} = 0.001$, this method overestimates the factor of safety by 41 per cent when compared to that given by finite element method. For cases with the combination of i and λ_{ms}, both the methods suggest similar factors of safety.

A designer will find it quite convenient to use these charts to try various alternatives by choosing any of the methods of analyses i.e. finite element or limit equilibrium methods adopting any failure criterion developed either from Mohr-Coulomb (Eq. 17) or Griffith (Eq. 8) approaches i.e. either using c and ϕ or m and s parameters of rock mass.

The primary objective of preparing Figs. 26 to 29, and 35 and 37 was to bring the rigorous and extensively computer oriented analyes within the reach of the designer.

STABILITY OF SQUEEZING GROUND

For the design of support system for tunnels in rock mass, estimation of rock pressures on the supports for any allowed deformation of both the rock mass and the supports is an important consideration for the

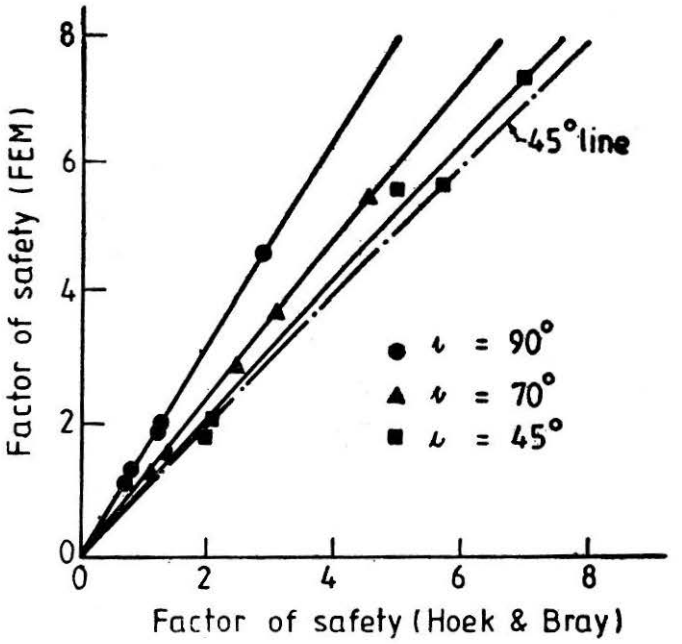

FIGURE 36 Comparison of Factors of Safety from FEM and Hoek-Bray Method (1977)

stability of the tunnel. More often, the magnitude of rock load is estimated based on the qualitative description of the rock mass (Terzaghi 1946). In such cases deformations produced on the tunnel walls do not figure. Such an analysis to predict rock loads is empirical, solely based on experience gained from the study of designs and some of their failures under specific conditions. This approach in course of time lead to the development of rock mass classification to aid estimation of rock loads.

Rock Mass Classifications

The most popular rock mass classifications for the estimation of rock loads are :

(*i*) Terzaghi's approach (1946), extensively used in India and the USA with steel support system,

(*ii*) Lauffer's (1958) concept of stand up time, emerging from Stini's work (1950),

(*iii*) Deere's (1964) classification introducing rock quality index (RQD) to borelog data and incorporating as such in the classifications developed later on,

(*iv*) Bieniawski's (1973) rock mass rating (RMR) varying from 0 to 100 and taking into consideration of Deere's RQD, strength of intact rock, extent of weathering, joint spacing, their separation and continuity, ground water flow conditions and orientation of attitudes of joints—an approach attracting considerable attention,

(*v*) Barton, Lien and Lunde (1974) defining the quality of rock mass (*Q*) in terms of RQD, joint number, joint roughness, joint

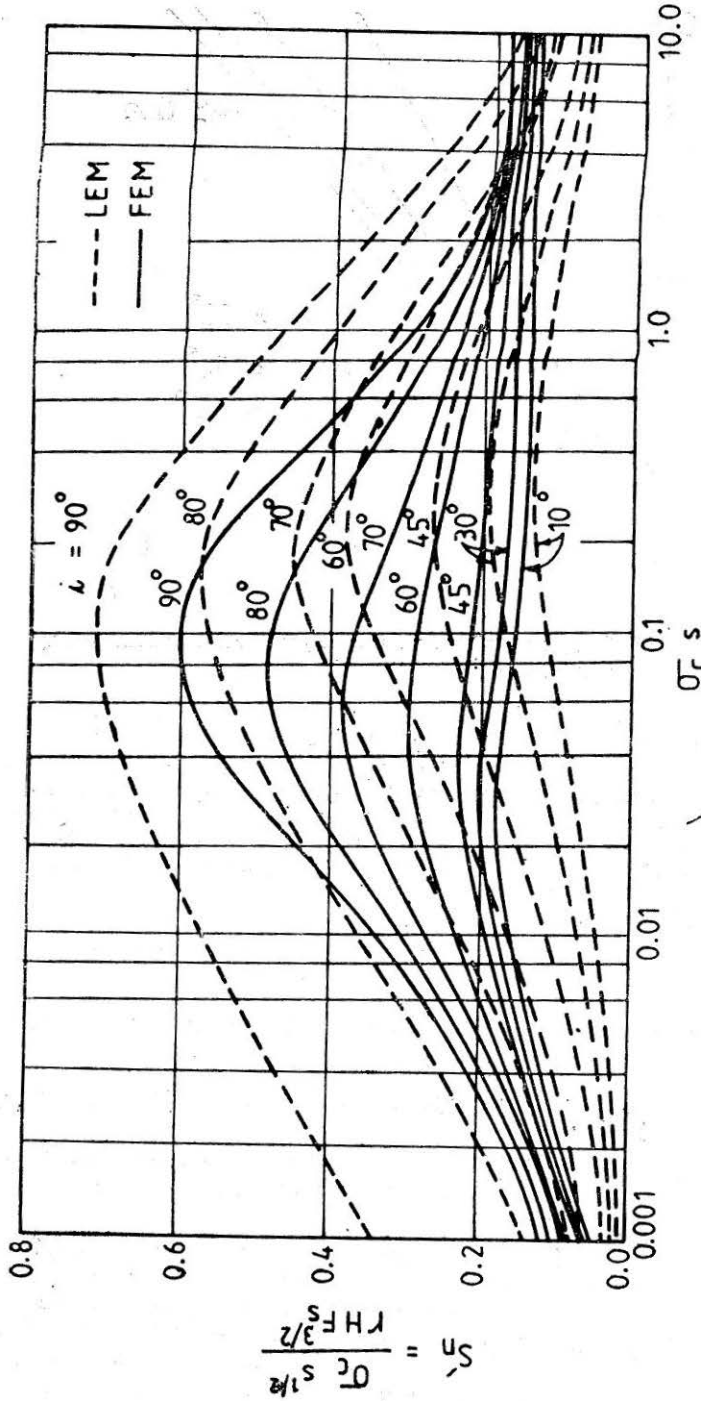

FIGURE 37 Slope Stability Chart by LEM and FEM using m and s Values

alteration, joint water condition and stress reduction factor with the range of rating varying from 0.001 to 1000.

New Austrian Tunnelling Method (Rabcewicz 1965, 1969) is essentially a design-construct-modify approach falling into the category of observational approach. Instrumentation, observation and monitoring of tunnel behaviour during construction and modifying suitably the support system is adopted to achieve the desired performance of the tunnel boundaries.

Analytical approaches have been extensively used and verified with the empirical approaches for the estimation of rock pressures and deformations predicted. No theoretical approach is able to consider comprehensively the influence of method of excavation, rigidity of supports in relation to the surrounding mass, time of installation of supports, progress of broken zone around the tunnel, the mechanism of contraction and expansion within this zone, the nature of variation of modulus and strength, in addition to the factors effecting the rock mass performance as indicated by RMR or Q-systems. Because of the complexities involved in characterising the rock mass it is often simplified to arrive at a workable solution. The assumption of a continuum so as to characterise rock mass with average properties has been made for massive unfractured or very heavily fractured rock mass. This assumption of continuum is not valid when well defined joint sets are present. But recently, use of RMR or Q-system of classifying discontinuous rock mass is also being treated as a continuum (Hoek and Brown 1980 as per Eq 8).

Squeezing ground condition results when the rock mass rating is low and the insitu or overburden pressure is high. Upon excavation, the tunnel walls advance slowly without perceptible volume changes due to overstressing of rock mass around the tunnel. Squeezing ground will also be noticed on the advancing face and heaving of invert.

For squeezing ground around circular tunnels, realistic solutions are available from

(*i*) elasto-plastic analysis, and

(*ii*) elasto-strain-softening-plastic analysis.

Elasto-Plastic Analysis

Assuming rock mass to be isotropic, homogenous and semi-infinite, an approximate analysis of the stress around a circualr opening located above water table and subjected to an anisotropic stress field was given by Daemen (1975). The support pressures required at the crown and spring levels can be estimated from the extent of circular broken zone developed around the circular tunnel. Though the broken zone is supposed to develop instantaneously, and no variation of shear strength parameters is supposed to take place, the corresponding displacements cannot be predicted. The rock in the broken zone is supposed to have reached residual stage while the zone beyond broken mass is to respond as per Mohr-Coulomb criterion. For hydrostatic insitu rock stress, the support pressure p_i is given by

$$p_i = [p_o (1-\sin \phi) - c \cos \phi + c_r \cot \phi_r] M_\phi - c_r \cot \phi_r \qquad ...(37)$$

where

p_o = hydrostatic insitu stress equal to the over burden pressure,

ϕ = friction angle of rock mass in the elastic zone, (outside the broken zone)

c = cohesion of rock mass in the elastic zone,

ϕ_r = residual friction angle in the broken zone,

c_r = residual cohesion in the broken zone,

$M_\phi = (a/b)^{\alpha_1}$,

a = radius of tunnel,

b = radius of broken zone, and

$$\alpha_1 = \frac{2 \sin \phi_r}{1 - \sin \phi_r}.$$

Assuming $c_r = 0$ for the broken rock mass, Eq. 37 reduces to

$$p_i = [p_o (1 - \sin \phi) - c \cos \phi] M_\phi \qquad ...(38)$$

The above expression provides only the support pressure without referring to the closure occuring in the tunnel due to squeezing ground condition. In order to generate a ground reaction curve with Eq. 38, Labasse's (1949) expression for estimating radial rock deformation accounting for volume expansion during fracturing is often adopted (Singh 1978, Dube 1979, Jethwa, Dube and Singh 1985). The radial deformation u_i is given as per Labasse (1949)

$$u_i = a - \sqrt{a^2 - (b^2 - a^2)\, k} \qquad ...(39)$$

where

k = coefficient of volumetric expansion of broken rock mass.

For different ratio of b/a, corresponding values of u_i are obtained for the estimation of ground reaction curve. Though Labasse suggested $k = 0.12$—0.15 for soft rocks, but Jethwa, Dube and Singh (1985) suggested much lower values as given in Table 13. Why a soft plastic clay is supposed to have higher volume of expansion than the fractured rock is not understandable ?

The values of c and ϕ for the rock mass are obtained from the known values of RMR as suggested by Bieniawski (1974). These values cannot be considered to be constant irrespective of the confining stress (hydrostatic stress). A better way to estimate c and ϕ would be by using Eq. 17. The residual friction angle may be obtained either from laboratory tests or from published literature. From back analysis, Jethwa, Dube and Singh (1985) provide guidelines for choosing ϕ_r as per Table 14 based on the extent of broken zone, b.

TABLE 13

Suggested Values of k for Different Materials (Jethwa, Dube and Singh 1985)

Rock	k
Highly jointed phyllites	0.003
Soft Sandstones	0.004
Crushed and sheared shales	0.005
Soft plastsic clays	0.01

TABLE 14

Suggested Values of ϕ_r (Jethwa, Dube and Singh 1985)

Radius of broken zone, b / Radius of tunnel, a	ϕ_r
2—4	(ϕ--5°)
4—8	(ϕ—8°)
8—12	(ϕ—10°)

Published literature suggests much lower values of ϕ_r than those given in Table 14. Arenaceous, chemical and other fine grained rocks often show values of ϕ_r less than 15°.

The very fact that the value of ϕ_r decreases with increasing extent of broken zone suggest that residual stage is not reached in the broken mass. The value of friction angle in the broken zone could as well be estimated depending upon the extent of change that has taken place in RMR. The change in RMR in the broken zone should enable estimation of the change in the friction angle as per Eq. 17. The rating of the rock mass has to be estimated only after the excavation is carried out. No data is available to guide the estimation of the change in the rating of rock mass with change in stress field.

The extent of broken zone can be estimated by either

(*i*) assuming $b/a = 3$,

(*ii*) measuring radial closure in the tunnel and using Eq. 39, or

(*iii*) instrumenting the broken zone around the tunnel and measuring the radial displacements at various locations along the radial directions.

Ultimate Rock Pressure

The ultimate rock load which is likely to act on the support system was suggested (Jethwa, Singh and Singh 1984) on the basis of Daeman's

(1975) solution and also considering circular tunnel as a thick cylinder. The ultimate rock load p_{ult}, is given as

$$\frac{p_{ult}}{p_o} = D\ M_\phi\ (1-\sin\phi)\ (1-\frac{\sigma_{cm}}{2p_o}) \qquad \ldots(40)$$

where

σ_{cm} = uniaxial compressive strength of rock mass which can be estimated from Eq. 15,

p_o = hydrostatic stress around the tunnel,

$$D = \frac{(r_c/a)^{\alpha_1} - (a/r_c)^2}{1-(a/r_c)^2}, \qquad \ldots (41)$$

r_c = radius of compacting zone (assumed equal to $0.4b$), and

b = radius of the broken zone.

Other symbols are as defined for Eq. 37.

Equation 40 implies that when the hydrostatic stress field has a value of about half that of the unconfined compressive strength of the rock mass, the ultimate rock load is insignificant. On the contrary, in the case of weak rocks this pressure was found to be about 30 per cent of the overburden while in strong rocks it is about 15 per cent.

This approach is also not adoptable directly to develop ground reaction curve to arrive at the design of suitable support system to absorb radial convergence.

Elasto-strain-softening-plastic Analysis

When a rock mass is excavated for creating a circular tunnel, insitu stress release results in redistribution of stresses on the tunnel walls and in the surrounding mass. Under squeezing ground conditions, radial movements set in resulting in reduction of stresses in the surrounding rock mass. If a support system is introduced, it is supposed to counter the rock load and arrest or permit only desired magnitude of closure. The load transferred to the support is a function of the closure of tunnel allowed and the deformability or adoptability of the support system. Figure 38 explains this ground support interaction. Ground reaction curves for short term and long term basis are represented by AE and AF respectively. Long term load on supports is higher due to creep or deterioration in the surrounding rock mass. If a support has to be placed immediately after the excavation (*i.e.* without any closure), the lining has to be rigid to withstand the load corresponding to OA or corresponding to B or D with increasing flexibility of support on a short term basis. On long term basis this flexible support when placed would have to counter ground reaction corresponding to B' instead of B.

To optimize the support system it is always essential to allow closure of tunnel and erect the support system either rigid as GC or flexible as GD. The support system is best when it is installed either at H with a rigid system or earlier to H with a flexible system, alternatively with a

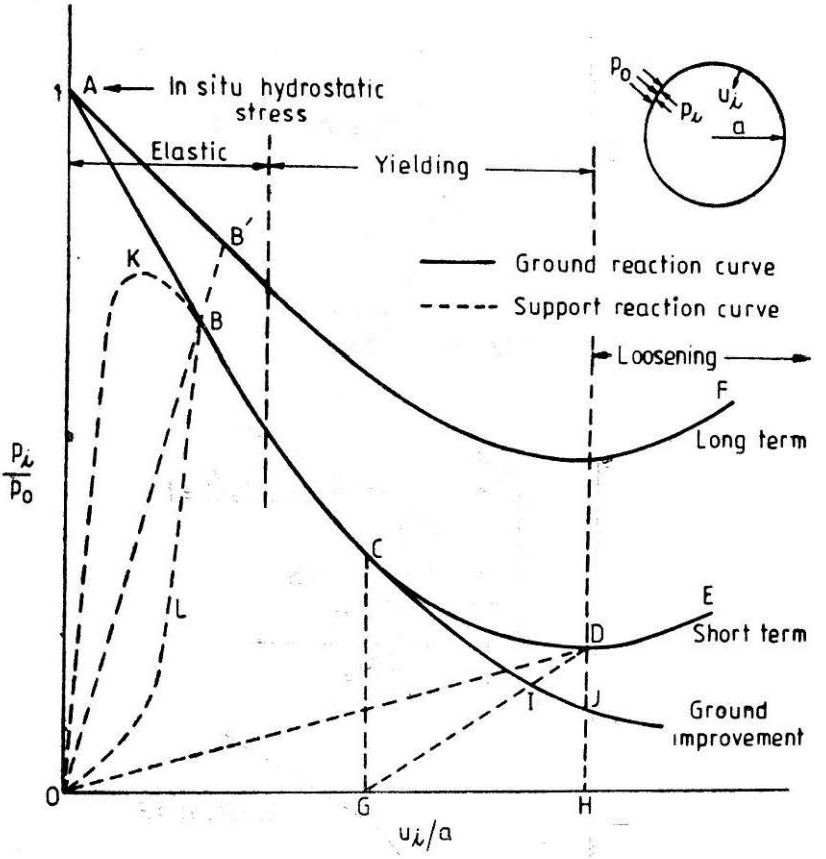

FIGURE 38 Ground Support Reaction Curves

rigid system leaving cushioning behind the lining. If shotcreting or any ground improvement is adopted, the support system will have to withstand lower rock load, may be as given by GI or HJ. The support reaction curve need not necessarily be straight as OB, it could as well follow along OKB in the case of a collapsing support or OLB for a stiffening support.

This convergence confinement approach appears to be the only method of evolving an optimal design for circular tunnels. Brown *et al* (1983) suggested a method for determining the ground convergence utilizing the finite differnce technique to work out the stresses, strains and displacements. Hoek-Brown nonlinear criterion was adopted for the solution of circular tunnel under hydrostatic stress field. The rock material is assumed to respond as an elastic-strain-softening-plastic material having three distinct zones around the tunnel, namely,

(*i*) an elastic zone away from the tunnel,

(*ii*) an intermediate plastic zone in which the stresses and strains respond to strain softening stage, and

(*iii*) an inner plastic zone in which the stresses are limited by the residual strength of rock mass.

This model of rock mass behaviour is presented in Fig. 39.

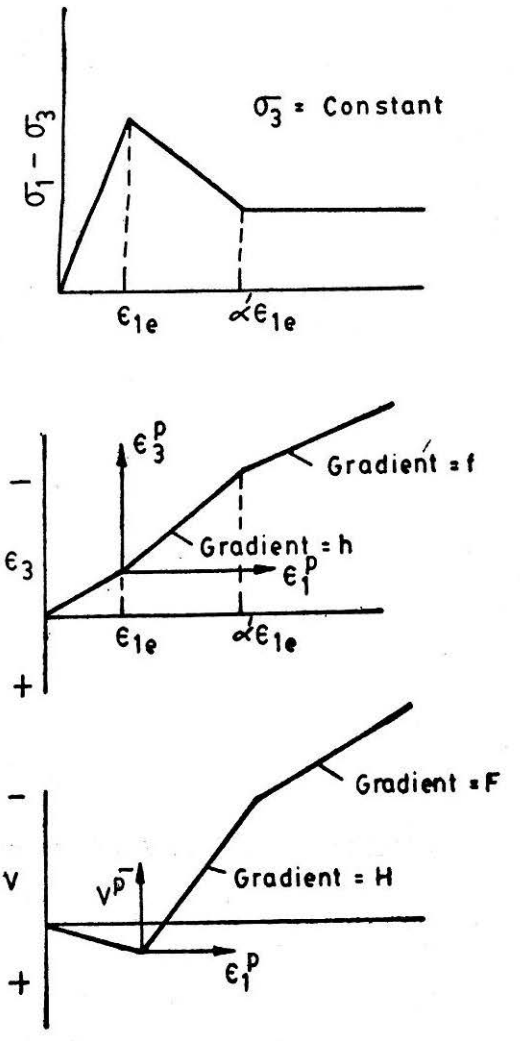

FIGURE 39 Material Behaviour Model used by Brown et al (1983)

The entire zone around the tunnel is assumed to consist of a number of thin concentric annuli. The radii, stresses, and strains at the two surfaces of the annular ring are assumed as

$$r_1,\ \sigma_{r_1},\ \sigma_{\theta_1},\ \epsilon_{r_1},\ \epsilon_{\theta_1} \text{ and } r_2,\ \sigma_{r_2},\ \sigma_{\theta_2},\ \epsilon_{r_2},\ \epsilon_{\theta_2}$$

respectively. If the stresses at one surface and the radii and the strains at both the surfaces are known, the corresponding stresses at the other radius can be determined by using finite difference technique. To start with the radius of the broken zone, the stresses and the strains are determined assuming the material to be elastic-brittle-plastic for which case closed form solution is available. The first ring has one radius as the elasto-plastic boundary and the other within strain softening zone. Utilizing known

values at one radius from the closed form solution, the parameters at the second radius are determined. The procedure is repeated for each annular ring, till the calculated radial stress equals the given internal pressure of the tunnel. Since this happens only at the actual tunnel boundary, all the radii calculated earlier are suitably modified. This gives the radius of yielding zone and the stresses and strains within it.

Brown *et al*'s (1983) method of calculating ground convergence, based on finite difference techniques, has been modified to incorporate integration within the thin annular rings. Comparing the results for particular cases for which closed form solutions are available, it is seen that the modified procedure is more efficient as the iteration cycle converges faster and the results are closer to those obtained from closed form solutions.

The finite difference approximation gives

$$r_2 = r_1 \left[\frac{2\epsilon_{\theta 1} - \epsilon_{r_1} - \epsilon_{r_2}}{2\epsilon_{\theta 2} - \epsilon_{r_1} - \epsilon_{r_2}} \right] \qquad \ldots(42)$$

The exact integration gives

$$r_2 = \frac{r_1}{\left[\frac{(h+1)\,\epsilon_{\theta 2}}{2\,\epsilon_{\theta 1}} - \frac{(h-1)}{2} \right]^{1/(h+1)}} \qquad \ldots(43)$$

Experimental evidence from tests conducted using a stiff testing machine shows that the relationship between axial and radial strains in a failing rock is non-linear. The following relationship has been used for calculating tunnel convergences,

$$\epsilon_3 = -h \,.\, \epsilon_1 \qquad \ldots(44)$$

where $h = h_1 - h_2\left(1 - \frac{\epsilon_{1e}}{\epsilon_1}\right)$,

ϵ_3 = minor principal strain in yielding zone,

ϵ_1 = corresponding major principal strain,

h_1 = constant, equal to initial tangent of ϵ_1 vs. ϵ_3 curve,

h_2 = constant by which amout, the tangent of ϵ_1 vs. ϵ_3 reduces as ϵ_1 goes to infinity, and

ϵ_{1e} = major principal strain corresponding to peak yield strength.

With the modified approach of Brown et al (1983) as suggested by Sharma (1985), a parametric study of various factors affecting ground convergence, radius of broken zone and stress distribution was carried out in order to establish the relative importance of these factors in the design of tunnel. The influence of the following parameters was studied for a range of values of

(*i*) peak strength,

(*ii*) residual strength,

(*iii*) modulus of elasticity,

(*iv*) rate of strain softening; defined by α' as the ratio of principal strain to reach residual strength to the strain required to reach peak strength, and

(*v*) dilation characteristics of rock mass.

The following are some of the salient observations:

(*i*) The convergence curve and the radius of broken zone are marginally influenced by changes in the dilation characteristics of rock mas and ratio of peak strength to residual strength for varying values of residual strength with constant peak strength.

(*ii*) The rate of strain softening as defined by α' has significant influence on ground reaction curve and the radius of broken zone for values of α' less than 3.5. *But, for values of* $\alpha' = 3.5$ to infinity, the influence is negligible. Most fractured rock masses, particularly in the Himalayan region, exihibit a value, of α' greater than 3.5. Therefore, the influence of rate of strain softening from peak to residual stage may not be important, as shown in Fig. 40.

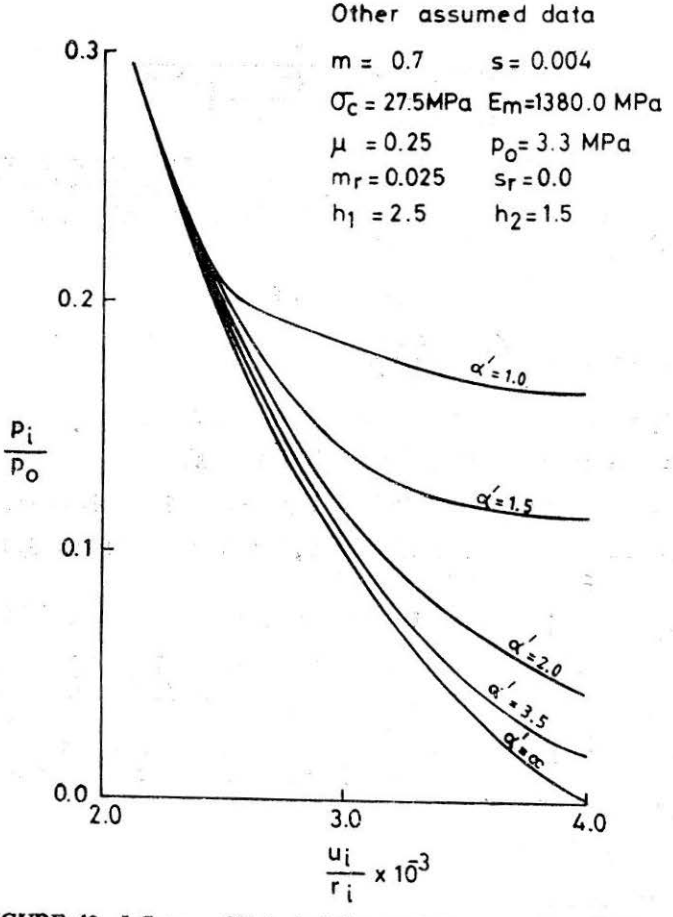

FIGURE 40 Influence of Extent of Ground Softening on Tunnel Closure

(*iii*) The peak strength and modulus of elasticity have pronounced effect on the ground reaction curve and radius of broken zone around the circular tunnel. Figure 41 shows typical strength envelopes in terms of Mohr-Coulomb criterion for uniaxial compressive strength of intact rock of 27.5 MPa. The corresponding values of m and s as per Hoek-Brown criterion are also indicated on these strength envelopes along with rock mass rating values. The analysis revealed (Sharma 1985) that for strong rock masses the ground reaction curve is essentially a straight line (for $m = 3.5$, $s = 0.1$). For weaker rocks it decays exponentially.

Figure 42 suggests that for strong rocks the radius of the broken zone is the same as the radius of the tunnel i.e. no plastic zone is developed. For a weak rock mass with $RMR = 44$ having $m = 0.34$ and $s = 0.0001$, for $p_i/p_o = 0.1$, the radius of broken zone would be about 4 times the radius of the tunnel. Figure 43 shows that the plastic strains are negligible in the case of strong rock mass and the ratio of total radial deformation (due to elastic and plastic strains), u_{it}, increases rapidly in the case of weak rock formations. The variation of closure (u_i/r_i) with rock mass

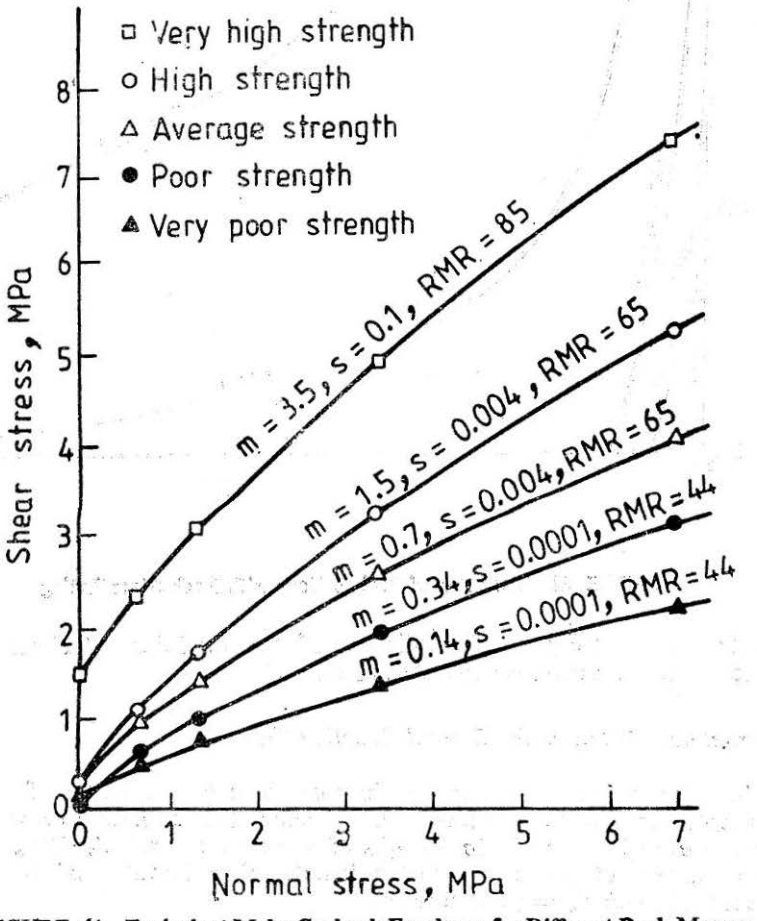

FIGURE 41 Equivalent Mohr-Coulomb Envelopes for Different Rock Masses

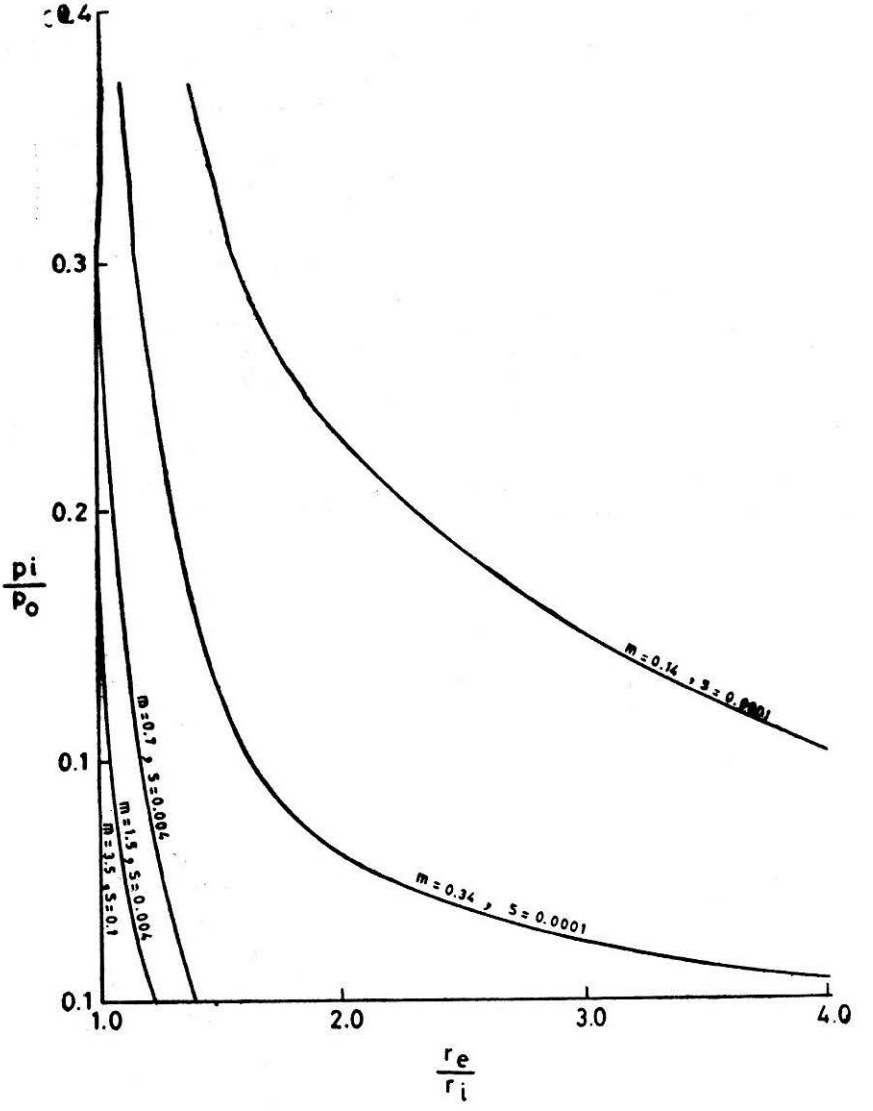

FIGURE 42 Variation of Broken Zone with Rock Mass Rating

rating is shown in Fig. 44. The influence of the modulus of elasticity on the radial deformation is presented in Fig. 45.

Approximate Relation for Ground Reaction Curve

In order to avoid rigorous calcultations as suggested in the foregoing, a simple approximate expression is suggested linking u_i/r_i with p_i/p_o through σ_c of intact rock, $(\sigma_1 - \sigma_3)_m$ of rock mass and $J_n\ E/K_n$, where J_n = number of joints per meter length, E = modulus of elasticity of intact rock, and K_n = joint stiffness.

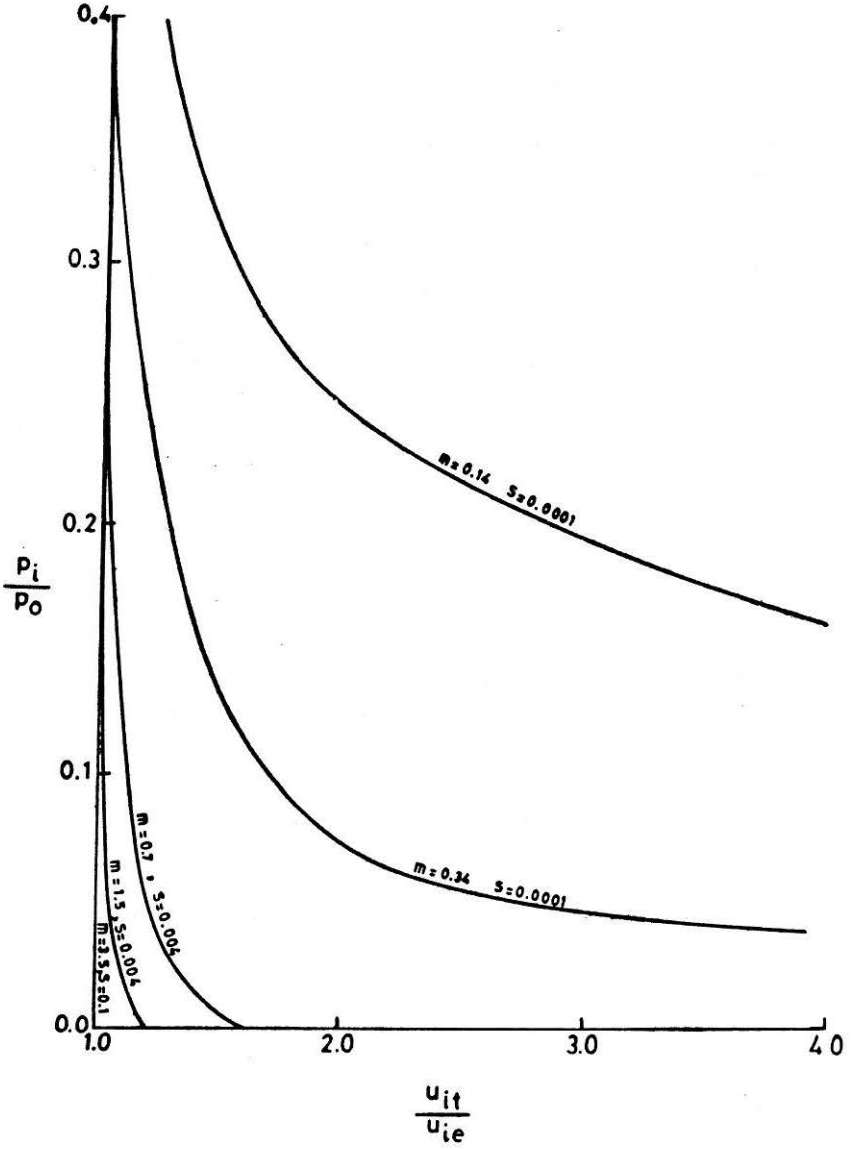

FIGURE 43 Influence of RMR on Elastic and Plastic Components of Closure

From theoretical analysis (Singh 1973), $J_n\, E/K_n = \left(\frac{E}{E_m} - 1\right)$.

This relationship is given as

$$(u_i/r_i)\ 10^{-3} = 1 + \frac{0.0525\ J\ R_1}{(p_i/p_o)^{R_2}} \qquad \ldots(45)$$

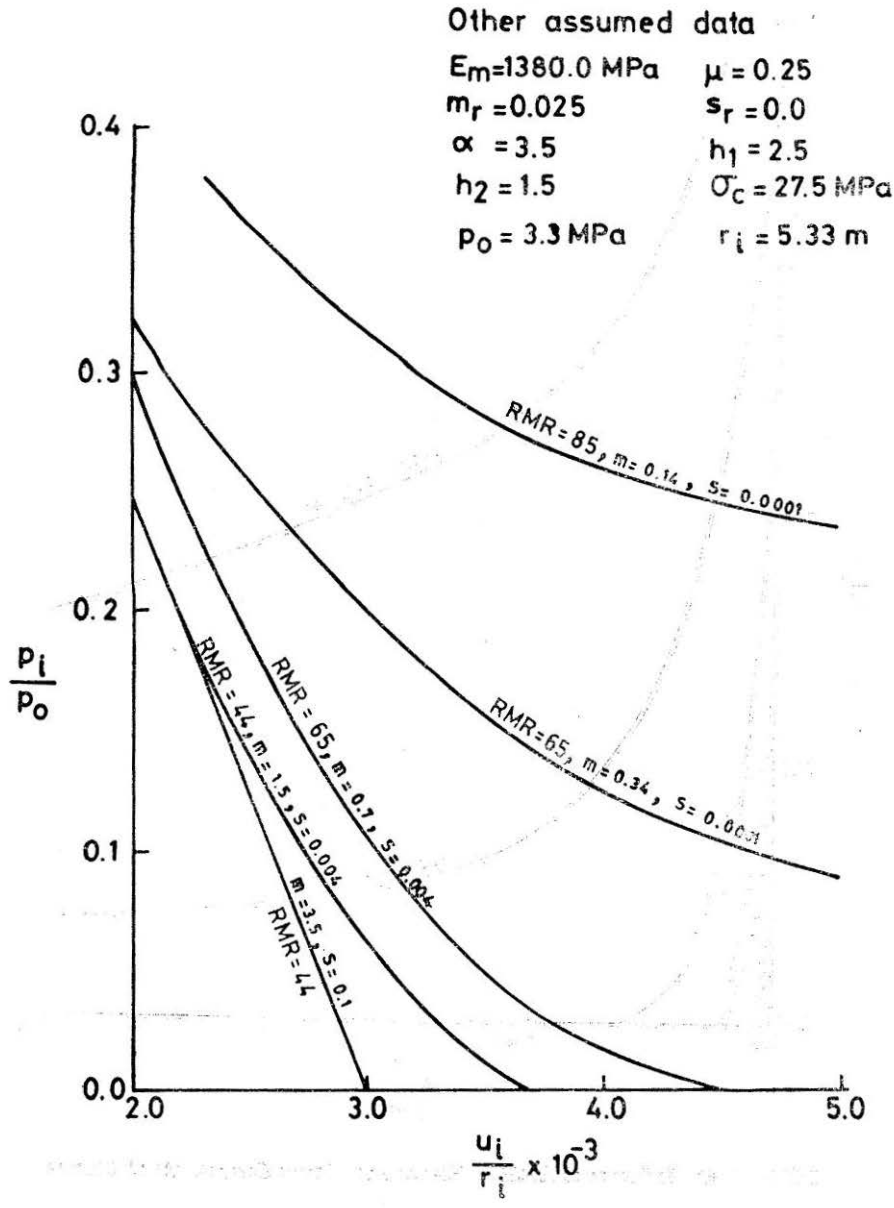

FIGURE 44 Influence of RMR on Tunnel Closure

where

$$J = J_n\, E/K_n,$$

$$R_1 = \left[\, 1/\ln \frac{(\sigma_1 - \sigma_3)}{p_o} \,\right]^{0.5}, \text{ and}$$

$$R_2 = \left[\, 1/\ln \frac{(\sigma_1 - \sigma_3)}{p_o} \,\right]^{0.15}.$$

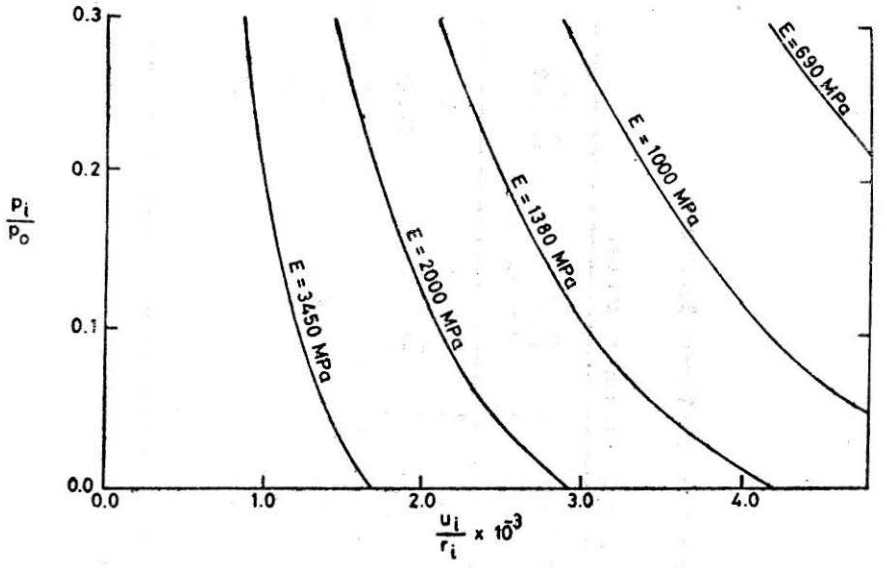

FIGURE 45 Influence of Modulus of Rock on Closure

The values of $(\sigma_1 - \sigma_3)$ of rock mass can be obtained from Eq. 17 whereas E_m/E may be obtained from Eq. 24 or Eq. 25 or from the tests conducted in the laboratory and field to evaluate J_n, E and K_n.

A comparison of radial deformation obtained from this simple empirical Eq. 45 with the rigorous approach presented in Table 15 suggest its reliability.

A comparison of ground reaction response predicted for Giri and Yamuna tunnels with the observed values of support pressures and actually measured radial deformations is shown in Figs. 46 and 47. The comparison is definitely encouraging. Even in the case of the Kielder experimental tunnel, a reasonably good agreement has been observed as shown in Fig. 48.

Rock Mass Classification Based on Ground Convergence

Based on an extensive study of parameters influencing ground reaction curve as indicated above one could suggest categorisation of rock mass based on the prediction of ground convergence value. Such a classification will enable making a decision on the type of support system to be adopted. The classification proposed is presented in Table 16.

In Eq. 13 by inserting $\sigma_3 = p_o$ and assuming $p_0 = \sigma_c$ this equation reduces to

$$\frac{\sigma_1 - \sigma_3}{\sigma_3} = B$$

$$\text{i.e. } \frac{\sigma_1}{\sigma_3} = B + 1 \qquad \ldots(46)$$

TABLE 15

Comparison of Ground Convergence obtained from the Correlation with that from Rigorous Procedure

p_i/p_o	$u_i/r_i \times 10^{-3}$ for different rock mass strength parameters					
	$m = 0.34$, $s = 0.0001$ $(\sigma_1-\sigma_3)/p_o = 1.6969$ $E = 1380.0\ MP_a$		$m = 0.14$, $s = 0.0001$ $(\sigma_1-\sigma_3)/p_o = 1.0909$ $E = 1380.0\ MP_a$		$m = 0.7$, $s = 0.004$ $(\sigma_1-\sigma_3)/p_o = 0.047$ $E = 1380.0\ MP_a$	
	by Rigorous Method	by Eq. 45	by Rigorous Method	by Eq. 45	by Rigorous Method	by Eq. 45
0.05	8.7	8.8	50.1	54.6	3.5	5.6
0.10	4.6	4.6	22.2	20.7	3.1	3.3
0.20	3.0	2.7	6.9	8.3	2.5	2.1
0.30	2.3	2.1	3.2	5.0	2.1	1.8

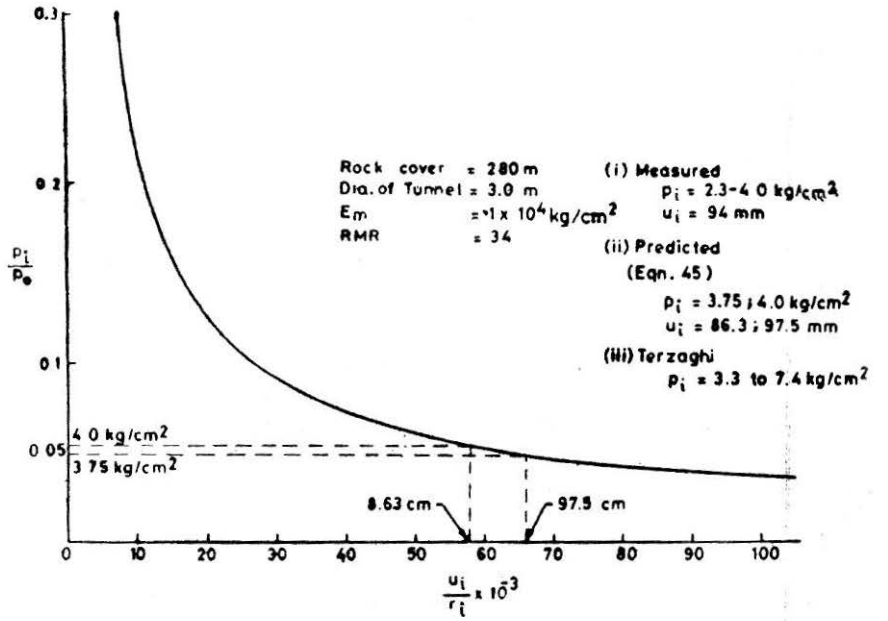

FIGURE 46 Ground Convergence Curve—Yamuna Hydel Project—Stage 2, Part II

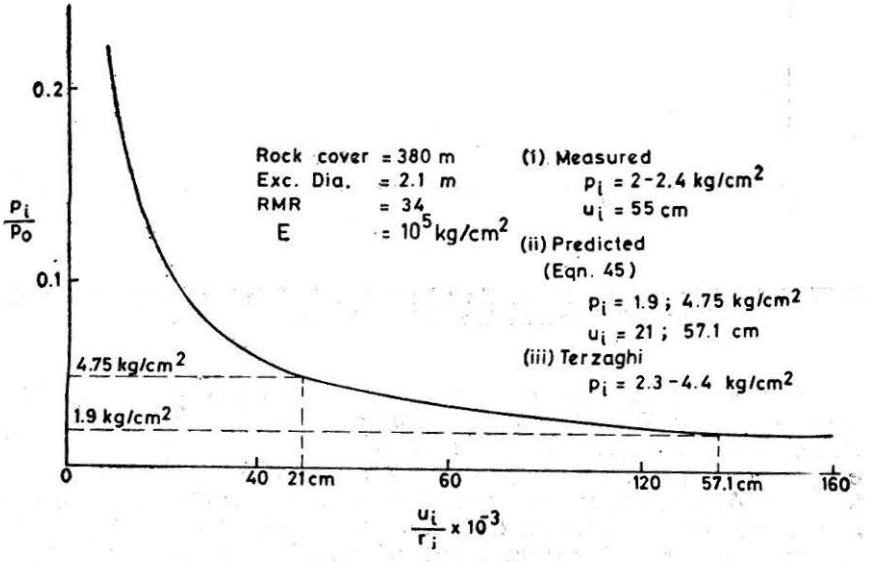

FIGURE 47 Ground Convergence Curve—Giri Hydel Project

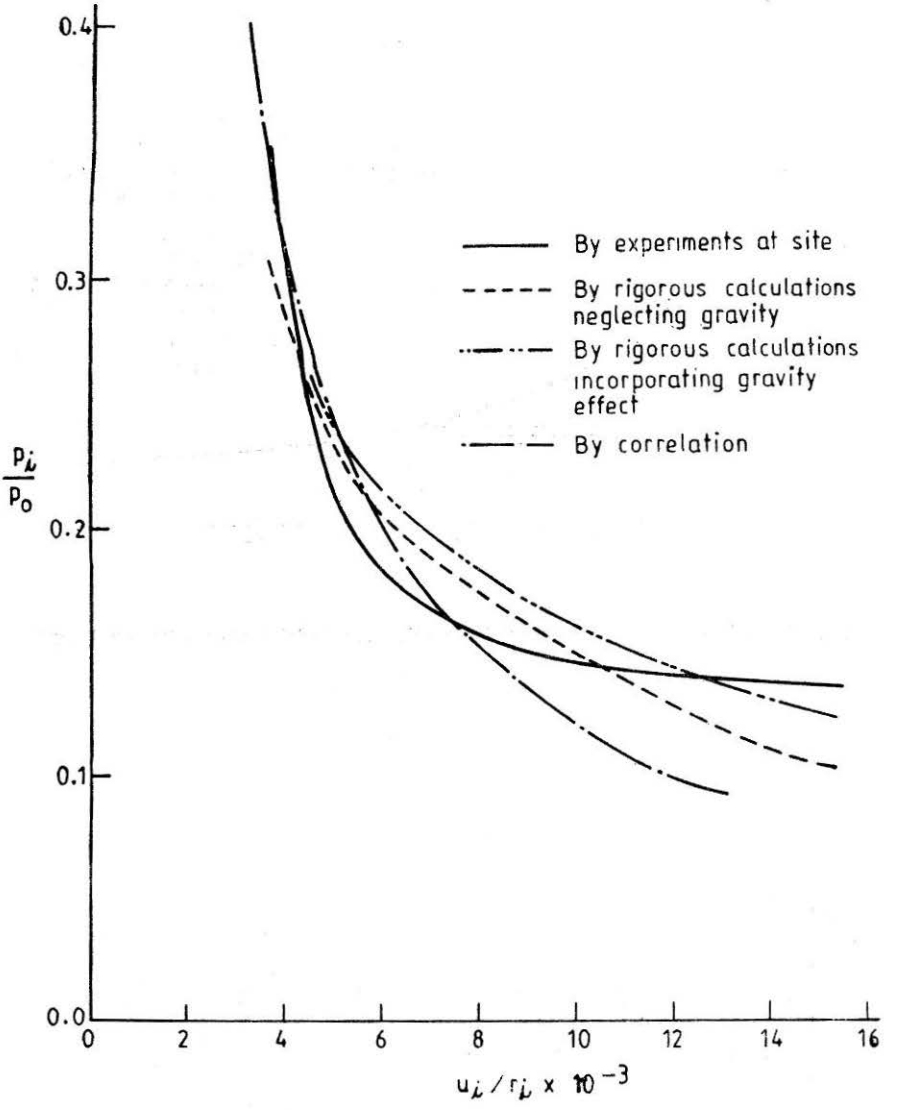

FIGURE 48 Comparison Between Experimental and Calculated Ground Reaction Curves—Kielder Experimental Tunnel, U.K.

By referring to various values of B (from 1.8 to 3.0) suggested for different rocks in Table 5, Eq. 46 gives σ_1/σ_3 varying from 2.8 to 4.0. The brittle-ductile boundary as suggested by Mogi (1965) exists for values of σ_1/σ_3 varying from 3 to 5; more often 3.4 is assumed. This comparison (with Eq. 46) suggests that when the confining pressure (or insitu hydrostatic stress) is same or higher than the unconfined compressive strength of rock, one would expect onset of ductile behaviour of the rock. Therefore, by adopting the ratio of confined compressive strength to insitu stress, one may also suggest the possibility of the occurrence of

TABLE 16

Convergence Classification and Squeezing Ground Condition

Category	1	2	3	4	5
Convergence $u_i/r_i \times 10^{-3}$	Elastic	< 5	5-20	20-100	> 100
Rock mass response	non-squeezing	slightly squeezing	moderately squeezing	highly squeezing	very highly squeezing
Squeezing Condition, σ_{cm}/p_o	> 1	1-0.75	0.75-0.5	0.5-0.25	< 0.25
Suggested support system	no support	rock bolts	rock bolts with shotcrete		yielding arch with rock bolts and shotcrete

squeezing ground condition when tunnels are excavated. Based on the parametric study, consideration of Eqs. 13 and 46 and the finding of Mogi. the guide lines suggested tentatively for estimating the extent of squeezing ground condition are presented in Table 16. This table provides a useful link between squeezing ground condition, corresponding convergence and the possible support system to be adopted for the stability of tunnel walls.

Concluding Remarks

In this lecture my attempt has been to bring out how strength of (both intact-isotropic and anisotropic) rocks and rock mass could be predicted in a simple manner from the unconfined compressive strength of intact rock, quantification of lithology and rock mass quality. The failure criterion proposed for rocks and rock masses appears to be promising. In quantifying the quality of rock mass the location, orientation and spatial distribution of *joints, presence or otherwise of anisotropic effect in relation to* σ_c/p_o and modulus of rock mass should find more prominent place in the rock mass classification in addition to the strength and condition of joints. The criterion proposed for rock mass requires to be examined in the light of the field data forthcoming in future.

Stability of slopes in rock mass could be assessed with the help of more accurate methods of analyses like variational and finite element methods and could be compared with conventional approaches by using charts prepared on the basis of modified Mohr-Coulomb and Griffith theories.

Under squeezing ground conditions, estimation of ground reaction curve from field and laboratory test data using a simple expression enables designers to carry out the analysis of circular tunnels with speed and reliability.

Whatever works we undertake either for dams, tunnels or roads, we

should make a conscientious effort to adopt at least the following line of action :

(*i*) Classify rock and rock mass as per lithology, rock mass rating and rock mass quality,

(*ii*) Estimate unconfined and confined strengths of intact rock and develop strength envelope,

(*iii*) Conduct field tests to estimate unconfined compressive strength and modulus of rock mass.

(*iv*) Estimate insitu stress state,

(*v*) Using the above data develop strength envelope for rock mass, and obtain c and ϕ or m and s for the rock mass,

(*vi*) Using the strength parameters. design rock slopes with the help of charts. Whenever a rock slope has failed, assess its stability and refine the data obtained from steps (*i*) to (*v*). In the case of tunnels in the Himalayan region, prepare ground reaction curve as suggested, measure rock loads and closures by instrumenting. Design the support system and study its performance. Refine the paramete in steps (*i*) to (*v*).

We should concentrate on judicious instrumentation and monitoring, and initiate active research on rock mass.

I hope with this approach we should be able to refine our present state of understanding of rock mass in unconfined and confined states.

Acknowledgements

Most of the work presented in this lecture is drawn from the research work of my students, Dr. C.G.P. Narayan, Dr. K.S. Rao, Dr. R.K. Yaji, Dr. V.M. Sharma, Dr O.P. Ailawadi and Mr. V.K. Arora. Only some aspects of the ongoing research in rock mechanics at IIT Delhi are highlighted. I am also indebted to Prof. G.V. Rao, Prof. A. Varadarajan and Dr. K.G. Sharma for the numerous discussions I had with them and to Prof. Rao, Dr. K.K. Gupta and Dr. K.G. Sharma for making useful suggestions in the manuscript. Very healthy and helping atmosphere created and preserved by these and other colleagues Prof. S.K. Gulhati, Dr. C.G.P. Narayan Dr. R. Kaniraj, Dr. J.M. Kate, Dr. M. Datta is gratefully acknowledged. This work would not have been possible without the liberal funding provided by IIT Delhi and the encouragement of our Director Prof. N. M. Swani.

The manuscript was neatly typed by ever cooperating and cheerful Mrs. V. Menon, Mrs. S. Sarna and Mrs. M. Khushalani. Figures were drawn elegantly by Mr. N.L. Arora and Mr. R.V. Aggarwal. To them I am indeed grateful.

My special indebtedness to my wife Kamala for all her encouragement, patience and forebearance, and to Raju and Ravi for their love and affection.

References

AILAWADI, O.P. (1985). "*Elasto-plastic Finite Element Analysis of Rock Slopes*". Ph. D. Thesis, Indian Institute of Technology, Delhi, India.

ALDRICH, M.J. (1969). "Pore Pressure Effects on Berea Sandstone subjected to Experimental Deformation." *Bull. Geol. Soc. Am.*, 80; 1577-1586.

ATTEWELL, P.B. and SANDFORD, M.R. (1974). "Intrinsic Shear Strength of a Brittle, Anisotropic Rock. I. Experimental and Mechanical Interpretation." *Int Jnl. Rock Mech. Min. Sci.* 11; 423-430.

BARTON, N.R. (1970). "A Low Strength Material for Simulation of the Mechanical Properties of Intact Rock in Rock Mechanics in Models." *Proc. 2nd Congr. Rock Mech.*, Belgrade, 3-15 : 90-110.

BARTON, N.R., (1973). "Review of Shear Strength Criterion for Rock Joints." *Engg. Geol.*, 7 : 287-332.

BARTON, N.R. and CHOUBEY, V.D. (1977). "The Shear Strength of Rock Joints in Theory and Practice." *Rock Mech* , 10 : 1 : 1-54.

BARTON, N.R., LIEN, R. and LUNDE, J (1974). "Engineering Classification of Rock Masses for the Design of Tunnel Support." *Rock Mech.*, 6:4:189-236.

BELL, F.G. (1978). "Petrological Factors Relating to Porosity and Permeability in the Fell Sandstones." *Qrt. Jnl. Engg. Geol.*, 11: 113-126.

BIENIAWSKI, Z.T. (1973). "Engineering Classification of Jointed Rock Masses" *Trans. South African Instn. Civ. Engr.*, 15: 12: 335-344.

BIENIAWSKI, Z.T. (1974). "Geomechanics Classification of Rock Masses and its Application in Tunnelling." *Proc. 3rd Int. Congr Rock Mech* , Denver, Part A, pp. 27-32.

BIENIAWSKI, Z.T. (1978). "Determining Rock Mass Deformability: Experience from Case Histories." *Int. Jnl. Rock Mech. Min. Sci.*, 15: 237-248.

BISHOP, A.W. (1955). "The Use of the Slip Circle in the Stability Analysis of Slopes." *Geotechnique*, 5: 1: 7-17.

BOOZER, G.D., HILLER, K. and SERDENGECTI, S. (1962). "Effects of Pore Fluids on the Deformation Behaviour of Rocks Subjected to Triaxial Compression." *Proc. Symp. Rock Mech.*, 5th, Pergamon, p. 578.

BRACE, W.F. (1964). "*Brittle Fracture of Rocks, State of Stress in the Earth's Crust.*" Judd, W.R., ed., Elsevier, New York, pp. 111-174.

BROCH, E. (1974). "The Influence of Water on Some Rock Properties". *Advances in Rock Mech.*, National Academy of Science, pp. 33-38.

BROCH, E. and FRANKLIN, J.A. (1972). "The Point Load Strength Test." *Int. J. Rock Mech. Min. Sci* , 9: 669-697.

BROOK, N. (1979). "Estimating the Triaxial Strength of Rocks." *Int. J. Rock Mech. Min. Sci. Geomech. Abstr.*, 16 : 261-264.

BROWN, C.B. and KING, I.P. (1966). "Automatic Embankment Analysis ; Equilibrium and Instability Conditions." *Geotechnique, 16: 3:* 209-219.

BROWN, E T., BRAY, J.W., LADANYI, B. and HOEK. E. (1983). "Ground Response Curves for Rock Tunnels." *Jnl. Geotech. Engg.* ASCE, 109: 1: 15-39

CHENVERT, M.E. and GATLIN, C. (1965) "Mechanical Anisotropic of a Laminated Sedimentary Rocks." *Soc. Pet. Engrs. J.*, pp. 67-77.

CHERNOVS'KO, F.L (1965). "A Local Variational Method for the Numerical Solutions of Variational Problems." *U.S.S.R. Computational Mathematics and Mathematical Physics*, 5 : 4: 234-241.

CHUGAEV. R.R (1964). "Stability Analysis of Earth Slopes, Jerusalem". Trans. from Russian, *Israel Programme of Scientific Translations*, 1966.

COLLIN, A. (1846). "*Glissement Spontanes des Terrains Argileux,*" Paris, Charilian Goeury and Dulmont (English Translation Publ. 1956 by Uni-Toronto Press).

COOLING, I.F. and GOLDER, H.Q. (1942). "The Analysis of the Failure of an Earth Dam during Construction." *Jnl. Instn. Civ. Engrs.*, 19 : 38-55.

COULOMB, C.A. (1973). "Application des Ragles de Maximis at Minims a Quelques Problems de Statique Relatifs a 1' Architecture," *Memoires de Savants Etrangers de 1' Academic des Science de Paris*, 7: 343-382.

DAEMEN, J.J.K. (1975). "*Tunnel Support Loading Caused by Rock Failure.*" Ph. D. Thesis, University of Minnesota, Minnesota, USA.

DEERE, D.U. (1964). "Technical Description of Rock Cores for Engineering Purposes." *Rock Mech. and Engg. Geology*, 1 : 1 : 17-22.

DEERE, D.U. and MILLER, R. P. (1966). "Engineering Clasification and Index Properties for Intact Rock." Tech. Rept. No. AFWL-TR-65-116, *Air Force Weapons Lab*, New Mexico.

DONATH, F.A. (1964). "Strength Variation and Deformational Behaviour of Anisotrophic Rocks." *State of Stress in the Earth's Crust*, W.R. Judd, ed., Am. Elsevier Publ. Comp., New York, pp. 281-298.

DONATH, F.A. (1970). "Some Information Squeezed Out of Rock," *Am. Scientist*, 58: 54-72.

DONATH, F.A. (1972), "Faulting Across Discontinuities in Anisotropic Rock, Stability of Rock Slopes," *Proc 13th Symp. Rock Mech.*, Urbana, New York, Am. Soc. Civ. Eng., pp. 753-772.

DONATH, F.A and FRUTH, L.S. (1971). "Dependence of Stress rate Effects on Deformation Mechanism and Rock Type," *J. Geol.*, 79: 347.

DUBE, A.K. (1979). "*Geomechanical Evaluation of Tunnel Stability under Failing Rock Conditions in a Himalayan Tunnel.*" Ph. D. Thesis, University of Roorkee, India.

FELLENIUS, W. (1936). "Calculation of the Stability of Earth Dams," *Trans. 2nd Cong. on Large Dams*, Vol. 4, Washington.

FRANKLIN, J A. (1971). "Triaxial Strength of Rock Materials." *Rock Mech.*, 3 : 86-98.

GELFAND, I.M. and FOMIN, S.V. (1963), "*Calculus of Variations,*" Prentice-Hall, Inc., Englewood Cliffs. New Jersey, pp. 54-63.

GNIRK, P.F. and CHEATHAN, J.B. (1965). "An Experimental Study of Single Bit-Tooth Penetration into Dry Rock at Confining Pressures of 0 to 5000 psi," *Soc. Pet. Engrs. J.*, 5 : 2 : 117-130.

GOLDSTEIN, I.M. (1969). "Application of Calculus of Variations to Investigations of Bases and Slopes." *Soil Mech. and Foundation Engg.*, 1 : 3-9.

GRIGGS, D.T. (1936). "Deformation of Rock Under High Confining Pressure." *J. Geol.*, 44: 541-577.

GRIGGS, D.T., TURNER, F.J. and HEARD, H.C. (1960). "Deformation of Rocks at 500° to 800°C., in Rock Deformation." *Geol Soc. Am. Mem.*, 79 : 39-104.

HANDIN, J. and HAGER, R.V. (1957). "Experimental Deformation of Sedimentary Rocks under Confining Pressure : Tests at Room Temperature on Dry Samples." *Bull. Am. Assoc. Petrol. Geol.*, 41 : 1-50.

HANDIN, J. and HAGER, R. V. (1958). "Experimental Deformation of Sedimentary Rocks under High Confining Pressure : Tests at High Temperature." *Bull. Am. Soc. Petrol Geol.*, 42: 2894-2934.

HANDIN, J., HAGER, R.V., FRIEDMAN, M. and FEATHER, J.N. (1963). "Experimental Deformation of Sedimentary Rocks under Confining Pressure : Pore Pressure Effects." *Bull. Am. Assoc. Petrol. Geol.*, 47: 717-755.

HOEK, E. (1968). "Brittle Failure of Rock". *Rock Mechanics in Engineering Practice*, Stagg and Zienkiewicz, eds., Wiley, London, pp. 99-124.

HOEK, E. (1970). "Estimating the Stability of Excavated Slopes in Opencast Mines". *Trans. Inst. Mining and Metallurgy*, London, 79: A 109-A131.

HOEK, E. (1983). "Strength of Jointed Rock Masses." *Geotechnique*, 33 : 3 : 187-223.

HOEK, E. and BRAY, J. (1977) "*Rock Slope Engineering.*" Inst. Mining and Metallurgy, London, (2nd Edn.).

HOEK, E. and BROWN, E.T. (1980). "*Underground Excavations in Rock.*" Institution of Mining and Metallurgy, London.

HOEK, E. and BROWN, E.T. (1983). "Empirical Strength Criterion for Rock Masses", *Jnl. Geotch. Engg. Div.*, ASCE, 106: GT9: 1013-1035.

HOFER, K.H. and THOMA, K. (1968). "Triaxial Tension Salt Rocks." *Int. Jnl. Rock Mech. Min. Sci., Geotech. Abstr.*, 5: 195-203.

HORINO, F.G. and ELLIKSON, M.L. (1970). "A Method of Estimating the Strength of Rock Containing Planes of Weakness," *U.S. Bureau Mines Report Investigation* 7449.

HOSHINO, K., KOIDE, H., INAMI, K., IWAMURA, S. and MITSUI, S. (1972). "Mechanical Properties of Japanese Tertiary Sedimentary Rocks under High Confining Pressure." *Geol. Surv Jpn.*, Rep. No. 244, pp. 1-200.

HOUPERT, R. (1970). "La Resistance a low Rupture des Roches on Compression Simple." *Proc. 2nd Congr. Int. Rock Mech.*, Belgrade, 2: 49-55.

HUTCHINSON, J.N. (1961). "A Landslide on a Thin Layer of Quick Clay at Furre, Central Norway." *Geotechnique*, 11: 2: 69-94.

JAEGER, J.C. (1960). "Shear Failure of Anisotropic Rocks," *Geol. Mag.*, 97: 65-72.

JAEGER, J.C. (1971). "Friction of Rocks and Stability of Rock Slopes". *Geotechnique*, 21: 2: 97-134.

JAEGER, J.C. and COOK, N.G.W. (1979). "*Fundamentals of Rock Mechanics,*" Chapman and Hall, London. p. 593.

JANBU, N. (1954). "Application of Composite Slip Surfaces for Stability Analysis". *Proc. European Conf. Stability of Earth Slopes*, Stockholm, 3: 43-49.

JANBU, N. (1965). "Soil Compressibility as Determined by Oedometer and Triaxial Tests". *Proc. European Conf. Soil Mech. and Found. Engg.*, Wiesbaden, *1: 19-25.*

JETHWA, J.L., DUBE, A.K. and SINGH B. (1985). "Tunnelling under Squeezing Rock Conditions—Indian Case Histories." Tech. Session V. *Proc. of 52 Annual* Session, *R & D*, CBIP pp. 95-109.

JETHWA, J.L., SINGH, B. and SINGH, B. (1984). "Estimation of Ultimate Rock Pressure for Tunnel Linings under Squeezing Rock Conditions—a New Approach". *Proc. Int. Symp. on Design and Performance of Underground Excavations*, Cambridge, pp. 231-238.

KOBAYASHI, S. (1970). "Fracture Criterion for Anisotropic Rocks," *Mem. Fac. Eng.*, Kyoto Univ., 32: 307-333.

KWASNIEWSKI, M. (1983). "Deformational and Strength Properties of the Three Structural Varieties of Carboniferous Sandstones", *5th Int. Congr. Rock Mech.*, Melbourne, 1: A105-A115.

LABASSE, H. (1949). "Les Pressons de Terrains Author des puits." *Revue Universalle des Mines*, 92e Annee, S-9, V-5, Mass., pp. 78-88.

LADANYI, B. and ARCHAMBAULT, G. (1970). "Simulation of Shear Behaviour of a Jointed Rock Mass". *Proc. 11th Symp. Rock Mech.*, Am. Inst. Min. Met. Petrol. Engrs., pp. 105-125.

LAUFFER, H. (1958). "Gebirgsklassifizievung for den Stollenbau." *Geologie and Bauwesen*, 24: 1: 46-51.

LEGGET, R.F. (1962). "*Geology and Engineering.*" McGraw Hill New York, p. 426.

MATALUCCI, R.V., ABDEL HADY, M and SHELTON, J.W. (1970). "Influence of Grain Orientation on Direct Shear Strength of a Loessial Soil." *Eng. Geol.*, 4: 121-132.

McLAMORB, R. and GRAY, K E. (1967). "The Mechanical Behaviour of Anisotropic Sedimentary Rocks." *Trans. Am. Soc. Mech. Engrs.*, Series B, 89: 62-76.

MOGI, K. (1965). "Deformation and Fracture of Rocks under Confining Pressure, Elasticity and Plasticity of Some Rocks " *Bull. Earthquake Res. Inst.*, Tokyo Univ., 43: 349-379.

MOGI, K. (1972). "Effect of the Triaxial Stress System on Fracture and Flow of Rocks." *Phys. Earth Planet Interiors*, 5: 318-324.

MOGI, K. (1974), "On the Presure Dependence of Strength of Rocks, and the Coulomb Fracture Criterion." *Tectonophysics*, 21: 273-285.

MORGENSTERN, N.R. and PRICE, V.E., (1965) "The Analysis of the Stability of General Slip Surfaces." *Geotechnique*, 15: 1: 79-93.

MURRELL, S.A.F. (1965). "The Effect of Triaxial Stress Systems On the Strength of Rock at Atmospheric Temperatures." *Int, J. Rock Mech. Min. Sci.*, 3: 11-43.

NARAYAN, C.G.P., BHATKAR, V.P. and RAMAMURTHY, T. (1976). "Slope Stability Analysis by Variational Technique." *Indn. Geotech. Jnl.*, 6:2: 67-90.

NARAYAN, C.G.P., BHATKAR, V.P. and RAMAMURTHY, T. (1978). "Slope Stability Coefficients by Variational Method." *Proc. Geocon-India*, Conf. on Geotechnical Engg., New Delhi, 1: 80-85.

NARAYAN, C.G.P. BHATKAR, V P. and RAMAMURTHY. T. (1982). "Nonlocal Variational Method in Stability Analysis". *Jnl. Geotech. Engg. Div.* ASCE, 108: 11: 1443-1459.

OLSSON, W.A. (1974). "Effects of Temperature, Pressure and Displacement Rate on the Frictional Characteristics of a Limestone." *Int. Jnl. Rock Mech. Min. Sci.*, 11: 267-278.

PATTON, F.D. (1966). "Multiple Modes of Shear Failure in Rock." Proc. *Ist In. Congr. Rock Mech.*, Lisbon, 1: 509-513.

POMERAY, C.D., HOBBS, D.W. and MAHMOUD, A. (1971). "The Effect of Weakness Plane Orientation on the Fracture of Bornsley Hards by Triaxial Compression." *Int. Jnl. Rock Mech. Min. Sci.*, 8: 3: 227-238.

PRICE, N.J. (1960). "The Compressive Strength of Coal Measure Rocks." *Coll. Eng.*, 37: 283-292.

PRICE, D.G. and KNILL, J.L. (1960). "A Study of the Tensile Strength of Coal." *Brit. Jnl. Appl. Phys.*, 7: 7: 243-246.

RABECEWICZ, L.V. (1965)." The New Austrain Tunnelling Method, Parts I to III." *Water Power*, London. Nov. and Dec. 1964 and Jan. 1965.

RABECEWICZ, L.V. (1969). "Stability of Tunnels under Rock Load Parts I to III" *Water Power*, London. June pp. 225-234; July pp. 266-273, Aug. pp. 297-302.

RAMAMURTHY, T. (1975). "A Simple Triaxial Cell." *Annual Report of Indian Institute of Technology, Delhi.*

RAMAMURTHY, T. (1984). "Stability to Check Landslides," *Proc. Spl. Session. Sym. Geotech. Aspects of Mass and Material Transportation*, Bangkok, pp. 47-86.

RAMAMURTHY, T. and GOEL, S.C. (1973). "Strength of Sandstones in Triaxial Compression" *Symp. Rock Mech. & Tunnelling Problems*, Kurukshetra, India, 1: 204-209.

RAMAMURTHY, T., NARAYAN, C.G.P. and BHATKAR, V.P. (1977). "Variational Method for Slope Stability Analysis." *Proc. 9th Int. Conf. SMFE*, Tokyo, 2: 139-142.

RAMAMURTHY, T., RAO, G.V. and RAO, K.S. (1985). "A Strength Criterion for Rocks." *Proc. Indn. Geotech. Conf., Roorkee*, Vol. 1, pp 59-64.

RAMAMURTHY., T., SHARMA, K.G. and AILAWADI. O.P. (1985). Elasto-plastic Finite Element Analysis of Slopes in Rock Mass." *Proc. Int. Conf. on Finite Element Computational Mechanics*, Bombay, 1: 291-300.

RAO, K.S., (1984). "*Strength and Deformation Behaviour of Sandstones.* Ph. D. Thesis, Indian Institute of Technology, Delhi India.

RAO, K.S., RAO, G.V. and RAMAMURTHY, T. (1985). "*Rock Mass* Strength from Classification." *Proc. of Wokshop on Engg. Classification of Rocks*, Central Board of Irrigation and Power, New Delhi, pp. 27-50.

RUMMEL, F. and FAIRHURST, C. (1970). "Determination of the Post Failure Behaviour of Brittle Rock using a Serve-controlled Testing Machine." *Rocks Mech*, 2: 189-204

RZHEVSKY. V. and NOVIK, G. (1971). "*The Physics of Rocks.*" MIR Publishers, Moscow, p. 320.

SCHNEIDER, H.J. (1976). "Friction and Deformation Behaviour of Rock Joints." *Rock Mech.*, 8: 169-184

SCHWARTZ, A.E. (1964). "Failure of Rock in the Triaxial Shear Test," *Proc. of the 6th Symp. on Rock Mech.*, Rolla, MO, pp. 109-151.

SEIFERT, K.E. (1969). "Strength of Adirondack Anorthosite at Elevated Temperatures and Pressures." *Geol. Am. Bull.*, 80; 10: 2053-2059.

SERDENGECTI, S. and BOOZER, W.S. (1961). "The Effects of Strain Rate and Temperature on the Behaviour of Rocks Subjected to Triaxial Compression." *Proc. 4th Symp. Rock Mech. Univ. Park, Penn.*, pp. 83-97.

SHARMA, V.M. (1985). "*Predication of Closure and Rock Loads for Tunnels in Squeezing Grounds.*" Ph.D. Thesis Indian Institute of Technology Delhi, India.

SHARMA, K.G., RAMAMURTHY, T. and AILAWADI, O.P. (1984). "Elasto-plastic Finite Element Analysis of Rock Slopes." *Proc. 5th Int. Conf. Numeri, Methods in Geomech*, Japan, 2; 891-987.

SINGH, B. (1973). "Continum Characterization of Jointed Rock Masses." *Int. Jnl. Rock Mech. Min. Sci, and Geomech. Abst.*, 1: 4: 311-349.

SINGH, B. (1978). "Analysis and Design Techniques for Underground *Proc. Geocon-India, Conf. on Geotech, Engr.*, New Delhi, 2: 102-112.

SKEMPTION, A.W. (1964). "Long term Stability of Clay Slopes." *Geotechni*, Structures." *due*, 14: 2: 77-101

SMART, B.G.D., ROWLANDS, N. and ISAAC. A.K. (1982). "Progress Towards Establishing Relationships between the Mineralogy and Physical Properties of Coal Measures Rocks." *Int. Jnl. Rock Mech. Min. Sci. and Geomech. Abstr.*, 19: 81-89.

SOKOLOVSKY, V.V. (1960). "*Statics of Soil Media.*" Butterworths Scientific Publication.

SPENCER, E. (1967). "A Method of Analysis of the Stability of Embankments Assuming Parallel Interslice Forces." *Geotechnique*, 17: 1: 11-26.

SPENCER, E. (1968). "Effect of Tension on Stability of Embankments." *Jnl. Soil Mech. & Found, Div., ASCE*, 94 : 5 : 1159-1173.

SPENCER, E (1969). "Circular and Logarithmic Spiral Slip Surface." *Jnl. Soil Mech. & Found. Div., ASCE*, 95 : 1 : 277-234.

SRIVASTAVA, L.S., GUPTA, R.P. and BEHARI, S. (1970). "Evaluation of Strength from Porosity and Durability Measurement of Rocks." *Jnl. Ind. Nat. Soc. Soil. Mech. Found. Eng.*, 9 : 2 : 225-233.

STINI, I, (1950), "*Tunnelbaugeologie*" Springer-Verlag, Vienna, p. 336.

STOW, R.L. (1969) "Strength and Deformation Properties of Granite, Basalt, Limestone and Tuff at Various Loading Rates." *U.S. Army Corps. Eng.*, Water: ways Exp. Station, Vicksburg, Miss., Misc. paper C-69-1.

STREET, N and WANG, F.D. (1966). "Surface Potentials and Rock Strength." *Proc. Ist Cong. Int. Soc. Rock Mech.*, Lisbon, 1 : 451-456.

SUBASH BABU, L., MARKANDEY, and ULABHAJE, A.V. (1977). "Mineral Compositions and Strength Properties of some Sandstones from Singrauli Coal Fields." *Jnl. Mines, Metals, Fuels*, 25 : 7.

TAYLOR, D.W. (1948), "*Fundamentals of Soil Mechanics.*" John Wiley Publications, New York.

TERZAGHI, K. (1946). "*Rock Tunnelling with Steel Supports.*" by proctor, R.V. and White, T.L., The Commerical Shearing and Stamping Co. Youngstown, Ohio.

VON KARMAN (1911). "The Festigskeitsversuche under Auseitigem Druck." *Zeits, Verein Deutsch. Ing.*, 55 : 1749-1757.

VUTUKURI, V.S , LAMA, and SALUJA, S.S. (1974). "*Hanbook on Mechanical Properties of Rock,*" *Vol. I-IV*. Trans. Tech. Publications.

WALSH, J.B and BRACE, W.F. (1964). "A Fracture Criterion for Brittle Anisotropic Rocks," *Geophysics Research Jnl.*, 69 : 3442.

WAWERSIK, W.R, and BRACE, W.F. (1971). "Post-failure Behaviour of a Granite and a Diabase." *Rock Mech.*, 3 : 61-85.

WAWERSIK, W.R. and FAIRHURST, C. (1970). "A Study of Brittle Rock Fracture in Laboratory Compression Experiments." *Int. Jnl. Rock Mech. Min. Sci.*, 7 : 561-575.

WILHELMI, B. and SOMERTON, W.H. (1967). "Simultaneous Measurement of Pore and Elastic Properties of Rocks under Triaxial Stress conditions." *Jnl. Soc. Petrol. Eng.*, AIME, 7 : 283-294.

WOLFSKILL, L.A. and LAMBE, T.W. (1957). "Slide in the Siburua Dam." *Jnl. Soil Mech. & Found. Div.* ASCE, 93 : 4 : 107-133.

YAJI, R.K. (1984). "*Shear Strength and Deformation Response of Jointed Rocks.*" Ph. D. Thesis, Indian Institute of Technology, Delhi, India.

YUDHBIR, LEMANZA, W. and PRINZL, F. (1983), "An Empirical Failure Criterion for Rock Masses." *5th Int. Congr. Rock Mech.*, Melbourne, 1 : B1-8.

ZIENKIEWICZ, O.C. and CORMEAU, I.C. (1974). "Visco-plasticity-plasticity and Creep in Elastic Solids—A Unified Numerical Solution Approach." *Int. Jnl. Numerical Methods in Engg.*, 8 : 821-845.

VOTE OF THANKS

Prof. G.V. Rao, Honorary Secretary of the Indian Geotechnical Society proposed the vote of thanks.

On behalf of the Indian Geotechnical Society it is my pleasant privilege to propose a hearty vote of thanks to Prof. Ramamurthy for delivering the 8th Annual Lecture of the Society.

We know of Prof. Ramamurthy as a geotechnical engineer of eminence and the abiding interest he has taken in developing teaching and research on rock mechanics in the country. To-day we have heard him unfolding the behaviour of the much "maligned" behaviour of rock masses into simple and easy to understand concepts and their application for solving field problems. I am personally happy to listen to him, the years of his meticulous work and many candles burnt, coming to fruition. On hehalf of all of you, Ladies and Gentleman, I congratulate him for the lucid manner in which he went through the Lecture and thank him for the painstaking efforts he has putin in bringing out the Text of the Lecture on a subject which has endeared him, if I may say so, more than his family. Probably that is the reason why we fondly call him TRM—RM standing for Rock Mechanics.

We are all greatly indebted to Prof. Ramamurthy for having accepted to deliver this lecture and sparing his valuable time. May I request you to join me in showing our appreciation to him in our usual way.

Now, on your behalf, I request him to accept a token of our appreciation and request Prof Shashi Gulhati to present him this token gift cheque on behalf of the Society (The token gift was then presented).

Our gratitudes to Dr. R.K. Bhandari for ably conducting this Session and the Organising Committee of IGC-85 for enabling this lecture session to be a total success, with their active co- operation and support.

Finally, I thank all of you, ladies and gentleman for your patient hearing.

List of Symbols, Units and Definitions*

Introduction

The list of symbols, units and definitions adopted in 1977, published in the proceedings of the 9th I.S.S.M.F.E. Conference held in Tokyo, and later in 1981, in the 5th edition of the Lexicon in 8 languages, has been revised and enlarged.

The main changes in the old list affect :

— length symbols, for which small letters have been added when necessary, in accordance with the International Standard Organization, which requires small letters for length symbols ;

— a few consolidation parameters.

New subjects have been treated; they are mainly: soil and foundation dynamics, soil fabric, anchors, geotextiles, retaining structures other than walls.

The organization of the new list had been recast.** It now appears as follows :

I. General

II. Stress and strain

III. Properties of soil

- (*a*) soil identification
- (*b*) hydraulic properties
- (*c*) sampling
- (*d*) consolidation (one-dimensional)
- (*e*) shear strength
- (*f*) in-situ tests
- (*g*) dynamics
- (*h*) soil-fabric
- (*i*) other

IV. Geotechnical structures

- (*a*) earth retaining structures
- (*b*) foundations
- (*c*) slopes

---

* International Society of Soil Mechanics and Foundation Engineering

** By the ISSM & FE Sub-committee

(*d*) ground anchors

(*e*) geotextiles

V. Foundation vibration and earthquake engineering

VI. Main subindexes

The symbols, units and names of the present list are those now recommended by the International Society of Soil Mechanics and Foundation engineering.

To make a proper use of them, the reader should be already familiar with Soil Mechanics. The definitions given are not necessarily exhaustive. Their purpose is primarily to clarify the meaning of the symbols.

The units shown are those recommended in most cases, but other multiple or submultiple of the basic SI unit may be used, if more convenient for the particular case under consideration, e.g. :

— kPa is recommended; Pa, MPa...may be also used.

— m is recommended; mm... may be also used.

The main subindexes given in Section VI, as well as the signs given in Section I can be used by the reader to specify a general symbol given in the proceeding sections, e.g. :

φ'_{cu} will denote an effective angle of shearing resistance measured in a consolidated-undrained test. :

Conventions Used

— for dimensions : L = length
M = mass
T = temperature
— dimensionless

— for units : m, s, kg, N, Pa

(SI units) —° degree (angle)
rad radian (,,)
—°C degree Centigrade
—°K degree Kelvin

multiples : k ($=10^3$), M ($=10^6$),...

submultiples : m ($=10^{-3}$), μ ($=10^{-6}$),...

— for a dimensionless parameter which expressed in actual figure (e.g. $S_r = 0.93$)

% for a dimensionless parameter which can also be expressed in percentage (e.g. $S_r = 93$ %)

SYMBOL	DIMENSION	UNIT	TERM DEFINITION
1 General			
$L,1$[1]	L	m	length
B,b[1]	L	m	breadth
H,h[1]	L	m	height
D,z[1]	L	m	depth
d,D[1]	L	m	diameter
A	L^2	m^2	area
V	L^3	m^3	volume
t	T	s	time
v	$L\,T^{-1}$	m/s	velocity
s	$L\,T^{-2}$	m/s^2	acceleration
g	$L\,T^{-2}$	m/s^2	acceleration due to gravity $g=9{,}81$ (m/s^2)
m	M	kg	mass
ρ	$M\,L^{-3}$	t/m^3 (or Mg/m^3)	density
γ	$M\,L^{-2}T^{-2}$	kN/m^3	unit weight
F[2]	—		factor of safety
π	—		3.1416
e	—		2.7183
$ln\,x$	—		natural logarithm of x
$lg\,x$	—		logarithm of x base 10
Signs			
			A "prime" applies to effective stress.
			A "bar" above a symbol relates to a mean value of a property.
			A "dot" above a symbol denotes derivative with respect to time.
			Prefix "δ" or "$\triangle$" denotes an increment or a change.
Stress and Strain			
u	$ML^{-1}T^{-2}$	kPa	pore pressure. pressure (above atmospheric pressure) in the water in the voids of a fully saturated soil.

(1) According to the International Organization of Standardization, small letters should be used for length symbols. As a provisional measure, both small and capital letters are proposed herein, but small letters are strongly recommended.

(2) The symbol "γ", adopted for the design of structures by the International Organization for Standardization in its Standard ISO-3898, is also used (instead of f) in Soil Mechanics, but only when calculating the loads for the design of structures.

U_w	$ML^{-1}T^{-2}$	kPa	pore water pressure. pressure in the water in the voids of a partially saturated soil.
U_a	$ML^{-1}T^{-2}$	kPa	pore air pressure. pressure in the air in the voids of a partially saturated soil.
U_s	$ML^{-1}T^{-2}$	kPa	static pore water pressure.
U_e	$ML^{-1}T^{-2}$	kPa	dynamic excess pore water prsssure. $u = u_s + u_e$
σ	$ML^{-1}T^{-2}$	kPa	total normal stress. stress (above atmospheric pressure) acting perpendicularly to a given plane.
σ'	$ML^{-1}T^{-2}$	kPa	effective normal stress. normal stress transmitted by intergranular contacts ($\sigma' = \sigma - u$ for saturated soils). Note : $\bar{\sigma}$ should be avoided.
τ	$ML^{-1}T^{-2}$	kPa	shear stress. stress acting tangentially to a given plane.
σ_1	$ML^{-1}T^{-2}$	kPa	major principal stress. maximum stress acting on one of the three orthogonal planes where shear stresses are equal to zero.
σ_2	$ML^{-1}T^{-2}$	kPa	intermediate principal stress. intermediate stress acting on one of the three orthogonal planes where shear stresses are equal to zero.
σ_3	$ML^{-1}T^{-2}$	kPa	minor principal stress. minimum stress acting on one of the three orthogonal planes where shear stresses are equal to zero.
σ_{oct}	$ML^{-1}T^{-2}$	kPa	mean stress or octahedral normal stress defined as : $(\sigma_1+\sigma_2+\sigma_3)/3$
τ_{oct}	$ML^{-1}T^{-2}$	kPa	octahedral shear stress. defined as : $\sqrt{(\sigma_1-\sigma_2)^2+(\sigma_2-\sigma_3)^2+(\sigma_3-\sigma_1)^2}/3$
p	$ML^{-1}T^{-2}$	kPa	mean normal stress in triaxial test : $p = \frac{1}{3}(\sigma_1+\sigma_2+\sigma_3)$
q	$ML^{-1}T^{-2}$	kPa	deviatoric stress in triaxial test : $q = \sigma_1-\sigma_3$
ϵ	—	—, %	linear strain. change in length per unit length in a given direction.
γ	—	—, %	shear strain. change of the angle between two planes originally perpendicular to each other (expressed in radians).

ϵ_1	—	—, %	major principal strain. maximum strain corresponding to one of the three orthogonal directions in which the shear strains are equal to zero.
ϵ_2	—	—, %	intermediate principal strain. intermediate strain corresponding to one of the three orthogonal directions in which the shear strains are equal to zero.
ϵ_3	—	—, %	minor principal strain. minimum strain corresponding to one of the three orthogonal directions in which the shear strains are equal to zero.
ϵ_v	—	—, %	volumetric strain : $\epsilon_v = \epsilon_1 + \epsilon_2 + \epsilon_3$
ϵ_s	—	—, %	shear strain : $\epsilon_s = \sqrt{\frac{2}{3}}\,[(\epsilon_1-\epsilon_2)^2+(\epsilon_2-\epsilon_3)^2 + (\epsilon_3-\epsilon_1)^2]^{\frac{1}{2}}$ Note : for axial symmetry ($\epsilon_2 = \epsilon_3$), these strains becomes : $\epsilon_v = \epsilon_1 + 2\,\epsilon_3$ $\epsilon_s = \frac{2}{3}\,(\epsilon_1-\epsilon_3)$
ϵ_{oct}	—	—, %	average or octahedral linear strain : $\epsilon_{oct} = \frac{1}{3}\,\epsilon_v$
γ_{oct}	—	—, %	octahedral shear strain : $\gamma_{oct} = \sqrt{2}\,\epsilon_s$
$\dot{\epsilon}$	T^{-1}	s^{-1}	linear strain rate. rate of change of ϵ.
$\dot{\gamma}$	T^{-1}	s^{-1}	shear strain rate. rate of change of γ.
ν	—	—	Poisson's ratio (μ is also used). ratio between linear strain changes perpendicular to and in the direction of a given uniaxial stress change.
E	$ML^{-1}T^{-2}$	kPa	modulus of linear deformation. ratio between a given normal stress change and the linear strain change in the same direction (all other stresses being constant).
G	$ML^{-1}T^{-2}$	kPa	modulus of shear deformation. ratio between a given shear stress change and the corresponding shear strain change (all other stresses being constant).
K	$ML^{-1}T^{-2}$	kPa	modulus of compressibility. ratio between an isotropic stress change and the corresponding volume change per unit volume.

μ	—	—	coefficient of friction. maximum ratio between shear and normal stress at point of contact between two solid bodies.
η	$ML^{-1}T^{-1}$	$kPa.s$	coefficient of dynamic viscosity. quotient of shear stress over corresponding shear strain rate in a viscous material.

Properties of Soil

Soil Identification

ρ_s	ML^{-3}	t/m^3	density of solid particles. ratio between mass and volume of solid particles.
γ_s	$ML^{-2}T^{-2}$	kN/m^3	unit weight of solid particles. ratio between weight and volume of solid particles.
ρ_w	ML^{-3}	t/m^3	density of water.
γ_w	$ML^{-2}T^{-2}$	kN/m^3	unit weight of water.
ρ	ML^{-3}	t/m^3	density of soil. ratio between total mass and total volume of soil.
γ	$ML^{-2}T^{-2}$	kN/m^3	unit weight of soil. ratio between total weight and total volume of soil.
ρ_d	ML^{-3}	t/m^3	dry density. ratio between mass of solid particles and total volume of soil.
γ_d	$ML^{-2}T^{-2}$	kN/m^3	dry unit weight. ratio between weight of solid particles and volume of soil.
ρ_{sat}	ML^{-3}	t/m^3	density of saturated soil. ratio between total mass and total volume of completely saturated soil.
γ_{sat}	$ML^{-2}T^{-2}$	kN/m^3	unit weight of saturated soil. ratio between total weight and total volume of completely saturated soil.
γ'	$ML^{-2}T^{-2}$	kN/m^3	unit weight of submerged soil. difference between unit weight of soil and unit weight of water.
e	—	—	void ratio. ratio between volume of voids and volume of solid particles.
n	—	—, %	porosity. ratio between volume of voids and total volume of soil.

w	—	—	water content. ratio between weight of pore water and weight of solid particles (expressed in percentage).
S_r	—	—, %	degree of saturation. ratio between volume of pore water and volume of voids.
w_L	—	—	liquid limit. water content of remoulded soil at transition between liquid and plastic states (determined by a standard laboratory test).
w_P	—	—	plastic limit. water content of a remoulded soil at transition between plastic and semi-solid states (determined by a standard laboratory test).
w_S	—	—	shrinkage limit. maximum water content at which a reduction of water content will not cause a decrease in volume of the soil mass.
I_P	—	—	plasticity index. difference between liquid and plastic limits.
I_L	—	—	liquidity index. defined as $(w-w_P)/I_P$
I_C	—	—	consistency index. defined as $(w_L - w)/I_P$
e_{max}	—	—	void ratio in loosest state. maximum void ratio obtainable by a standard laboratory procedure.
e_{min}	—	—	void ratio in densest state. minimum void ratio obtainable by a standard laboratory procedure.
I_D	—	—, %	density index. defined as $(e_{max}-e)/(e_{max}-e_{min})$
D, d(1)	L	mm	grain diameter. grain size as determined by sieve analysis or wet mechanical analysis.
D_n, d_n(1)	L	mm	n percent-diameter. diameter corresponding to n percent by weight of finer particles.
C_U	—	—	uniformity coefficient. defined as : d_{60}/d_{10}.

(1) Use preferably big letter

C_Z	—	—	curvature coefficient. defined as : $d_{30}^2/(d_{60}.d_{10})$
X_n	—	—	fine fraction — the subscription denotes the diameter adopted for the upper limit of fines and expressed in μm.

Hydraulic Properties

h	L	m	hydraulic head or potential. sum of pressure height (u/γ_w) and geometrical height(z) above a given reference level.
q	L^3T^{-1}	m^3/s	rate of discharge. volume of water seeping through a given area per unit of time.
v	LT^{-1}	m/s	discharge velocity. rate of discharge per total unit area perpendicular to direction of flow.
i		—	hydraulic gradient. loss of hydraulic head per unit length in direction of flow.
k	LT^{-1}	m/s	coefficient of permeability (or hydraulic conductivity). ratio between discharge velocity and corresponding hydraulic gradient (v/i).
j	$ML^{-2}T^{-2}$	kN/m^3	seepage force. the force due to flow with which the seeping water acts upon the soil particles in a unit volume of soil $(j=i.\gamma_w)$
h_e	L	m	capillary rise.

Sampling

C_a	—	%	area ratio (of a sampler). defined as $(d_2^2 - d_1^2)/d_1^2$ with d_1 = inner diameter of cutting nose, d_2 = outer-diameter of cutting nose.
C_i	—	%	inside clearance ratio (of a sampler). defined as $(d_3-d_1)/d_1$, with d_1 = inner diameter of cutting nose, d_3 = inner-diameter of container.
C_o	—	%	outside clearance ratio (of a sampler). defined as $(d_2-d_4) : d_4$ with d_2 = outer diameter of cutting nose, d_4 = outer diameter of barrel shaft.

Consolidation (one-dimensional)

E_{oed}	$ML^{-1}T^{-2}$	kPa	Oedometric modulus : $E_{oed} = d\sigma'/d\epsilon$
m_v	$ML^{-1}LT^2$	kPa^{-1}	coefficient of volume compressibility. $m_v = d\epsilon/d\sigma' = 1/E_{oed}$ for a loading phase.
m_{ve}	$ML^{-1}LT^2$	kPa^{-1}	coefficient of volume expansibility. $m_{ve} = d\epsilon/d\sigma'$ for an unloading phase.
C_c	—	—	compression index. slope of virgin compression curve in a semi-logarithmic plot "effective *pressure-void ratio*": $C_c = -\triangle e/\triangle lg\sigma'$
C_s	—	—	swelling index. average slope of an unload-reload cycle in a semi-logarithmic plot of effective pressure-void ratio : $C_s = -\triangle e/\triangle lg\sigma'$
C_α	—	—	rate of secondary consolidation. defined as : $C_\alpha = d\epsilon/d\ lgt$ during the secondary consolidation phase.
c_v	L^2T^{-1}	m^2/s	coefficient of consolidation. defined as $c_v = k/(m_v\gamma_w)$
d	L	m	drainage path. thickness of layer drained on one side only, or half thickness of layer drained on both sides.
h	L	m	thickness of a layer.
T_v	—	—	time factor. defined as $T_v = t\ c_v/d^2$, t being the time elapsed since application of a change in total normal stress.
U	—	—, %	degree of consolidation.
U_ϵ	—	—, %	local degree of consolidation for strains : $U_\epsilon = \epsilon(t)/\epsilon_f$ where : $\epsilon(t)$ = strain at time t ϵ_f = final strain
U_σ	—	—,%	local degree of consolidation for stresses : $U_\sigma = (\sigma' - \sigma'_0)/(\sigma'_f - \sigma'_0)$ where : σ' = stress at time t σ'_0 = initial stress σ'_f = final stress

U_S	—	—,%	degree of consolidation for settlement: $U_S = S(t)/S$ where: $S(t)$ = settlement at time t S = settlement at the end of consolidation
σ'_{vo}	$ML^{-1}T^{-2}$	kPa	effective overburden pressure. in-situ effective vertical pressure existing prior to sampling or excavation.
σ'_p	$ML^{-1}T^{-2}$	kPa	preconsolidation pressure. maximum vertical effective pressure which has occurred in the soil $(\sigma'_p \geqslant \sigma'_{vo})$.
σ'_c	$ML^{-1}T^{-2}$	kPa	consolidation yield pressure. vertical effective pressure at which soil changes from the so-called "overconsolidated state" to "normally consolidated state" in consolidation process.

Shear strength

τ_f	$ML^{-1}T^{-2}$	kPa	shear strength. shear stress at failure in rupture plane through a given point.
c	$ML^{-1}T^{-2}$	kPa	cohesion intercept.
φ, ϕ	—	—°	angle of shearing resistance. $\tau_f = c + \sigma . \tan \varphi$
c'	$ML^{-1}T^{-2}$	kPa	effective cohesion intercept.
φ', ϕ'	—	—°	effective angle of shearing resistance. $\tau_f = c' + \sigma' . \tan \varphi'$
c_u	$ML^{-1}T^{-2}$	kPa	undrained shear strength. *Note*: to specify the type of test from which c and/or φ are obtained, please refer to the list of subindexes.
c_r	$ML^{-1}T^{-2}$	kPa	remoulded undrained shear strength. shear strength of remoulded soil in undrained situation.
S_t	—	—	sensitivity. ratio between undrained shear strength of undisturbed and of remoulded soil: $S_t = c_u/c_r$.
τ_R	$ML^{-1}T^{-2}$	kPa	residual shear strength. ultimate shear strength in rupture plane which a soil maintains at large displacement.

c'_R	$ML^{-1}T^{-2}$	kPa	residual cohesion intercept.
φ'_R or ϕ'_R	—	—°	residual angle of shearing resistance.

residual shear strength parameters with respect to effective stresses, defined by the equation :

$$\tau_R = c'_R + \sigma' \tan \varphi'_R$$

In-situ Tests

Static Probing

q_c	$ML^{-1}T^{-2}$	kPa	static point resistance (or cone resistance). average pressure acting on the conical point in the standard static penetration test.
f_s	$ML^{-1}T^{-2}$	kPa	local side friction. average unit side friction acting on the friction sleeve in the standard static cone penetration test.

Dynamic Probing

q_d q_{dA}, q_{dB}	$ML^{-1}T^{-2}$	kPa	dynamic point resistance. average pressure acting on the conical point in the standard dynamic penetration test (q_{dA} and q_{dB} for tests of type A and B, respectively).
r_d r_{dA}, r_{dB}	$ML^{-1}T^{-2}$	kPa	dynamic resistance. standardized result of the dynamic penetration test (r_{dA} and r_{dB} for test of type A and B, respectively).
N_d N_{dA}, N_{dB}	—	—	number of blows per 0.20 m. standardized result of the dynamic penetration test (N_{dA} and N_{dB} fo tests of type A and B, respectively).

Standard Penetration Test

N	—	—	SPT blow count. standardized result of the Standard Penetration Test (number of blows for 0.30 m)

Weight Sounding Test

N_{ht}	—	—	number of half-turns for 0.20 m. standardized result of the weight sounding test.

Pressuremeter Test

P_1	$ML^{-1}T^{-2}$	kPa	pressuremeter limit pressure. limit pressure defined in the standard Ménard pressuremeter test.
E_M	$ML^{-1}T^{-2}$	kPa	pressuremeter modulus. Conventional defined in the standard Ménard pressuremeter test.

Dynamics

β	—	—, %	damping ratio. defined as : $\beta = \triangle W/(4\pi W)$ where : $\triangle W$ = energy loss during one cycle W = maximum strain energy
F_L	—	—	safe factor against liquefaction. $F_L = (\tau/\sigma')_L/(\tau/\sigma')$ where : $(\tau/\sigma')_L$ = shear stress ratio causing liquefaction (τ/σ') = induced shear stress ratio
V_P	LT^{-1}	m/s	speed of compression (or primary) wave (P-wave).
V_S	LT^{-1}	m/s	speed of shear (or secondary) wave (S-wave).
V_L	LT^{-1}	m/s	speed of Love wave
V_R	LT^{-1}	m/s	speed of Rayleigh wave (R-wave).

Soil fabric

B_g	—	%	grain breakage. sum, over all sieved fractions, of the *positive* changes of retained percentage per fraction between initial and final gradation curves.
F_{ij}	—	—	fabric tensor. tensor describing the distribution of the relative position of particles which are in mutual contact.
N_g	—	—	coordination number. average number of contacts per grain. *Note* : subindex g refers to grains or soil particles.

Other

Critical State Model Parameters

λ	—		slope of isotropic virgin consolidation line) (or of normal consolidation line)
κ	—		$\lambda = C_c/2.303$ slope of Isotropic swelling reloading lines. $\kappa = C_s/2.303$
M	—		slope of the projection of the critical state line on to the (p', q) plane.
Γ	—		ordinate of critical state line. ($\Gamma = 1 + e$, at $p = 1\ kPa$)

Creep Model Parameters

τ_c	$ML^{-1}T^{-2}$	kPa	Creep threshold. shear stress below which no creep occurs.
τ_l	$ML^{-1}T^{-2}$	kPa	rupture threshold. shear stress beyond which creep ends in failure.
γ_{ml}	—	—,%	mobilization limit. shear strain corresponding to minimum shear strain rate (end of mobilization phase of creep at intermediate and high shear stresses, $\tau > \tau_c$).
γ_{sl}	—	—,%	stabilization limit. shear strain corresponding to maximum shear strain rate (beginning of stabilization phase of creep at intermediate shear stresses, $\tau_c < \tau < \tau_l$).

Geotechnical Structures

Earth retaining structures

K	—	—	coefficient of earth pressure.
K_a, K_p	—	—	active and passive earth pressure coefficients. dimensionless coefficients used in expressions for active and passive earth pressure.
K_o	—	—	coefficient of earth pressure at rest. ratio of lateral to vertical effective principal stress in the case of no lateral strain and a horizontal ground surface.
q	$ML^{-1}T^{-2}$	kPa	surcharge on surface.

Retaning Walls, Diaphragm Walls

δ	—	—°	angle of wall friction. angle of friction between wall and adjacent soil.
a	$ML^{-1}T^{-2}$	kPa	wall adhesion. adhesion between wall and adjacent soil.
β	—	—°	inclination of ground level to horizontal.
α	—	—°	angle of back face of retaining wall to vertical.

Reinforced Earth

l	L	m	length of reinforcing element.
l_a	L	m	length of adherence between soil and reinforcing element.
d	L	mm	diameter or thickness of reinforcing element.
μ^*	—	—	coefficient of apparenent friction ($\mu^* = \tau/\gamma\, z$).
T	$ML\,T^{-2}$	kN	tension force in reinforcing element.

Foundations

$b, B^{(1)}$	L	m	breadth of foundation.
$l, L^{(1)}$	L	m	length of foundation.
$d, D^{(1)}$	L	m	depth of foundation beneath ground.
Q	$ML\,T^{-2}$	kN	applied (axial) load.
q	$ML^{-1}T^{-2}$	kPa	applied (axial) pressure.
q_1	$ML^{-1}T^{-2}$	kPa	limit pressure.
Q_p	$ML\,T^{-2}$	kN	point resistance force.
q_p	$ML^{-1}T^{-2}$	kPa	point resistance pressure.
Q_s	$ML\,T^{-2}$	kN	total shaft resistance.
q_s	$ML^{-1}T^{-2}$	kPa	unit shaft resistance.
q_{dw}	$ML^{-1}T^{-2}$	kPa	dowel penetration resistance. resistance to penetration of dowel in base of a gravity platform to penetration into the seabed.

(1) Use preferably the small letter

q_{sk}	$ML^{-1}T^{-2}$	kPa	skirt penetration resistance. resistance to penetration of the skirt structure at the base of a gravity platform to penetration into the seabed.
R_d	MLT^{-2}	kN	soil resistance against driving. resistance to penetration of pile during driving.
H	$ML\,T^{-2}$	kN	lateral force applied to a foundation.
s	L	m	settlement.
e	L	m	eccentricity. *distance of point of application of* force to center line of the base of the foundation.
δ	—	—°	inclination of load. angle of load force with perpendicular to base of foundation.
k_s	$ML^{-2}T^{-2}$	kN/m^3	modulus of subgrade reaction. ratio between change of vertical stress on a rigid plate and corresponding change of vertical settlement of the plate.
N_c, N_q	—	—	bearing capacity factors.
N_γ			dimensionless coefficients used in expressions for bearing capacity as a function of c and ϕ.
i_c, i_q		—	correction factors for inclination.
i_γ			correction factors for the bearing capacity factors in the case of an inclined load.
Slopes			
h, H(1)	L	m	vertical height of slope.
d, D(1)	L	m	depth below toe of slope to hard stratum.
β	—	—°	angle of slope to horizontal.
$\bar{\tau}$	$ML^{-1}T^{-2}$	Pka	average shear strength mobilized along sliding surface.
R	—	—	residual factor. defined as : $R = \frac{\tau_f - \tau}{\tau_f - \tau_R}$
r_u	—	—	pore pressure ratio. ratio between the in-situ pore pressure and the total overburden pressure : $u/\gamma z$.

(1) Use preferably the small letter

Ground anchors

α	—	—°	angle of anchor inclination to horizontal.
T	MLT^{-2}	kN	anchor load.
T_u	MLT^{-2}	kN	ultimate load of prestressing tendon.
T_l	MLT^{-2}	kN	limit load of fixed anchor zone.
ΔT_{rel}	MLT^{-2}	kN	loss of load due to relaxation.
l_f	L	m	free tendon length.
l_{eff}	L	m	effective free tendon length.
l_b	L	m	calculated tendon bond length.
P_{inj}	$ML^{-1}T^{-2}$	kPa	grout injection pressure.

Geotextiles

ρ_f	ML^{-3}	kg/m^3	density of fibres or filaments.
d_f	L	μm	diameter of fibres or filaments.
λ	ML^{-1}	kg/m	linear mass of fibre. Note: the unit "tex" is also used: 1 tex = 1 mg/m.
o_n, $O_n^{(1)}$	L	$mm,\mu m$	filter opening of a geotextile.
ψ	T^{-1}	s^{-1}	permittivity. quotient of water permeability, perpendicularly to the geotextile, by the geotextile thickness.
θ	L^2T^{-1}	m^2/s	transmissivity. product of water permeability in the geotextile plane by the geotextile thickness.

Foundation vibration and earthquake engineering

f	T^{-1}	s^{-1}	frequency.
T	T	s	period of vibration. $T = 1/f$
ω	T^{-1}	rad/s	circular frequency. $\omega = 2\pi f$
c	MT^{-1}	kg/s	viscous damping coefficient. quotient of resisting force by velocity.
c_{cr}	MT^{-1}	kg/s	critical damping coefficient. minimum viscous damping coefficient that will allow a displaced system to return to its initial position without oscillation.

(1) Use preferably the small letter

D	—	—, %	percentage of critical damping defined as c/c_{cr}
k	MT^{-2}	kN/m	spring constant for vibration. quotient of resistance force by displacement.
k_h	MT^{-2}	—	horizontal seismic coefficient. ratio between the horizontal acceleration and gravity.
k_v	—	—	vertical seismic coefficient. ratio between the vertical acceleration and gravity.
λ	L	m	wave length.
M	—	—	magnitude of earthquake.
M_s	—	—	magnification factor for amplitude of motions of various modes.
I	—	—	intensity of an earthquake. a numerical index describing the effects of an earthquake on the earth surface, on man and on built structures. If necessary, the type of scale should be specified, e.g. I_{MM} for the intensity according to modified Mercalli scale.
T_C	T	s	fundamental period of ground. highest period of mode where resonance occurs, giving in general largest magnification factor (It may be calculated as $4\ h/v_s$, where h is the thickness of a layer).
T_P	T	s	predominent period. period at which spectral acceleration is a maximum.
S_a	LT^{-2}	m/s^2	absolute spectral acceleration. maximum dynamic response of a single-degree of freedom system to earthquake excitation [= (1)].
S_v	LT^{-1}	m/s	relative spectral velocity.
S_d	L	m	relative spectral displacement.
S_{pv}	LT^{-1}	m/s	relative spectral pseudovelocity. spectrum.
SI	LT^{-1}	m/s	spectral intensity or spectrum intensity.

Main Subindexes

Subindexes	Applies to
a	air, active (earth pressure) or allowable.
b	suspension, slurry (usually of bentonite).
c	cohesion or consolidation or critical or capillary.
cd	consolidated-drained test.
cu	consolidated-undrained test.
d	drained or dry state or dynamic.
e	excess (pore pressure).
f	failure or final.
g	soil grains or particles.
G	ground.
h	horizontal.
i	immediate or initial.
l	limit.
p	passive (earth pressure) or preconsolidation or point or predominant.
q	surcharge.
r	radial or remoulded.
R	residual.
s	solids or static or shear.
t	time.
u	undrained conditions or pore-pressure.
uu	unconsolidated-undrained test.
v	vertical or volumetric.
w	water.
x,y	two orthogonal horizontal axes.
z	vertical exis.
γ	weight of soil or rock.
ϕ	angle of internal friction.
$_o$	at rest or initial conditions
1,2,3	principal directions.